TAMPEREEN TEKNILLINEN YLIOPISTO

OLLI KURKELA

ANALYSIS OF ATTACHMENT, PROLIFERATION AND MATURATION OF HUMAN EMBRYONIC STEM CELL–DERIVED RETINAL PIGMENT EPITHELIAL CELLS ON SPESIFIC SUBSTRATA

Master of Science Thesis

Examiners: Professor Minna Kellomäki, Adjunct Professor Heli Skottman, PhD Kati Juuti-Uusitalo
Examiners and topic approved in the Faculty of Science and Environmental Engineering Council meeting on March 9th, 2011

ABSTRACT

TAMPERE UNIVERSITY OF TECHNOLOGY
Master´s Degree Programme in Biotechnology
KURKELA, OLLI: Analysis of attachment, proliferation and maturation of human embryonic stem cell-derived retinal pigment epithelial cells on specific substrata
Master of Science thesis, 100 pages
June 2011
Major: Tissue engineering
Examiners: Professor Minna Kellomäki, Adjunct Professor Heli Skottman, PhD Kati Juuti-Uusitalo
Keywords: Human embryonic stem cell, retinal pigment epithelium

Most severe degenerative diseases of retina are often due to malfunctions of retinal pigment epithelium (RPE). Absence of effective treatments has led to development of cell-biomaterial constructs with the aim of creating RPE equivalents for transplantation. Presently, the poor biocompatibility of allologous and xenologous culture substrata in addition with limited amount of source tissue poses the major issues. Well-defined synthetic substrata together with utilization of human embryonic stem cell-derived RPE cells (hESC RPE) are suggested to be potential solutions. In addition, need exists for an effective method to determine the developmental status of cells during the culturing period. This need could be addressed with automated image analysis.

The aim of this thesis was to examine the capability of a few specific cell culture substrata to enable attachment, proliferation and maturation of hESC RPE cells. Study included total of 17 xeno-free synthetic materials including 12 BioMaDe™ Gelators, Purecoat™ amine and carboxyl, poly(D,L-lactic-*co*-glycolic acid) (75:25), poly(D,L-lactic acid) (96:4) and poly(L-lactic acid-*co*-ε-caprolactone) (70:30). In addition five materials with natural-origin were studied including chitosan, type I collagen, Matrigel™ and Substrate X. Type IV collagen was used as control. Growth and maturation were monitored by taking images with specific time intervals. At the end point cellular developmental status was determined by assessing the expression of maturation specific mRNAs by PCR techniques and proteins by immunofluorescence microscopy. In addition, images were used to determine the potential of ImageJ-software as user-friendly image analysis tool for RPE cell analysis.

Study demonstrated poor attachment and cell survival on every xeno-free synthetic substrate with cells retaining their initial developmental phase throughout the culturing period, which was supported by gene expression analysis. On the contrary, cells on natural materials attached and proliferated readily. Maturity was further confirmed with immunofluorescence labeling. Image analysis with ImageJ, in turn, confronted many problems mainly arising from heterogeneity of the images.

As a conclusion, xeno-free synthetic materials tested in this study show low potential as RPE cell substrata. However, means to enhance their performance are suggested. Despite the good results obtained with natural materials, their ill-defined structure prone to alterations in physiological conditions remains an obstacle for entering clinical experiments. Further experiments should concentrate on combining the strengths of both approaches, that is, incorporation of attachment-related functional groups into well-defined xeno-free synthetic body. In order to increase image homogeneity imaging conditions should be more carefully considered. This way the benefits of automated image analysis could be more effectively exploited.

TIIVISTELMÄ

TAMPEREEN TEKNILLINEN YLIOPISTO
Biotekniikan koulutusohjelma
KURKELA, OLLI: Ihmisen kantasoluista erilaistettujen verkkokalvon pigmenttiepiteelin solujen kiinnittymisen, kasvun ja kypsymisen analysointi erilaisilla soluviljelyalustoilla
Diplomityö, 100 sivua
Kesäkuu 2011
Pääaine: Kudosteknologia
Tarkastajat: Professori Minna Kellomäki, Dosentti Heli Skottman, FT Kati Juuti-Uusitalo
Avainsanat: ihmisen alkion kantasolu, verkkokalvon pigmenttiepiteeli

Monet verkkokalvon sairaudet, vakavimpana näistä silmänpohjan rappeuma, on usein seurausta verkkokalvon pigmenttiepiteelin (RPE) vajaatoiminnasta. Ongelman laajuuden ja tehokkaiden hoitojen puuttuessa kudosteknisen RPE:n siirtoistutuksesta etsitään ratkaisua ongelmaan. RPE on potentiaalinen kohde kudosteknologiselle lähestymistavalle, johtuen sen yksinkertaisesta rakenteesta mutta tärkeästä roolistaan verkkokalvon toimintakyvyn ylläpidossa.

Nykyisten soluviljelyalustojen huono bioyhteensopivuus sekä RPE kudoksen rajoitettu saatavuus ovat suurimmat ongelmat kudosteknologisen RPE:n kehittämisessä. Ihmisen alkion kantasoluista erilaistettujen RPE-solujen (hESC RPE) hyväksikäyttö voi tuoda ratkaisun tähän ongelmaan. Viljelyn aikainen solujen kehityksen tehokas seuranta ei myöskään ole nykymenetelmillä mahdollista. Ongelman ratkaisemiseen automaattinen kuva-analyysi voi olla soveltuva vaihtoehto.

Diplomityön tavoitteena oli tutkia erilaisten materiaalien kykyä toimia hESC RPE-solujen soluviljelyalustana. Tutkimus sisälsi 17 synteettistä ja viisi luonnonperäistä materiaalia. Mielenkiinnon kohteena olivat solujen kiinnittyminen, lisääntyminen sekä kypsyminen, mitä seurattiin kuvaamalla solut säännöllisin väliajoin. Viljelyjakson päätyttyä, kypsyneille hESC RPE-soluille tyypillisten lähetti-RNA - molekyylien sekä proteiinien ekspressio selvitettiin soveltaen PCR-menetelmää sekä vasta-ainevärjäyksiä.

Tutkimus osoitti, että valitut synteettiset soluviljelyalustat tukivat heikosti RPE solujen kiinnittymistä ja kasvua. Kiinnittyneet solut säilyttivät pääosin alkuperäisen kehitysasteensa. Geenien ekspression määritys tuki tätä havaintoa. Luonnonperäiset soluviljelyalustat puolestaan tukivat erinomaisesti solujen kiinnittymistä sekä kasvua ja vasta-ainevärjäykset vahvistivat solujen täysikasvuisuuden. Kuva-analyysi kohtasi monia ongelmia, mitkä pääosin johtuivat kuvien erilaatuisuudesta.

Johtopäätöksenä valitut synteettiset materiaalit soveltuvat heikosti hESC RPE-solujen kasvualustaksi. Selkein toimenpitein niiden suorituskyky on kuitenkin parannettavissa. Huolimatta luonnonperäisten kasvualustojen hyvästä suoriutumisesta, niiden huonosti tunnettu koostumus sekä alttius muutoksille kehossa ovat esteenä etenemiselle kliinisiin kokeisiin. Paremmat tulokset voitaisiinkin saavuttaa yhdistämällä molempien materiaalityyppien vahvuudet. Kiinnittymistä edistävien funktionaalisten ryhmien eristäminen luonnonproteiineista ja liittäminen synteettisesti valmistettuun kasvualustaan voisi parantaa solujen kiinnittymistä ratkaisevasti. Yhdenmukaistamalla kuvausolosuhteita, voitaisiin automaattisen kuvankäsittelyn tehokkuutta puolestaan parantaa huomattavasti.

PREFACE

This study was carried out in the Ophthalmology Group of REGEA Institute of Regenerative Medicine (presently known as Institute of Biomedical Technology) at the University of Tampere and partly at the Department of Biomedical Engineering at Tampere University of Technology.

First, I would like to thank BioMaDe Technology Foundation (presently known as NanoFM) and Finnish Red Cross for providing substrates for this study. Second, I would like to express my gratitude to my supervisors, professor Minna Kellomäki and adjunct professor Heli Skottman, for valuable counseling throughout the process. Furthermore, I am grateful to professor Kellomäki for providing materials and processing facilities for this study.

I owe my gratitude to my supervisor MSc Heidi Hongisto for invaluable guidance and help during the process in both practical work and writing process. Furthermore, I would like to thank MSc Anne-Marie Haaparanta, MSc Ville Ellä and MSc Kaarlo Paakinaho for help with material processing.

I also want to thank my family for support and encouragement. Finally, I would like to express my sincere gratitude to my supervisor, PhD Kati Juuti-Uusitalo, for guidance and support throughout the thesis process and also for valuable advices when choosing my future path.

Tampere, 19.5.2011

Olli Kurkela

CONTENTS

ABBREVIATIONS

AMD	Age-related macular degeneration
ARPE19	Spontaneously transformed human adult RPE cell line
bFGF	Basic fibroblast growth factor
BSA	Bovine serum albumin
cDNA	Complementary DNA
CHX10	Homeodomain transcription factor Chx10
CRALBP	Cellular retinaldehyde binding protein 1
DAPI	4', 6'-diamidino-2-phenylindole
DNA	Deoxyribonucleic acid
DPBS	Dulbecco's Phosphate Buffered Saline
D407	Spontaneously transformed human adult RPE cell line
EB	Embryoid body
ECM	Extracellular matrix
EDM	Euclidian distance map
EDTA	Ethylenediaminetetraacetic acid
FBS	Fetal bovine serum
FDA	US Food and Drug Administration
GADPH	Glyceraldehyde 3-phosphate dehydrogenase
GAG	Glycosaminoglycan
GF	Growth factor
GMP	Good Manufacturing Practice
HA	Hyaluronic acid
hASC	Human adipogenic stem cell
hESC	Human embryonic stem cell
hESC RPE	hESC-derived RPE
hMSC	Human mesenchymal stem cell
ICM	Inner cell mass
IPE	Iris pigment epithelium
IVF	*In vitro* fertilization
LHX2	LIM HOX gene 2
MITF	Microphthalmia-associated transcription factor
mRNA	Messenger RNA
MW	Molecular weight
NaOH	Sodium hydroxide
N-glycan	Asparagines-linked glycoprotein glycan
OCT3/4	Octamer-binding transcription factor 3/4
OTX2	Orthodenticle-homeobox 2 variant 1
PAX6	Paired box gene 6
PCL	Poly(ε-caprolactone)

PCR	Polymerase chain reaction
PDLLA (96:4)	Poly(D,L-lactic acid) with 96:4 ratio of D- and L-lactid acid monomers
PEDF	Pigment epithelium-derived factor
PEG	Poly(ethylene glycol)
PFA	Paraformaldehyde
PHA	Polyhydroxyalkanoates
PHBV	Poly(hydroxybutyrate-*co*-valerate)
PLA	Poly(lactic acid)
PLCL (70:30)	Poly(lactic acid-*co*-ε-caprolactone) with 70:30 ratio of lactic acid and ε-caprolactone monomers
PLGA (75:25)	Poly(lactic-*co*-glycolic acid) with 75:25 ratio of lactic acid and glycolic acid monomers
PLLA	Poly(L-lactic acid)
PMEL	Premelanosome protein
PMMA	Poly(methacrylamide-*co*-methacrylic acid)
RAX	Anterior neural fold homeobox
RGD	Integrin binding peptide arginine-glycine-aspartic acid
RNA	Ribonucleic acid
RP	Retinitis pigmentosa
RPE	Retinal pigment epithelium
RPE65	Retinal pigment epithelium-spesific 65 kDa protein
RPE DM-	Serum-free culture medium used to induce differentiation of hESC towards RPE cells
RT	Room temperature
RT-PCR	Reverse transcriptase polymerase chain reaction
SOX2	SRY (sex determining region Y)-box 2
SIX3	Sine oculis homeobox homolog 3
SIX6	Sine oculis homeobox homolog 6
TBE	Buffer solution containing tris base, boric acid and EDTA
TCEP	Tris(2-carboxyethyl)phosphine
UEP	Ultimate eroded point
VEGF	Vascular endothelial growth factor
Xeno-free	Free from animal-derived components
WS	Working solution
ZO-1	Tight junction protein zonula occludens 1

1. INTRODUCTION

Retinal degenerative diseases affect millions of people worldwide and due to increasing life expectancy and current demographics the number is expected to increase remarkably in forthcoming years [77]. Most common conditions are age-related macular degeneration (AMD) and retinitis pigmentosa (RP). Malfunctions in the innermost layer of retina, the retinal pigment epithelium (RPE), may ultimately lead to impaired vision. [12] RPE is a monolayer of pigment cells that is essential in maintaining overall retinal health. For example RPE regulates homeostasis of the neural retina and choroidal blood vessels including nutrient and ion transport to outer parts of retina. [12, 88, 89] At the moment, absence of effective treatments creates high clinical demand to find therapeutic interventions for retinal diseases. RPE, due to its relatively simple structure, provides a potential target for tissue engineering. [77] An approach first introduced by Lu et al. utilizes a biodegradable substrate as a scaffold for RPE transplantation which among many other advantages provides structural support for monolayer organization [60, 39].

Tight prerequisites have been set concerning biocompatibility, mechanical properties and degradation behavior of the material selected for RPE scaffold [68, 58, 90, 60]. The biocompatibility of allologous or xenologous substrata meets the requirements poorly and may cause severe immune reactions in target individual [67]. In order to use the cultured cells in therapeutic transplantation operations, a xeno-free material is desired option [100]. Another issue hindering clinical experiments is the limited amount of source tissue. Human embryonic stem cell-derived RPE cells (hESC RPE) could provide means to overcome this shortage. [77] To date, reported studies combining RPE cells and biomaterials have been mainly carried out using fetal or spontaneously transformed RPE cell lines, such as ARPE-19 and D407. In addition culture conditions have often contained fetal bovine serum (FBS) which enhances cellular attachment, however, may have other ill-defined effects. [58, 90, 97, 38, 105, 92, 110, 84, 30, 59, 93, 1] Recently, many studies with long term goal to develop xeno-free Good Manufacturing Practice (GMP) growth and maturation producing conditions for hESC RPE cells have been reported [87, 104, 74, 15, 49, 100]. In addition, need exists for a non-invasive, simple and accurate method to determine the proliferative and differential status of cells while they are still in the culture. The image analysis is one step forward on this goal. To date many image analysis tools have been developed for image cytometry, among these, open-source ImageJ-software [2].

Aim of this master's thesis was to address the previously mentioned issues by investigating the capability of different well-defined synthetic and natural-based substrata to enable attachment, proliferation and maturation of hESC RPE cells in

serum-free conditions. If substrata showed potential it could be further applied in RPE transplant. Total of 17 synthetic materials including 12 BioMade™ Gelators, Purecoat™ amine and carboxyl, poly(D,L-lactic acid) (96:4) (PDLLA), poly(D,L-lactic-*co*-glycolic acid) (75:25) (PLGA) and poly(L-lactic acid-*co*-ε-caprolactone) (70:30) (PLCL) and five materials with natural-origin including chitosan, type I collagen, Matrigel™ and Substrate X were selected for the study. Type IV collagen was selected as control substrate. First, the hESC RPE cells were seeded on the materials and the growth and maturation was monitored by taking images with specific time intervals. At the end point the stage of cellular differentiation and maturation was determined by assessing the expression of maturation specific mRNAs by PCR techniques and proteins by immunofluorescence microscopy. Second aim was to define how successfully and easily ImageJ-software could be used to provide statistical data about the maturation stage of the RPE cells. Examined factors were cellular proliferation rate, morphology and the amount of pigmentation. ImageJ-software includes a possibility to create custom-made plugins [2], however, this possibility was ruled out in this study due to insufficient programming skills. The practical work was done at the REGEA Institute of Regenerative Medicine (presently known as Institute of Biomedical Technology) at the University of Tampere and partly at the Department of Biomedical Engineering at Tampere University of Technology.

The course of study is presented as follows. Thesis is divided into theoretical part and experimental part. Theoretical part provides essential background information and justifies the study by introducing basic concepts of RPE structure, functions and disorders. In addition potential cell sources are presented. Furthermore, candidate materials and existing literature concerning RPE culturing and transplantation are overviewed. Finally, state of image analysis involving RPE cells is briefly introduced. Experimental part, in turn, provides detailed description how the study was carried out. First, Materials and Methods-chapter describes practical arrangements and applied methods. Second, in the Results-chapter detailed results are viewed. In Discussion, outcome of the study is more thoroughly demonstrated. Finally, conclusions are drawn and future perspectives considered.

THEORETICAL PART

2. RETINA

2.1. Structure of retina

Retina is the innermost layer of the eye wall (Figure 2.1) receiving the light that enters the eye [36]. Consisting of approximately 55 distinct cell types it forms a highly organized structure that plays essential part in providing visual perception [47]. On the outer surface Bruch's membrane separates it from blood vessel-rich choroid. On the inner surface, in turn, it faces the vitreous body. Preliminary image modification begins already at retina although the eventual formation of an image takes place in the brain. [36]

The retina has two main layers, the neural layer and RPE layer (Figure 2.1), which have both structural and functional dependence on each other. Neural retina is the inner part of retina. The architecture is highly complex consisting of several layers of different neurons, glial cells and photoreceptor cells reactive to light. [47] The light that enters must pass the whole neural layer before being processed by the rod and cone photoreceptors, transformed into a signal and transmitted through ganglion cell layer to optic nerve and ultimately to brain. On the way, the signal is being processed by several horizontal, bipolar and amacrine cells each affecting the outcome. There are two specific areas on retina dense in color-sensing cone receptors: macula and fovea. Macula enables vision for sharp work. Fovea, with even denser population of cone receptors, provides sharpest possible vision. In addition to these, cells supporting and stabilizing the cellular environment such as astrocytes and Muller glial cells are present in the neural retina. [106]

Bruch's membrane separates RPE and choroid and therefore forms the outer limit of retina. The main functions of Bruch's membrane include anchoring of cells, creating barrier and filter for molecular transport and stabilizing the cell structures. [3] The Bruch's membrane together with RPE cells play crucial role in maintaining photoreceptor viability as well as overall retinal health [26]. The Bruch's membrane consists of five distinct layers. The inner basement membrane separates the Bruch's membrane from RPE cells. The inner collagenous layer separates the inner basement layer and elastic layer. Next to elastic layer is the outer collagenous layer before the outer basement membrane connects Bruch's membrane to choroid. Primary components of Bruch's membrane are type I and type IV collagens, elastin, laminin and fibronectin. [58] When individual ages, Bruch's membrane goes through several changes such as increase in thickness, decrease in collagen cross-linking, accumulation of lipids and decrease in hydraulic conductivity [109].

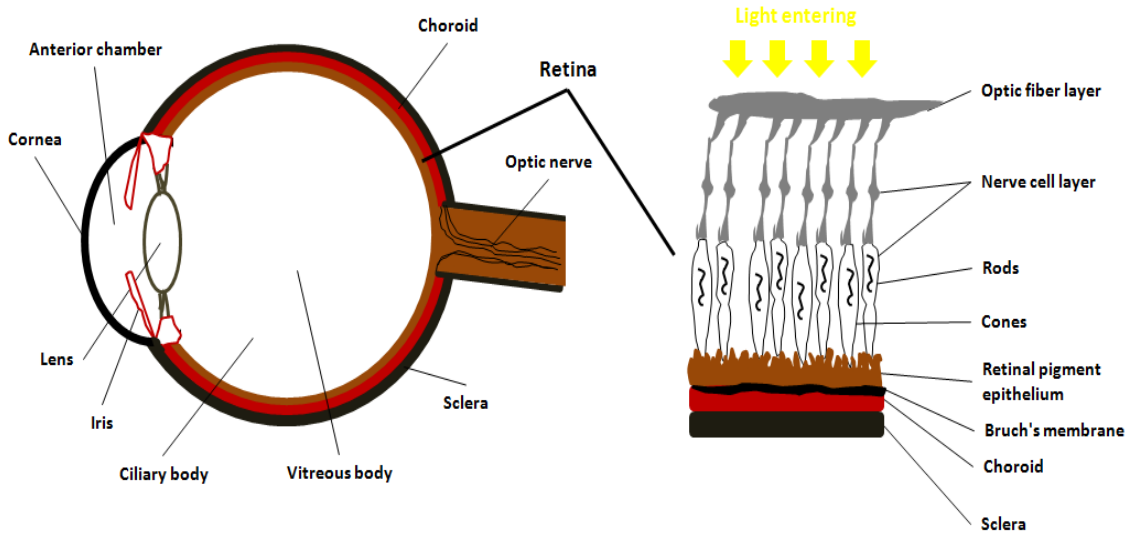

Figure 2.1 *The structure of eye and spesific structure of retina. Drawn according to [106].*

2.2. Retinogenesis

The early development of retina towards highly organized layer-structure results from complex interactions influenced by many intrinsic and extrinsic factors. Both retinal microenvironment and the progenitor cells alter according to different developmental phases in order to regulate the process. [47] Several genes, such as paired box gene 6 (PAX6), anterior neural fold homeobox (RAX), microphthalmia-associated transcription factor (MITF), orthodenticle-homeobox 2 variant 1 (OTX2), homeodomain transcription factor Chx10 (CHX10), Bestrophin and retinal pigment epithelium-spesific 65 kDa protein (RPE65) have been discovered to have effect on cellular fate during the process [28, 8, 100, 66, 74, 49, 104, 47]. Extrinsic factors, in turn, include for example growth factors (GFs), secreted transcription factors, extracellular matrix (ECM) molecules and retinoids [28, 8, 47]. Early development of embryo includes a formation of hollow sphere of cells containing outer cell layer and inner cluster of cells called inner cell mass (ICM). The outer cell layer develops into trophoectoderm and ultimately gives rise to placenta and other supporting tissues. The ICM on the other hand gives birth to tissues of body. [4]

Retina originates from embryonic ectoderm. In the early neural stage of embryo the eye field fold into structure called optic pit with first distinguishable morphological features of eye. [47, 100] Further invagination results in formation of optic vesicles which develop into a two-layered structure, optic cup. RPE originates from outer layer of the optic cup and the neural retina from the inner layer, respectively. [28, 8, 47] Ultimately, mature RPE cells appear as monolayer structure with brownish pigmentation [104, 100]. Despite the common embryological origin of neural and RPE cells they express different transcription factor profiles during development and exhibit quite distinct properties after differentiation [47].

3. RETINAL PIGMENT EPITHELIUM

3.1. Structure of retinal pigment epithelium

RPE is a monolayer of highly specified cells with multiple functions. In the normal *in vivo* environment RPE cells in a monolayer take cuboidal shape and form a cobblestone-like packing (Figure 3.1). The characteristic brownish color of RPE layer results from melanin and other pigments inside the RPE cells. [60] Throughout the individual's life, form of a RPE cell remains fairly static. The cell size depends on the cell's location on the retina and correlates with the individual's age. The height and width of a normal RPE cell in a young individual's macula is approximately 14 µm and 10-14 µm, respectively. Due to high structural and functional polarity the RPE cells are able to perform highly specified roles. [52]

Distinct surfaces separate RPE layer from surrounding tissues. The basal surface forms a twisted structure with high surface area creating connection between RPE and underlying Bruch's membrane and facilitating effective molecular transport. [52] The microvilli-covered apical surface actively interacts with light-sensitive outer segments of photoreceptors [58]. The lateral surfaces of the adjacent RPE cells are bind together by a specific setting of four junction types: tight junctions, adherent junctions, desmosomes and gap junctions [52].

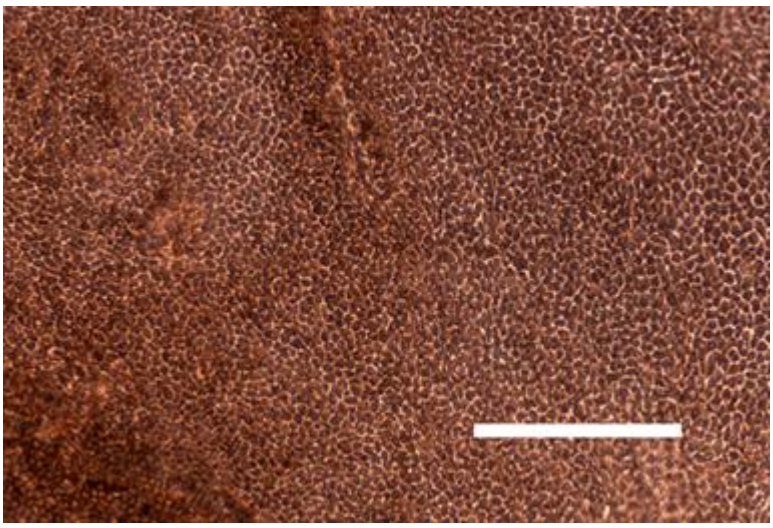

Figure 3.1. *hESC RPE culture in vitro on Matrigel™. Scale bar length 200 µm, magnification 100x. Image was taken at the end point of phase II in this study.*

3.2. Functions of retinal pigment epithelium

Due to RPE layer's location and characteristics it has essential functions in maintaining overall retinal health (Figure 3.2). These functions include controlling the molecular transportation between choroidal blood vessels and other parts of retina, participating in the visual cycle, light absorption and protection against photo-oxidation, regeneration of outer photoreceptor segments and secretion of several crucial factors affecting retinal structural integrity and immune privilege of eye. [89, 107]

Due to specific setting of tight junction proteins RPE layer forms part the outer blood-retina barrier and controls the transepithelial delivery of fluids, toxic molecules and plasma components between choroid and other parts of retina. Through RPE, retinol and nutrients such as glucose and fatty acids, ascorbic acid and vitamin A pass from blood to the tissue. Another transportation-related function is maintaining the proper amount of water in subretinal space mainly through the transportation of Cl^- and K^+ from the apical side to the blood. In addition, ion composition is stabilized by RPE through the control of K^+ concentration, which is crucial for maintenance of photoreceptor sensibility [89, 107]. Reduction in epithelial transport may cause retinal degeneration [89].

RPE has important role also in the visual cycle. Delivery of retinal, a protein with high significance in the visual cycle, is partly controlled by RPE. This metabolic pathway starts in visual pigment rhodopsin as light absorption in 11-cis retinal leads to isomeric change to all-trans form. Due to lack of proper enzyme, photoreceptors are unable to perform the retransformation and therefore retinal is transported to RPE. After retransformation retinal in cis-form is returned back to photoreceptors. [89, 107] Several types of inherited retinal and RPE degenerations are due to reduction in the activity of visual cycle. This is typically a result of defects in genes leading to altered function of various proteins in the reaction cascade. [89]

Primary function of pigments in RPE is to reduce reflections of light entering back to eye globe and this way prevent disturbance in visual perception [36]. Light can induce photo-oxidative damage to proteins and phospholipids on the outer segments of photoreceptors. This leads to lipid transformation into a form toxic for retinal cells and generation of reactive oxygen species. Pigments function to prevent this emerging oxidative stress by absorbing various wavelengths. However pigments can only partly prevent light-induced photo-oxidative damage and therefore different enzymatic and non-enzymatic antioxidants pose additional type of defense mechanism. [83] The occurred damage is repaired by continuous regeneration of outer segments occurring in cycles of 11 days in humans. Maintaining the right size of outer segments is essential and this is carried out by continuous phagocytosis by RPE cells and reassembly by photoreceptors. The regeneration process takes place on the surface of apical microvilli. In digestion process various essential substances are recycled and returned to photoreceptors. [89, 107]

The maintenance of previously mentioned functions requires efficient communication with adjacent tissues. This is accomplished by secretion of various GFs as well as other factors crucial for RPE integrity. Among these pigment epithelium-derived factor (PEDF) and vascular endothelium growth factor (VEGF) are most significant in maintaining health of endothelium in choriocapillaris yet preventing it to penetrate into retina. [83] Immune privilege of the eye, that is, the ability of eye to tolerate antigens without eliciting immune response, is mainly due to RPE layer's barrier function but also due to secretion of factors such as major histocompatibility complex molecules, adhesion molecules and cytokines that interferes the signaling pathways coordinating immune suppressive functions. [89, 107, 83]

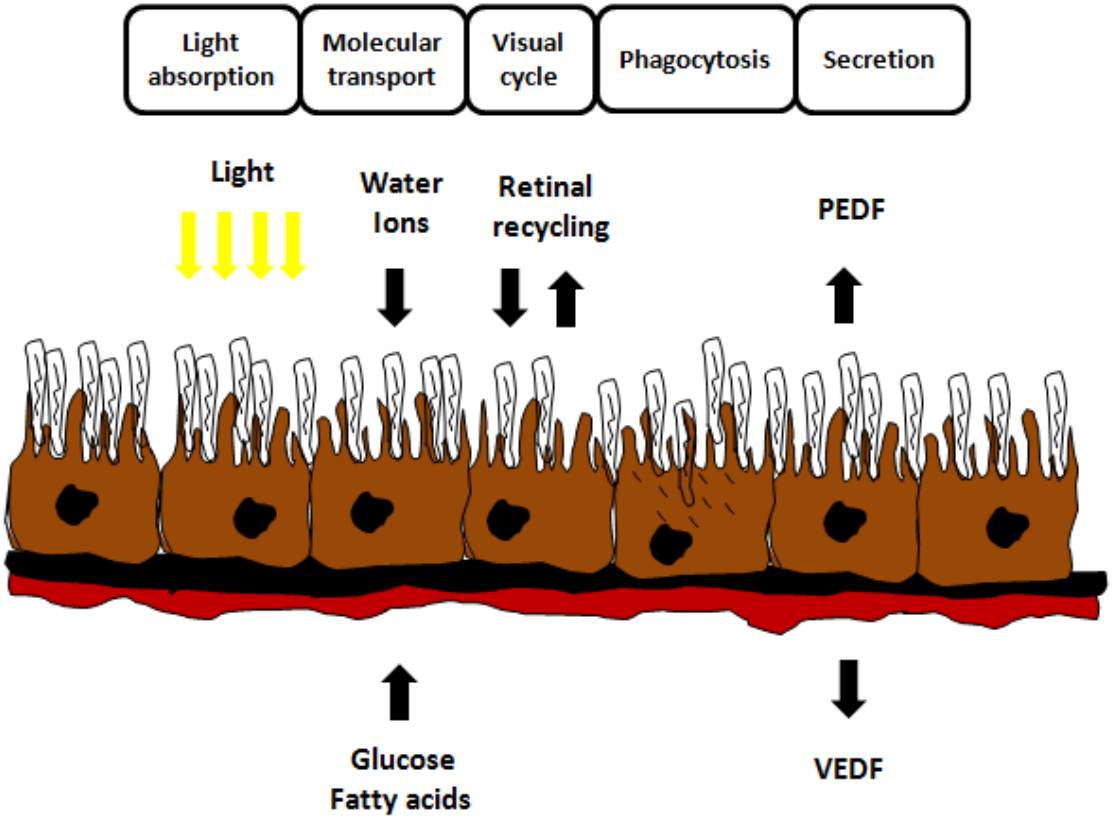

Figure 3.2 *The schematic representation of principal functions of RPE. The figure was drawn according to representation in [89].*

4. RETINAL DISEASES

4.1. Retinal disorders

Disorders of retina are cause of many ophthalmic diseases such as AMD and RP. Typical for these diseases is deterioration of Bruch's membrane and RPE ECM which leads to malfunctioning of RPE cells. Most often these changes affect the RPE layer's cell adhesion which is mainly organized by the proteins of ECM. The malfunctioning of RPE cells can disturb the visual perception by affecting the health of photoreceptors and, in the most severe cases, ultimately lead to total loss of vision. [40]

The most common condition is AMD which can lead to blindness. AMD is considered to be the leading cause of blindness among elder people in the western countries with approximately 16000 new cases of different forms of AMD reported annually. Since the studies have indicated correlation between ageing of people and occurrence of AMD the increasing life expectancy causes the number to increase in the future. [40, 77]

AMD can exhibit two morphologic forms. The atrophic form is characterized by RPE cell atrophy and choroid degeneration. [26, 60] Increased number of photo-oxidative reaction species and errors in secretion of GFs are considered to be initial steps in AMD pathogenesis [89]. At first the gradual loss of vision begins in one eye then spreading to the other [60]. Early stages include formation of drusen and alteration in pigmentation [77]. Characteristic for AMD is weakened ability of RPE cells to degrade photoreceptor waste products properly leading to accumulation of waste products in the membrane. Consequently, Bruch's membrane can thicken resulting in crucial changes in organization of RPE layer. This change leads to deteriorated nutrient transport into retina and ultimately to destruction of rods and cones. [77, 60]

On approximately 10-20% of the patients the atrophic type develops into neovascular form. The neovascular AMD has similar pathogenesis and is considered to be continuity of the atrophic form. In neovascular AMD, blood vessels from choroid start to penetrate through Bruch's membrane ultimately reaching RPE and neural layer [77]. This may cause hemorrhages in retina which damages retinal cells [26, 109]. The factors that cause AMD remain unknown but both genetic and environmental factors are believed to have influence. As an important non-genetic factor, smoking has shown correlation with AMD. [77]

RP is another major condition involving RPE cells. RP is a group of disorders characterized by slow degeneration of photoreceptors. Occurrence of RP is approximately 1/4000. Studies have shown that RP is hereditary with first symptoms emerging already at childhood or adolescence. RP exists with variation in rapidness and

severity of pathogenesis. Two main types of RP are rod-cone and cone-rod dystrophies, each name indicating the direction of pathogenesis. Rod-cone dystrophy is characterized by progressive deterioration of peripheral RPE leading to defective dark adaption and ultimately to total loss of vision. Rod receptors degrade first followed by cone receptors. The cone-rod dystrophy, on the contrary, results more in the loss of visual acuity than loss of vision field. To date, 45 genes have been identified with causative effect on RP resulting in variations in disease phenotype. Three different ways to inherit RP exists with decreasing severity: autosomal dominant, X-linked manner and autosomal repressive. [35]

RPE degeneration is typical for other retinal dystrophies as well including diabetic retinopathy, vitelliform macular dystrophy (Best disease), proliferative vitreous retinopathy, Stargardt's disease, pattern dystrophies, choroideremia and photic maculopathy. However, the prevalence of these diseases is minor compared to previously introduced. [3]

Current treatments for AMD include dietary supplementation of anti-oxidants, laser therapy, anti-VEGF treatment and combination therapy of laser with anti-VEGF [45]. In the case of RP most commonly applied treatments are vitamin A and protection against sunlight [35]. Despite the fact that injections of anti-angiogenic drugs have shown to delay the progress of neovascular AMD none of the treatments can completely stop the degeneration. [45] At worst the injections can imbalance the GF concentrations even further and lead to destruction of portions of outer retina which ultimately leads to other defects of RPE cells and Bruch's membrane. [89]

4.2. Cell transplantation experiments

Since the present treatments fail to restore vision a need for novel approaches in retinal treatment exists. The principal alternatives to date are gene therapy and RPE transplantation which both have various applications under research. For many of the diseases the RPE transplantation is not the most suitable alternative and superior results can be achieved by repairing gene defects. Yet diseases in which the RPE goes through severe structural damage and cell loss could be treated with the different applications of cell transplantation. [20] It is demonstrated that in many diseases the inner layers of retina maintain their organization for a significant period of time. Therefore transplantation of healthy cells capable to integrate and reconnect to the synaptic pathways of the host in the early stages of disease could restore vision. To date there are numerous studies about subretinal transplantation of RPE cells, mature photoreceptors, progenitor cells and retinal sheets on animals showing varying degrees of restored vision. [39]

RPE transplantation using cell sheets have been applied in order to cure AMD. Due to progress in surgical techniques and equipment safer incorporation of sheets into the eye have become possible. [9] Several different approaches have been applied including use of allologous adult RPE cells, fetal RPE cells [9, 39], autologous

peripherial RPE cells and iris pigment epithelium (IPE) cells [39]. However, these attempts have encountered severe problems including rejection by host, formation of multilayered structure and initiated de-differentiation of grafted RPE cells [20]. In addition, peripheral RPE cells have found to fail in creating connection to foveal RPE and IPE cells have difficulties maintaining typical RPE functions such as phagocytosis of photoreceptor outer segments [39].

Another approach widely studied is transplantation of *ex vivo* cultured or recently harvested RPE cells as a suspension into subretinal space. The attachment of RPE cells to Bruch's membrane can be aided with specific adhesion molecules. However, problems with this technique exist. Suspended cells tend to attach on the basal lamina of Bruch's membrane instead of other layers. [9, 20] Typically transplantation is performed on aged or diseased retina with Bruch's membrane undergone structural damage resulting in poor attachment and induced apoptosis. In addition, cells prefer to stack and form isolated islands instead of forming a typical monolayer [60] which can lead to other conditions such as retinal fibrosis or proliferative vitreoretinopathy. [90, 9, 20]

Promising results on animal trials concerning AMD and RP exist. In addition, human volunteer studies in which RPE has been grafted on the eyes of patients with AMD has taken place. [39] Unfortunately in the human trials the visual recovery at best has been limited [20, 60]. Failures could be due to the specific characteristics of RPE layer *in vivo:* polarity and distinct apical and basal characteristics. In order to carry out successful transplantation cell population needs to integrate to the cellular environment. This includes proper organization and differentiation into retinal cell types. [60]

4.3. The need for tissue-engineered constructs

The harvesting process of adult RPE cells separates the cells from their ECM and induces apoptosis. This indicates that the donor cells ability to function depend on the attachment to the Bruch's membrane. [20, 90] Due to this anchorage-dependency, reattachment to a substrate increases cell survival [21, 39]. The coating of the substrate with ECM components improves the survival even more [90, 39]. In addition differentiation of retinal progenitor cells has been more advanced on substrates [39]. Furthermore, by using a substrate cellular growth and organization could be directed. Therefore implantation of RPE cells on thin biodegradable films could provide means to achieve an organized structure that could more readily restore the subretinal anatomy and re-establish the crucial interactions between the RPE and photoreceptors. [60, 90, 20]

Lu et al. have proposed a four-step treatment strategy which applies a tissue-engineered construct (Figure 4.1) [60]. This strategy has later been supported by Hynes et al [39]. In the first step RPE cells are harvested from proper source and a xeno-free biodegradable substrate is prepared. If possible the RPE cells should be of autologous (harvested from the treated individual) origin in order to minimize rejection reactions.

However, typically unaffected RPE areas are rare in the patients and therefore allologous (harvested from different individual of same species) cells could be used. At this point the limited amount of source tissue creates a remarkable problem. [60] It is suggested that hESC RPE cells could provide means to overcome this shortage. [77] In addition it is demonstrated that immature cell populations integrate most readily to their environment [39]. The biodegradable substrate is processed into form of a film in order to easily establish a monolayer of RPE cells. In the second step the cells are cultured on the substrate *in vitro*. Cell growth and function could be manipulated for example by adding GFs and immunosuppressant drugs into the substrate. Furthermore the surface of the film could be micropatterned to enhance cell adhesion. After reaching confluency the cell culture together with the substrate is inserted into the subretinal space which constitutes the third step. In the last step the reattachment of retinal equivalent usually occurs spontaneously within 24-48 hours. The transplant then connects to the photoreceptors at the apical side and Bruch's membrane at the basal surface. Simultaneously, the polymer substrate slowly degrades. [60]

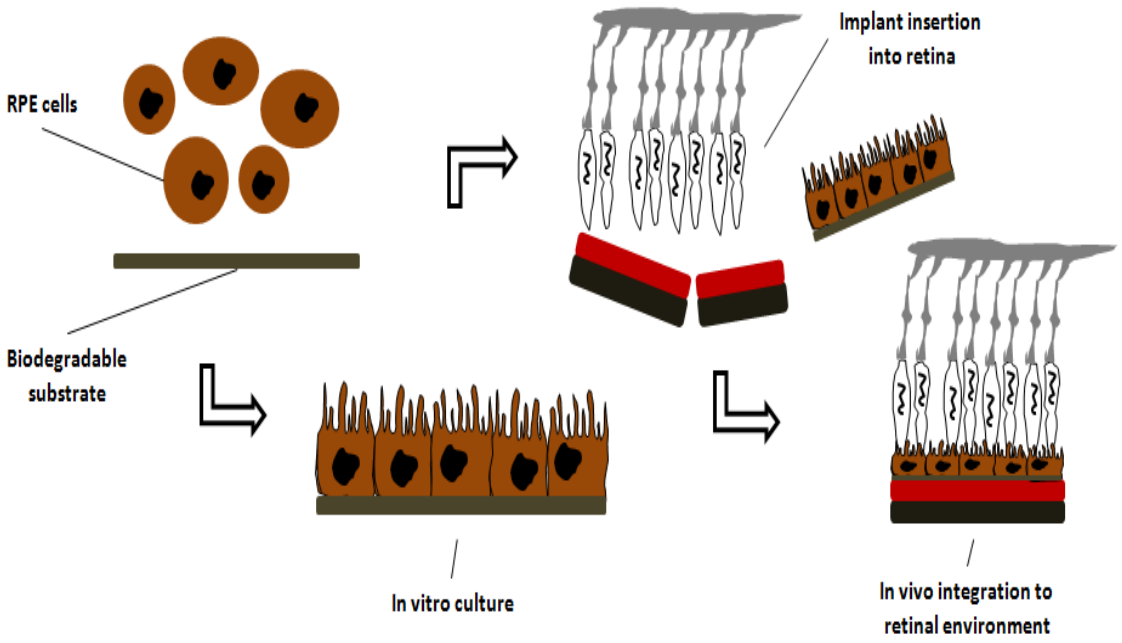

Figure 4.1 *The strategy for construction of RPE transplant. The figure was drawn according to [60].*

5. RPE CELL LINES

5.1. Overview

RPE cells exist with wide range of origin. In general, both human and animal derived cells have been studied (Table 5.1). These cells can be primary RPE cell-derived or transformed RPE cell-derived. Primary RPE cells can be of autologous or allologous origin and harvested at different stages in their lifespan, typically as adult mature or at early fetus stage. Transformed RPE cells, in turn, can be divided into genetically modified such as h1RPE7 cell line and spontaneously transformed such as ARPE-19 and D407 cell lines. Also non-RPE cells have been studied including IPE cells, Schwann cells, bone marrow stem cells, retinal progenitor cells and umbilical stem cells. [20]

Non-xeno origin of cells is considered more desirable in order to avoid possible rejection reactions and genetic disorders [100]. However the major problems with mature retinal cells concern the availability of donor tissue, batch-to-batch variation and issues concerning safety and ethics. In order to overcome the problem of shortage shift towards less mature cell types, for example progenitor and stem cells, has taken place. [39] Presently stem cells show potential as a primary cell source. Most importantly hESC, which have the ability to differentiate into every cell type in human body, could provide inexhaustible source for all types of cells. [20] To date, effective hESC differentiation towards RPE lineage has been studied extensively [49, 61, 74, 75, 31, 104, 15, 40, 66, 69]. Recent studies have also reported RPE cell derivation from induced pluripotent stem cells [37, 14, 66, 16].

5.2. Human adult ARPE-19 cell line

ARPE-19 is a spontaneously arising human RPE cell line originally obtained from primary RPE cell culture through trypsinization. The cell line was derived from the globes of 19-year old male donor in Sacramento, CA, USA. After enucleation globes were stored in cold room (12 h) before plating. After wash eyes were treated to detach anterior segment. RPE was then dissected away from the optic nerve and split from other retina. The eyecup was then rinsed and filled with dispersal solution including trypsin. The RPE was removed from the eyecup and transferred into culture

Table 5.1 *Cell sources. Information collected and modified from [20].*

Human	Type of cell	References
Primary RPE cell-derived	Adult	Gouras et al. (1985) He et al. (1993) Peyman et al. (1991) Castillo et al. (1997), Stanga et al. (2001), Binder et al. (2002) Van meuers and Van Den Biesen (2003)
	Fetal/Childhood	Algvere et al. (1994), Durlu and Tamai (1997), Castillo et al. (1997), Gabrielian et al. (1999b), Oganesian et al. (1999)
Transformed RPE cell-derived	Genetically modified	Lund et al. (2001a), Ogata et al. (1999), Lai et al. (1999,2000), Wang et al. (2002a), MacLaren et al. (2007)
	Spontaneously transformed (ARPE-19, D407)	Dunn et al. (1996, 1998), Davis et al. (1995), Coffey et al. (2002), Girman et al. (2003, 2005), McGill et al. (2004), Wang et al. (2005a, b), Pinilla et al. (2005), Sauve et al. (2006)
Non-RPE cells	Embryonic stem cell	Klimanskaya et al. (2004), Lund et al. (2006), Osakada et al. (2008, 2009)), Gong et al. (2008), Vugler et al. (2008), Carr et al. (2009), Idelson et al. (2009), Meyer et al. (2009), Nistor et al. (2010)
	Induced pluripotent stem cells	Hirami et al. (2009), Buchholz et al. (2009), Meyer et al. (2009), Carr et al. (2009)
	Iris pigment epithelial cells	Rezai et al. (1997a, b, c), Thumann et al. (1998),
	Schwann cell	Lawrence et al. (2000), McGill et al. (2004), Wang et al. (2005b)
	Bone marrow stem cell	Arnhold et al. (2006)
	Retinal progenitor cell	Kumar and Dutt (2006)
	Umbilical stem cell	Lund et al. (2006b)
Animal		
Primary RPE cell-derived	Adult (rat, mice, rabbit, bovine, porcine)	Li and Turner (1988b), Jiang et al. (1994), Lopez et al. (1987), Crafoord et al. (1999), Durlu and Tamai (1997), Wang et al. (2001, 2004), Nicolini et al. (2000), Grisanti et al. (2002), Eurell et al. (2003), Wiencke et al. (2003), Del Priore et al. (2004), Lane et al. (1989), Maaijwee et al. (2006), Wongpichedchai et al. (1992), Phillips et al. 2003)
	Fetal/Childhood/Infantile	Grisanti et al. (1997), Rizzolo et al. (1991), Rizzolo and Heiges, (1991), Li and Turner (1991), Del Priore et al. (2003a)
Transformed RPE cell-derived	Genetically modified (rat)	Faktorovich et al. (1990), Abe et al. (1999, 2005), Saigo et al. (2004), Dunaief et al. (1995), Osusky et al. (1995), Hansen et al. (2003)
Non-RPE cells	Embryonic stem cell (monkey)	Haruta et al. (2004)
	Iris pigment epithelial cells (rat, porcine)	Abe et al. (1999), Ohno-Matsui et al. (2006), Thumann et al. (1997)
	Neural stem and progenitor cell (rat, porcine)	Enzmann et al. (2003), Klassen (2006)
	Bone marrow stem cell (rat, mice)	Arnhold et al. (2006), Atmaca-Sonmez et al. (2006), Harris et al. (2006)
	Retinal progenitor cell (mice)	Warfvinge et al. (2003)

medium and ultimately to culture flasks. After reaching confluency and removal of weakly adherent cells and fibroblasts the cell line was purified by selective trypsinization. After repeating this procedure several times a uniform, highly epithelial culture of RPE cells was obtained. The cell line was shown to have potential for growth, heavy pigmentation and polygonal morphology. [23]

Dunn et al. have described the development and characterization of ARPE-19 cell line. ARPE-19 cells possess features characteristic for RPE including defined cell borders, an overall cobblestone-like appearance and prominent pigmentation. Maturation requires 3-4 weeks after cultures reach confluency. Typically the pigmentation becomes stronger as the culturing period advances. The karyology of ARPE-19 cells was studied to expose possible aneuploidy and other chromosomal defects that usually are related to cell transformation. Metaphase chromosome number was confirmed to be 46. Spesific RPE markers cellular retinaldehyde binding protein 1 (CRALBP) and RPE65 were detected. CRALBP protein was also detected by both immunocytochemistry and Western blotting method. [23]

5.3. Human embryonic stem cell-derived retinal pigment epithelial cells

Stem cell is defined as cell possessing capability to self-renew. Furthermore stem cells are regarded as pluripotent since they can differentiate into multiple mature cell types. Through asymmetric cell division, one daughter cell remains multipotent while another initiates differentiation towards maturity. [47]

hESC, in turn, are stem cells derived from the ICM of the blastocyst, an early-stage embryo. Thomson et al. pioneered the first stable hESC lines in 1998. Since then the utilization of hESCs has been extensive. [94] Typically, hESCs used in cell culturing origin from ICM of low quality early day embryo (4-5 days) donated by couples going through *in vitro* fertilization (IVF) treatments [57]. Cells of ICM are enzymatically extracted and proliferated on different types of feeder cells or alternatively on suitable ECM under feeder-free conditions [87].

As fulfilling the prerequisities of a stem cell, hESCs possess the capability to self-renewal due to the high level of telomerase activity which enables extended replication. In addition, hESCs are pluripotent. These two valuable properties have raised hopes to utilize hESCs as inexhaustible cell source for transplantation applications in many degenerative diseases. [94] In several studies research groups have examined the possible ways to differentiate hESCs to RPE cells (Figure 5.1). To date hESC RPE cells functionally equal to their native counterparts have been obtained. [104, 100, 40, 15, 49, 74, 75]

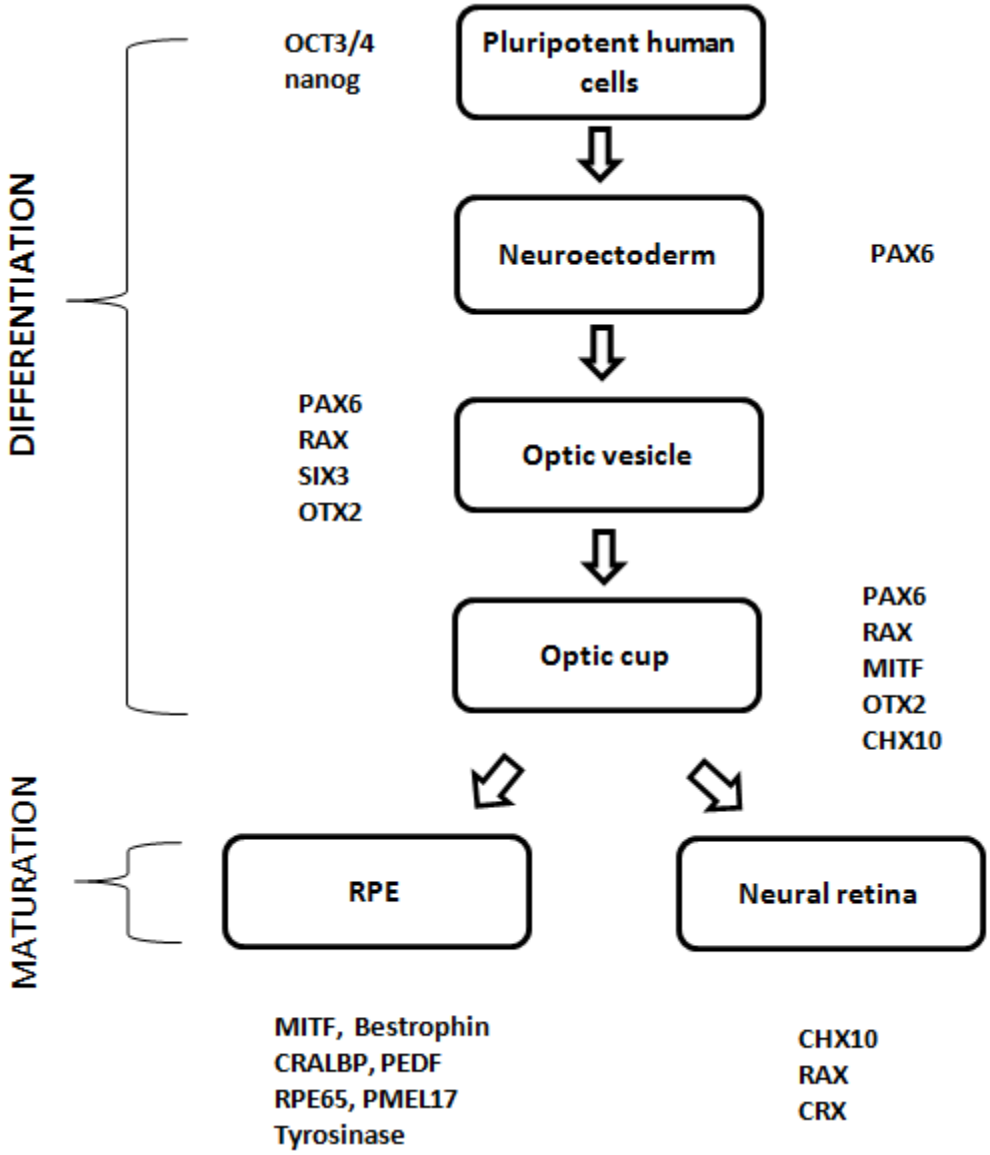

Figure 5.1 *Differentiation of RPE cells from hESCs and marker gene expression during different phases of differentiation compared to natural embryo development. Modified from [100].*

5.3.1. Phenotypical changes during development

RPE epithelium *in vivo* is very stable and cells remain fairly static throughout individual's life, however, RPE cell retain ability to proliferate and possess remarkable growth potential when exposed to culture conditions *in vitro* [47]. Early *in vivo* studies in vertebrates and *in vitro* cultures with specific conditions have indicated the RPE capability to transdifferentiation, that is, the ability to perform phenotypic switch and identity change into different cell types, in the case of RPE typically towards neural lineage [47]. This phenomenon partly plays role in RPE cell proliferation *in vitro* as cells obtain de-differentiated pheno- and genotype. Many *in vitro* studies, in which RPE cells have been maturated from differentiated RPE cells of different origin, have

demonstrated distinct stages of growth. In the first stage cells lose pigmentation and shift appearance towards fibroblast-like elongated morphology after cell attachment onto the substrate. Second stage includes reaching confluency and finally obtaining cobblestone-like morphology and re-appearance of pigmentation. [104, 40, 100] Vugler et al. have stated that these changes demonstrate typical RPE growth cycle [104]. In order to proliferate RPE cells de-differentiate including de-pigmentation and expression of key transcription factors involved in RPE differentiation and also proliferation indicator keratin 8. De-differentiation is followed by proliferation in which cells retain de-differentiated form. Finally, cells exit the cell cycle and re-differentiate with restarted melanogenesis and cobblestone-like appearance. [104, 40, 100]

5.3.2. Genotypical changes during development

Multiple genes together with extrinsic factors play role in determining cell fate in different phases of retinal development [47]. Nanog gene is considered to be key factor in maintaining the pluripotency in embryonic stem cells and is typically used as specific marker of undifferentiated state of embryonic stem cells [18, 100]. Another characteristic gene is octamer-binding transcription factor (OCT3/4), which also regulate pluripotency of embryonic stem cells [70]. RPE cell differentiation can be initiated *in vitro* by removal of basic fibroblast growth factor (bFGF) from the cell culture medium leading to spontaneous rise of RPE cells [100]. After induction of cells towards eye lineage expression of specific markers such as PAX6 can be observed [100, 66, 74, 49]. Also sine oculis homeobox homolog 3 (SIX3), sine oculis homeobox homolog 6 (SIX6) and LIM HOX gene 2 (LHX2) genes are being expressed [66]. As the differentiation proceeds cells typically retain PAX6 and SIX3 expression [100, 66] and increase the expression of RAX and OTX2 [100]. Also expression of MITF, a factor crucial for initiation of melanogenesis and maintenance of RPE cell identity, can be observed [104]. In the developmental point representing optic cup phase, in which the developing structure consists of mixed cell population, both neural and RPE markers are present [100, 104, 74, 66]. The expression of CHX10, a gene required in generation of bipolar cells in neural retina, can be observed in addition to the previously mentioned markers [47, 104]. At this point the fate of progenitor cells is determined by interplay between CHX10 and MITF [104]. PAX6 plays role in initiation of pigmentation however, as the cell culture further differentiates, expression decreases leading to absence in the mature RPE [104, 49].

A differentiated RPE epithelium is characterized by expression of mature RPE cell markers such as CRALBP gene and PEDF gene, premelanosome protein (PMEL) gene and tyrosinase [100]. In addition expression of MITF and Bestrophin is retained. [100, 66, 104] Also mature RPE marker RPE65 is expressed [100, 74, 66].

On the other hand, if cells differentiate towards neural lineage expression of RAX typically retain together with CHX10 [100, 47]. In addition cone-rod homeobox can be observed [74, 66]. Also recoverin and opsin are mature neural markers indicating the presence of differentiated photoreceptors [66]. During the process of

transdifferentiation, cells typically retain expression of specific RPE markers such as MITF, PAX6 and PMEL in the culture [104].

In protein expression of differentiated RPE cells early markers such as MITF and PAX6 proteins can be observed. Furthermore mature RPE markers, such as tight junction protein zonula occludens 1 (ZO-1), RPE65 protein, CRALBP and Bestrophin protein, can be observed [100, 40]. Typically in a mature RPE cell Bestrophin, CRALBP, and ZO-1 are located on the cellular membrane while MITF is typically located in nucleus [100].

6. SUBSTRATES FOR RPE TRANSPLANTATION

6.1. Introduction to scaffold materials

RPE cell cultures have been studied on various types of natural and synthetic substrates with differing results. In order to mimic the original RPE selection of a structure already existing in the nature provides a very straightforward approach often leading to superior biocompatibility. A few examples include human amniotic membrane, human lens capsule, and Bruch's membrane. These membranes and tissues can be isolated from the donor tissue and treated to remove harmful cellular components. The major problems concerning this approach are donor shortage and disease delivery [39].

Another approach in scaffold production is the use of nature-based polymers which to date have already been widely investigated in the eye [39]. These proteins include the main ECM proteins: type I and IV collagens and the collagen derivative gelatine. Also commercial Matrigel™, laminin, vitronectin, fibrin and a few different oligopeptides and aminoacid sequences have been studied. In addition a few polysaccharides such as chitosan, hyaluronic acid (HA) and alginate are suggested to have potential as growth substrata. [60, 39] Natural polymers outmatch synthetic materials in some aspects. As they are natural constituents of cellular environment they are better tolerated immunologically and have natural tendency to enhance cell adhesiveness. Natural materials also exit body through normal metabolic pathways. [64, 101] However, a few disadvantages also exist. As being complex in structure it is challenging to control the consistency of the naturally derived product and the mechanical properties of the resulting scaffolds. Concerns also exist regarding the purity of animal-derived materials, disease delivery and patient allergies of some components. [39]

Synthetic polymers are extensively used in various tissue engineering applications outmatching natural materials in some aspects. Even though they are not natural components from the body their advantages lay in properties such as microstructure, strength, degradation, permeability and processability which can be efficiently modified. [101] Additional advantage that can be gained by using synthetic materials is that possible disease delivery can be eliminated. Both non-degradable and degradable synthetic polymers exist and can be chosen for intended application. [39] In addition incorporation of bioactive ligands, such as integrin binding peptide arginine-glycine-aspartic acid (RGD) and HA [55, 68], have been investigated. Many synthetic polymers have potential to function as RPE vehicles. The use of poly-α-esters such as

poly(lactic acid) (PLA), poly(glycolic acid) and their copolymers, polyanhydrides, polyorthoesters and polycaprolactones has been extensive in tissue engineering applications since they fulfill most of the requirements that has been set for a RPE scaffold. [56, 60, 39] Also two experiments have been reported of utilizing poly(hydroxybutyrate-*co*-valerate) (PHBV) copolymer and PHBV/PLGA blend as substrate for RPE cells [90, 91]. Studies concerning poly(methacrylamide-*co*-methacrylic acid) (PMMA) properties and RPE cell culture have also been carried out [84, 7]. Other synthetic substrates showing potential are commercial Purecoat™ amine and carboxyl surfaces which have supported human adipogenic stem cell (hASC) and human mesenchymal stem cell (hMSC) differentiation into adipogenic and osteogenic lineages [76].

By utilizing different hydrogels, for example polyethylene glycol (PEG), three-dimensional matrixes can be created. Hydrogel is a highly hydrophilic network of polymer chains with natural or synthetic origin. Characteristic for a hydrogel is ability to hold large amount of water which result in high degree of flexibility. Main advantages are their multidimensionality and their ability to structurally and functionally respond to cellular environment. Hydrogels are considered to be applicable in several fields of biomedical engineering including contact lenses and controlled drug delivery and to date increasingly as cell culture substrates, especially in creating endothelial layers. [50] Production of hydrogel copolymers is carried out by cross-linking two co-monomer units. Co-monomer structure and concentration together with amount of cross-links in the material affects properties such as mechanical strength and swelling ratio. [7, 50] In addition hydrogel degradability can be directed by incorporation of hydrophilic or hydrophobic units. Furthermore by incorporation of biological cues cell-substrate interactions can be enhanced. However, the nature of the physical cross-linking limits their mechanical properties, such as network elasticity and mechanotransduction, limiting the ability to carry physiologically relevant loads. Moreover, incorporation of responsive units may result in high complexity which in turn can lead to unpredicted local changes in material. [50]

6.1.1. Requirements for ideal scaffold material for RPE transplantation

Scaffolds can be defined as follows: structures utilized to guide repairing and re-establishing of damaged tissue by providing structural support and aid in cell delivery. In addition, scaffold should direct cell behavior and able delivery of drugs or trophic molecules [39]. Effect of material on tissue is a sum of numerous chemical, physical and biological factors and varies depending on the degradation phase. Since scaffold material faces complex extracellular environment when transplanted, specific requirements must be met. [68]

Most important requirement is biocompatibility defined as follows: the ability of a material to perform with an appropriate host response in a specific application. In short, this includes non-toxicity, proper mechanical properties and enabling the

appropriate specific cellular activities and structures. Each following aspect falls under definition of proper biocompatibility. [68, 58]

Biomaterial must not induce sustained inflammatory or toxic responses in the host that can lead to local implant rejection. This includes also degradation products which should be naturally metabolized and cleared from the body. In addition biomaterial must promote structures and functions exhibited by RPE cells *in vivo*, such as regular epithelial monolayer, functional tight junctions, apical microvilli and phagocytosis of photoreceptor outer segments. [68, 58, 89, 52, 60]

Biomaterial should also support the RPE cell attachment, proliferation and differentiation on the surface [90]. The RPE cells are anchorage-dependent and require a supportive structure in order to proliferate and differentiate towards mature RPE [20, 90]. To achieve this, material should guide cell orientation and organization into monolayer with distinct apical and basal RPE characteristics [90, 52, 58]. After differentiation of the cells the biomaterial must be able to maintain the differentiated functions. [60, 89] Biomaterial should prevent any changes in the shape of neural retina and support the diffusion of nutrients. [90, 89]

Biomaterial should be effortlessly processed into a film structure with thickness [60] similar to original Bruch's membrane [58]. Other important factors are the surface chemistry and topography affecting the type and strength of interactions taking place between the biomaterial, cells and surrounding ECM. Topography affects the contact area between the cell and the substrate. When the optimum topography is achieved the cell adopts the form complementary to the surface profile achieving maximum contact area. Both factors also affect to adsorption of proteins. Surface roughness preferences vary between different cell types and it is suggested that RPE cells are more comfortable on smooth surfaces. [90]

Finally, proper degradation time is also important requirement. Through accumulation of degradation products into the tissue, the rate of degradation may affect cell behavior, structural regeneration and induction of rejection reactions. After implantation the biomaterial degradation must take place same pace as the regenerated RPE monolayer reconnects with Bruch's membrane. [60]

6.2. Natural substrates for RPE transplantation

6.2.1. Collagens

Different subtypes of collagen are the most abundant proteins in the human body with over 22 different collagen types discovered to date. Types I-IV are found in largest quantities acting as principal components of skin and other musculoskeletal tissues. Type I collagen is the most plentiful and most studied protein to date. [68] Due to its high strength provided by its fibrous structure it is present in structures such as the skin, tendon and bone that have to tolerate high forces [58, 27]. Type IV collagen in turn forms a loose fibrillar network with greatly specialized structure that interacts with

tissues affecting cell migration, attachment and differentiation [27, 46]. Different from other collagens type IV forms major constituent of basement membranes [29].

The primary, secondary, tertiary and quaternary structures of collagen (Figure 6.1) give rise to its unique physiological characteristics. The primary structure consists of amino acid chain. After synthesis the chain goes through modifications depending on its ultimate location in the body. [68] The amino acid chain then forms helical secondary structure which is followed by arrangement of three secondary structures into triple helical tertiary structure. Finally, tertiary structures self-assemble to fibrils after secretion into extracellular space. Fibrils have distinct periodicity and are further organized into fibers. [27] The orientation of the fibrils varies depending on the tissue and thus giving them the appropriate mechanical strength [68]. Also the length of the helix differs between various types and the size and nature of the portions outside the helical structure are not equal [27].

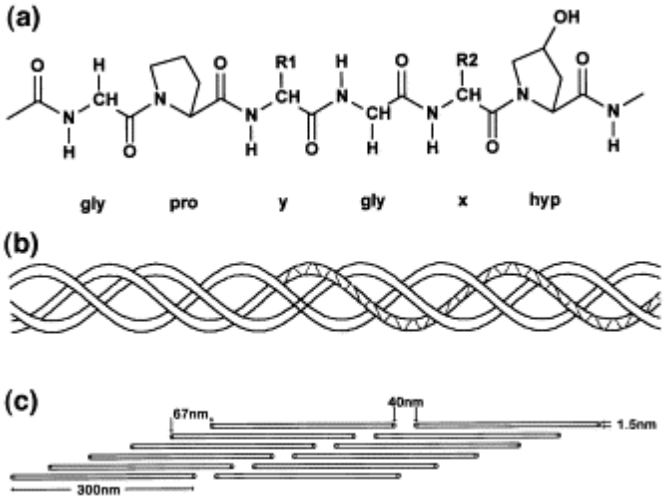

Figure 6.1 *Primary, secondary, tertiary and quaternary structures of collagen [27].*

Collagen degradation *in vivo* takes place enzymatically due to enzymes such as collagenases and metalloproteinases. The degradation rate is dependent on collagen type and can be scarcely controlled using enzymatic pre-treatment or cross-linking. For example, degradation of non-crosslinked collagen occurs within 2-7 weeks. Collagen can be easily processed into various shapes including sheets, sponges, foams, tubes, powders and injectable viscous solutions due to its solubility in acidic aqueous solutions. [68]

The major advantage of collagens is that by being natural components of ECM they provide a natural substrate for cell attachment, proliferation and differentiation [68]. Therefore numerous studies have been reported as its use in different biomedical applications such as implants, wound dressings, drug delivery systems and, in increasing amounts, as scaffold material [68, 58, 97, 38, 49, 13]. As a major

shortcoming with collagens alterations in physical and chemical properties bring uncertainty in material behavior. Other drawbacks are relatively high cost and mild immunogenicity varying greatly between different sources. [68] Collagen with bovine, porcine and sheep origin has been studied most but also sources such as human placenta and recombinant human collagen have been exploited [27].

Lu et al. have studied extensively different substrata for culture and transplantation of RPE cells. In an early study thin solvent casted type I collagen films (2.4±0.2 µm) with Teflon tape support were prepared and compared with native Bruch's membrane in order to assess the properties of the films and their performance with ARPE-19 cell culture. In addition, films were cross-linked via UV-radiation. The viability studies indicated that prepared collagen membranes could support nutrient flow across the RPE membrane up to 15 hours sufficiently maintaining RPE cell culture. ARPE-19 cells in medium containing FBS attached readily, reached confluency and formed a monolayer with cobblestone-like morphology and intercellular tight junctions. Phagocytosis assay was performed indicating the ability of ARPE-19 cells to phagozytise rod photoreceptor outer segments. Lu et al. suggested that results demonstrate high potential of type I collagen to function as RPE scaffold and future research could be focused on creating a full model of outer retinal membrane including capillary network. [58]

Thumann et al. studied ARPE-19 cell culture on thin (7 µm) type I collagen membranes with aim to assess the membrane biocompatibility and cell behavior. After reaching confluency cells were examined for morphology, characteristics of differentiation and viability using immunohistochemistry and phagocytosis assay. Degradation rate and long-term biocompatibility *in vivo* were determined by 24-week subconjunctival and subretinal implantation of cell-free films in rabbits. As a result ARPE-19 cells, seeded in medium containing FBS, adhered and proliferated readily into a monolayer of cells, possessed phagocytic ability and expressed RPE65 protein. Biocompatibility of the transplanted membranes was found excellent without any signs of inflammation or rejection. The collagen films remained stable for 10 weeks and degraded totally in 24 weeks. Study indicates that studied collagen membranes show potential as a vehicle and support for RPE cells. [97]

Type IV collagen has also been studied for RPE cell cultures however no clear transplant studies has been carried out. In an early study by Ho and Del Priore adult RPE cells harvested from human were seeded in medium containing FBS on RPE-derived ECM and Bruch's membrane with or without type IV collagen coating. As a result cells adhered more readily on type IV collagen coated substrates. [38] Klimanskaya et al. and Vaajasaari et al. have given their efforts on obtaining a consistent differentiation of hESCs towards RPE cells using type IV collagen coating in serum-free conditions with promising results [49, 100]. On the other hand, study by Braam et al. indicated low binding of HUES1 RPE cells to type IV collagen coating when defined medium supplements were used [13].

6.2.2. Laminins

The laminins form a large family of heterotrimeric ECM glycoproteins abundant mainly in basement membranes but also existing in the other parts of the body. In retinal environment laminins are produced by glial and RPE cells. [3] Since laminins take part in many interactions between RPE cells and surrounding ECM interest has raised in utilizing them as RPE cell culture substrates [105, 49].

Laminins consist of α, β, and γ chains with humans being able to produce five different α chains and three γ chains. These chains can combine to form at least 15 different laminins with different biological activity. [3] Their principal function is to affect the morphogenesis of tissue by interacting with surface receptors such as integrins initiating intracellular events that influence on cellular organization and differentiation [99, 98]. These interactions are enabled by binding sites that vary between different laminin forms. [99]

As first experiment with animal-derived cells, Ward et al. carried out an *in vitro* study concerning the maturation of porcine RPE cells in medium containing FBS on different substrates. The substrates used included Matrigel™ in different dilutions (1:2, 1:3, 1:4 and 1:5) and laminin with different concentrations (2.5 μg/cm^2, 5.0 μg/cm^2 and 15.0 μg/cm^2). Ward et al. discovered that the cultures on 5.0 μg/cm^2 laminin displayed most well-differentiated epithelial-like morphology with cells forming tightly packed cobblestone-like monolayer with junctional complexes and microvilli typical for RPE layer *in vivo*. Tight junction protein ZO-1 was present with strong staining pattern. Furthermore, pigmentation was increased compared to cells cultured on Matrigel™. These results indicate that the laminin matrix supports maturation of RPE cells. [105]

In an early study by Tezel & Del Priore the attachment of adult human RPE cells was assessed on laminin-coated plastic culture dishes. As a result these culture dishes supported RPE cell attachment in medium containing FBS compared to the uncoated ones and showed lower apoptosis. However, the collagen coatings studied in the same study slightly outmatched laminin ones. [92]

Recently Klimanskaya et al. have, in addition with type I and IV collagens, studied the laminin coating as a differentiation substrata for hESC towards RPE cells in serum-free conditions [49]. In addition Ho and Del Priore discovered that laminin coating on RPE-derived ECM and Bruch's membrane supported human RPE cell attachment compared to uncoated ones however in the presence of FBS [38]. Laminin has also been used extensively as a supporting matrix for attachment of hESC-derived neuronal cells [6].

6.2.3. Chitosan

Chitosan is a biodegradable polycationic polysaccharide obtained through deacetylation from chitin which is the main structural component of the exoskeleton of crustaceans [80]. Wide use in wound healing applications as drug delivery vehicle has raised interest

in use also as scaffold material for tissue-engineered constructs. Chitosan has also been approved by US Food and Drug Administration (FDA) for use as food additive. [68]

Chitosan has similarities with glycosaminoglycans (GAGs) present in the human body. Structurally chitosan is a linear polysaccharide with its chain consisting of β-(1-4) linked D-glucosamine. Degree of deacetylation is determined by the percentage of randomly located N-acetylglucosamine groups on the polymer backbone. [68] The structure of chitosan is presented in Figure 6.2.

Chitosan is highly biocompatible and non-toxic however it possesses high sensitivity for pH alterations. [80, 68] Chitosan is positively charged and dissolves easily in aquous solutions. This enables it to interact with negatively charged polymers, macromolecules and polyanions in an aqueous environment. [80]

In vivo chitosan is degraded enzymatically mainly by lysozymes. Degradation occurs through the hydrolysis of the acetylated residues. The factors affecting degradation rate are the degree of acetylation and crystallinity of the polymer. The high degree of deacetylation results in low degradation rate and may last several months *in vivo*. Physiological pH (7.4) is not optimal environment for chitosan degradation which limits its uses. In addition the fast adsorption of water leading to high swelling may rule out even more applications. [80]

Chitosan can be easily processed into different forms such as gels, particles and microspheres mainly due to its aqueous solubility. In addition, highly reactive amino groups present in the polymer chain enable chemical and biological functionalization. This way degradation rate and solubility can be remarkably altered which has made possible the development of numerous chitosan derivatives. [80, 68]

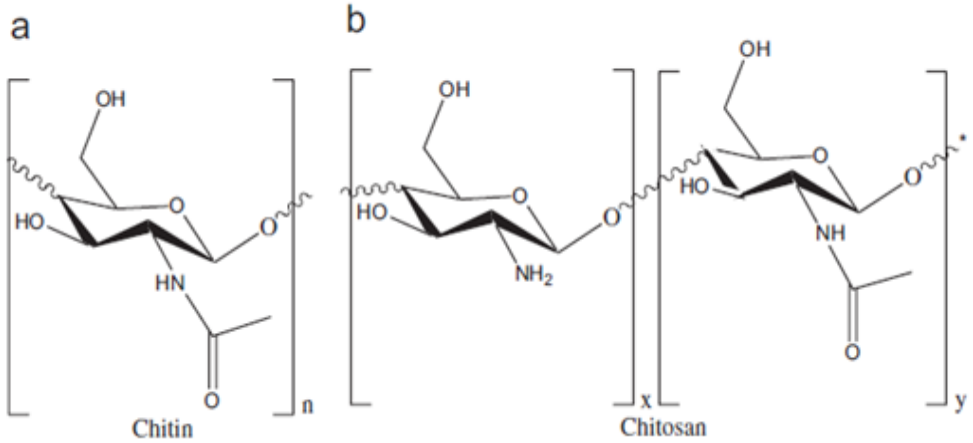

Figure 6.2 *The structure of chitosan [68].*

To date no study exists combining chitosan and RPE cells however promising results on hESC attachment on chitosan hydrogel have been reported. Doran et al. have developed method for presenting proteins and peptides on temporally stable self-assembled surface of chitosan. Protein deposition was found to be over 50%. hESCs were seeded in serum-free commercial StemPro® medium on generated surface and attachment was observed

for two hours. Surface was found to support attachment even though serum-free medium was used. This study provides two important results: first, it indicates chitosan's potential to support stem cell culture and second, it enables stem cell culturing in serum-free conditions necessary for use in clinical applications. [22]

6.2.4. Matrigel™

Commercial Matrigel Basement Membrane Matrix (Matrigel™) (BD Biosciences) is a widely used basement membrane equivalent for epithelial cell cultures. It has been utilized in many studies concerning three-dimensional cell cultures and in different assays concerning cell migration and invasion, drug metabolism and *in vitro* and *in vivo* angiogenesis. [72]

Matrigel™ is extracted from Engelbreth-Holm-Swarm mouse sarcoma which is a tumor rich in ECM proteins. Major components include laminin, collagen IV, heparin sulfate proteoglycans and entactin. Also various GFs are present including transforming growth factor-β, epidermal growth factor, insulin-like growth factor, FGF, tissue plasminogen activator and others naturally occurring in particular tumor. [72]

Material has shown to enhance cell attachment and differentiation on both normal and transformed anchorage dependent epithelial cells [72, 105]. Vugler et al. studied the phenotypical and genotypical changes of hESC RPE cells on growth factor-reduced Matrigel™. During the culturing period cells attached, proliferated to confluency and reached maturity on the substrate. [104] In addition, Gong et al. have studied effects of ECM and neighbouring cells on induction of hESC into retinal or RPE progenitors. In the study Matrigel™ was used as cell culture platform. [31]

6.2.5. Bioactive ligands

RGD is one of the most commonly utilized bioactive ligands originally present in fibronectin as an independent cell attachment site. By binding to cell-surface receptor integrin it creates connection between ECM and cytoskeleton. Extensive research exists concerning its use to improve cell attachment and organization in tissue engineering applications. [55]

Zhou et al. have incorporated RGDs into three-dimensional nanofibrous hydrogel scaffold for anchorage-dependent cells. Fabrication was carried out through self-assembly of two short peptide components: aromatic fluorenylmethoxycarbonyl-diphenylalanine and RGD. In this application RGDs had influence on the system as both structural and biological factor. The generated structure included cylindrical nanofibres interwoven within the hydrogel with the presence of RGDs on the fibre surfaces. As result, both materials were found to support adhesion of encapsulated dermal fibroblasts (in the presence of fetal calf serum) via specific integrin-RGD binding. Cells were found to spread and proliferate readily. Therefore, it offers a model for three-dimensional culture of anchorage dependent cells *in vitro*. [110]

Glycans are carbohydrate units of glycoproteins, glycolipids, and proteoglycans. By linking to the cell surface proteins and lipids on the extracellular side of the cells they form a dense, negatively charged layer called glykocalyx. The primary function of glycocalyx is to enable the communication between cell and the environment including cell-to-cell contacts and interactions with ECM components. Through their specific molecular structures they carry great amounts of biological data concerning cellular attachment. It is suggested that since glycans are abundant components on the cell surface, reagents that specifically recognize hESC glycans should be useful tools for identification, isolation and manipulation of stem cells. [82]

Satomaa et al. have studied asparagines-linked glycoprotein glycans (N-glycans) of hESCs and their differentiated progeny using mass spectrometric and NMR spectroscopic profiling. N-glycans functions in controlling protein folding and transportation. The N-glycan phenotype of hESCs was shown to reflect their differentiation stage. During differentiation hESC-associated N-glycan features were replaced by differentiated cell-associated structures. The results indicated that hESC differentiation stage can be determined by direct analysis of the N-glycan profile. These results provide the first overview of the N-glycan profile of hESCs and form the basis for future strategies to target stem cell glycans. Lectins, on the other hand, are proteins that recognize glycans with specificity to certain glycan structures. It is suggested that biocompatible lectins could provide specific differentiation platform for hESCs towards desired phenotype. [82]

HA was isolated from vitreous humor of the eye in 1934 by Meyer and Palmer. HA is present in high amounts in synovial fluid and vitreous humor affecting largely in the viscoelastic properties of surrounding tissues. Since HA plays part in controlling ECM metabolism and since it affects many biological processes including cell migration and differentiation during embryogenesis it has raised interest in many applications in biomedicine. [68]

HA is a linear polysaccharide belonging in the family of GAGs that are polymers consisting of alternating units of N-acetyl-D-glycosaminoglycan and glucuronic acid. However HA is not covalently bond to proteins which separates it from other GAGs. With molecular weights (MWs) up to several millions, HA is the largest GAG. [68]

HA is water soluble forming viscous solutions with unique viscoelastic properties. Typically in a solution HA forms three-dimensional structure which is enabled by extensive intramolecular hydrogen bonding. Structure of HA is presented in Figure 6.3. Due to its high functionality and charge density HA can be easily cross-linked with different methods. The degradation of HA occurs either enzymatically by lysozymes or by free radicals such as nitrix oxide. Enzymatic degradation results in mono- and disaccharides which enter to the Krebs cycle. [68]

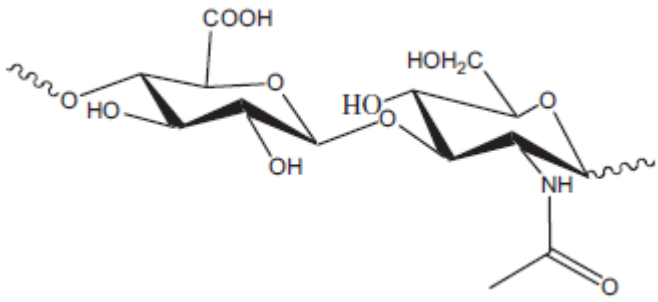

Figure 6.3. *The structure of HA. [68]*

Together with chitosan experiment Doran et al. tested hESC attachment on peptide-modified self-assembled HA hydrogel. Also with HA protein deposition was found to be over 50%. hESCs were seeded in serum-free commercial StemPro® medium on generated surface and attachment was observed for two hours. Surface was found to support hESC attachment even though serum-free medium was used. As result HA hydrogel provides defined stem cell culture conditions possibly applicable for stem cell-based therapies. In addition it enables stem cell culturing in serum-free conditions necessary for use in clinical applications. [22]

6.2.6. Other natural materials

Several natural materials including fibrinogen and various natural membranes have been studied as substrates for RPE cell culturing [71, 73, 85, 96]. Fibrinogen is a protein functioning as primary component of blood clots and is typically cross-linked in the presence of thrombin to form a dense network. In an early study by Oganesian *et al.* cross-linked **fibrinogen** spheres were utilized as three-dimensional carrier system for subretinal transplantation of human fetal RPE cells. However after successful transplantation the cells were not well tolerated *in vivo* causing mild inflammatory response. [71]

In the early studies concerning RPE culture and transplantation natural membranes obtained from different parts of the body have been under investigation. Natural membranes would provide good biocompatibility due to their natural occurrence in the human body however the shortage of donors creates barrier for their large-scale use. [39] One alternative is **amniotic membrane** which is a thin tissue creating the walls of the amniotic sac found in the embryo. These natural membranes are easily obtained from Ceasarian sections. [73] Another studied membrane for RPE is **Bruch's membrane** [85]. Also **human lens capsule** is available for studies from cataract surgeries and has been studied for RPE substrates [92]. In addition **Descemet's membrane**, a thin layer in the cornea next to endothelial layer, has been studied by Thumann *et al*. [96].

A remarkably different approach is to use thin membranes harvested from **cryoprecipitates**, that is, preparations which are collected from fresh human plasma that has been frozen and thawed. The main advantage of cryoprecipitates is that they are

derived from patients's own blood. Farrokh-Siar *et al*. studied an isolated human fetal RPE cell sheet on cryoprecipitates obtained from anonymous blood donors. As a result cells attached readily on the substrate and formed monolayer, maintained their cuboidal morphology and phagocytized isolated rod outer segments indicating that cryoprecipitates have potential as RPE cell substrates. [25]

6.3. Synthetic substrates for retinal pigment epithelium transplantation

6.3.1. Poly(ethylene glycol)

PEG is a hydrophilic polymer widely investigated for biomedical applications including tissue-engineered scaffolds. To date main uses have been surface modification, bio-conjugation and drug delivery however interest has raised towards utilizing them as three-dimensional matrix for cell cultures. Despite the fact that PEG does not degrade naturally in the body it possess good biocompatibility mainly due to biologically inert, non-adhesive chains. Additional properties beneficial in biomedical applications are non-immunogenicity and resistance to protein adsorption. [111]

The basic structure of PEG is presented in Figure 6.4. PEG monomer includes two hydroxyl groups and can appear in linear and branched structures. Hydroxyl groups can be substituted with wide variety of different functional groups. The cross-linking of PEG enables manipulation of gel properties. [55] Typical cross-linking methods include radiation of PEG polymers and free radical polymerization of PEG acrylates [111].

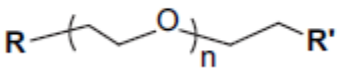

Figure 6.4 *The structure of PEG. [111]*

By incorporation of degradable segments such as different poly-α-esters PEG degradation can be modified. Introduction of bioactive ligands into naturally bio-inert PEG molecules could bring about principal ECM functions such as specific cell adhesion, proteolytic degradation and signal molecule binding [111]. These bioactive ligands include for example RGD and HA [33]. Despite the utilization of PEG as substrate for fibroblast, endothelial cell, chondrocyte, osteoblast, neural and stem cell cultures, no study of PEG with RPE cells exist. As a drawback anchorage-dependent cells encapsulated in PEG hydrogels have shown low viability. However additional knowledge must be gained on scaffold architecture and biological functions in order to reliably use PEG scaffolds in tissue engineering applications. [111]

6.3.2. Poly(D,L-lactic acid) and poly(D,L-lactic-*co*-glycolic acid)

PLAs are thermoplastic aliphatic polyesters derived from natural sources such as sugarcanes. Due to PLAs chirality they can obtain two optically active forms: L-lactic acid and D-lactic acid (Figure 6.5)**.** [68]. Polymerization of L-lactic acid monomers results in poly(L-lactic acid) (PLLA) while polymerization of D-lactic acid monomers creates poly(D-lactic acid). Furthermore when polymerizing both L-lactic acid and D-lactic acid monomers poly(D,L-lactic acid) is obtained. [62]

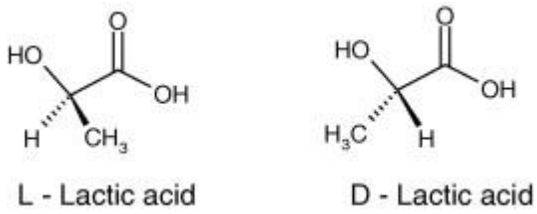

Figure 6.5 *The structures of lactic acid isomers. [34]*

PDLLA is amorphous polymer with glass transition temperature (T_g) around 60°C. Loss of strength takes place in 1-2 months when hydrolyzed. PDLLA degrades hydrolytically via bulk erosion mechanism. Degradation occurs through cracks in the ester backbone. [68] Degradation products are normal human metabolic by-products. These lactic acids are removed from body through respiratory and urinary systems. [95, 68] Due to rather fast degradation time it has been considered as potential candidate for drug delivery and low strength scaffold applications. [68]

When combining poly(D,L-lactic acid) with glycolic acid monomers PLGA is obtained [68]. The structure of PLGA is presented in Figure 6.6. PLGA has been under extensive research for different biomedical applications including sutures and controlled drug and protein delivery systems. To date extensive research also exists of its use as tissue-engineered scaffold. Despite the synthetic origin PLGA has shown to support cell adhesion and integration. [68, 30, 59, 93] An economically important factor is that both PLAs and PLGA have been approved by FDA for use in humans [30]. Additional benefit is good processability into wide variety of shapes [68].

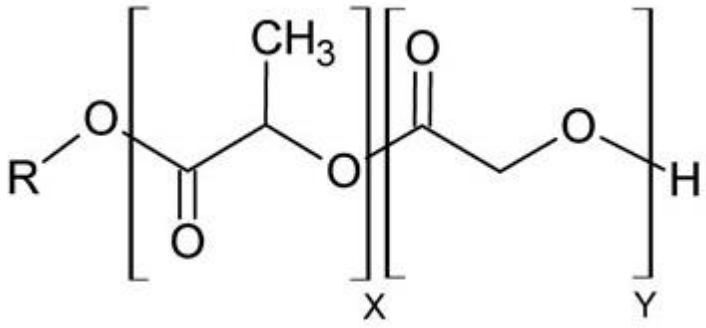

Figure 6.6 *The structure of PLGA polymer [11].*

Properties of PLGA, especially degradability can be tuned by altering the copolymer ratio. Increase in less hydrophobic glycolide content results in faster hydrolysis due to higher penetration of water. [60, 59] For example: PLGA with 50% lactic acid and 50% glycolic acid degrades in 1-2 months whereas PLGA 75:25 degrades in 4-5 months [68]. A factor playing part in PLGA degradation is autocatalytic effect, that is, accumulation of carboxylic groups in the center of material which leads to faster degradation. This phenomenon has more effect as the thickness of the specimen grows. [60, 59]

T_g of PLGA can be also extensively modified by altering the lactic acid content. Decrease in lactic acid content results in lower T_g. Typically PLGA possesses brittle characteristics since its T_g is above physiological temperature. [42] The degradation of PLGA occurs through same mechanism as with PLAs, that is, by cracking of ester bonds in the backbone. Other factors influencing the degradation rate are MW, size and shape of specimen and the surrounding environment. A major disadvantage with both PLAs and PLGA is development of acidic degradation products, lactic acid and glycolic acid, which can temporarily decrease the local pH of the tissue. Therefore the rate of degradation may have an effect on cell survival, tissue regeneration and drug release. [60, 68]

Early *in vitro* testing by Lu et al. and Thomson et al. has given valuable information about structural behavior, manufacturing conditions and optimization of shape and monomer ratio of PLGA. [59, 95] The typical processing method used extensively on studies is the solvent casting method resulting in flexible films with a smooth surface and controllable degradation rate [39]. In addition spheroid structures have been studied by Rezai et al. [81].

In a study by Thomson *et al*. films produced using solvent casting method out of high and low MW PLLA and PLGA (high and low MW 50:50 and high MW 75:25 copolymer ratios) were characterized for their thickness, surface morphology, porosity and flexibility. As result films with thickness of 12±3 µm was successfully obtained. Then fetal human RPE cells in medium containing FBS were cultured on high MW PLGA (75:25) films for eight days resulting in good attachment. [95] This is supported by study of Giordano et al. in which high MW 50:50 and 75:25 PLGA films outmatched other participants in cellular attachment and proliferation of human fetal RPE cells in medium containing FBS [30].

Further on, Lu et al studied PLGA (75:25) films *in vitro* as substrates for human D407 cell culture in medium containing FBS. Cell attachment, proliferation and phenotypic expression were assessed. During 7-day culturing period cells attached readily, proliferated to confluency and formed cobblestone-like morphology. [59]

In a recent *in vitro* study by Thomson et al. five blends of PLLA and PLGA (10:90, 25:75, 50:50, 75:25, and 90:10 blend ratio), manufactured by solid liquid phase separation technique, were evaluated as RPE cell substrates. Part of the samples was then coated with laminin in order to improve cellular attachment and seeded with ARPE-19 cells in medium containing FBS. Then cell attachment, viability and retention

of phenotype were determined. The cell phenotype of ARPE-19 cells remained constant with low cell death up to 4 weeks of culturing. Apoptotic cell death level was found to decrease during the culturing period. The study indicates that 25:75 blend could be most suitable for scaffold use in RPE cell transplantation. [93]

6.3.3. Poly(ε-caprolactone) and poly(L-lactic acid-*co*-ε-caprolactone)

Poly(ε-caprolactone) (PCL) is a synthetic semicrystalline poly-α-ester [68, 19]. When copolymerized with L-lactic acid PLCL is obtained [68, 43]. PCL and PLCL have been widely studied for use as tissue-engineered constructs mainly in vascular and bone regeneration but also in cardiac failures. However no study involving RPE cells has been carried out. [68, 102, 44, 143]

PCL and PLCL possess good biocompatibility [68, 43]. PCL has low melting point (55-60°C) and low T_g (-60°C) which brings elastic characteristics to the material. In addition PCL is soluble in most typical organic solvents which ease processing. Both PCL and PLCL degrade through breakage of aliphatic ester linkages which are prone to hydrolysis [68, 43]. Rate of PCL degradation, approximately 2-3 years, is rather low however can be accelerated remarkably by copolymerization with lactic acids. The rubbery characteristics of PCL allow high permeability. Despite the faster degradation of PLCL it has been found that applications of these copolymers have been limited due to poor mechanical properties. [68]

In the field of tissue engineering the main use of PCL has been in bone repair [68, 102, 19]. In one of these applications PCL has been reinforced with phosphate glass fibres for use as fixation pins for fractures and in craniofacial repair as tissue engineered constructs [19]. In an early study by Coombes et al. a precipitation-casted microporous PCL matrix with hydroxyapatite and inulin polysaccharide was studied for degradation behavior and cell interaction with primary human osteoblasts. As result PCL matrixes showed potential as particle-releasing cell culture substrates. [19] Jeong et al. have reported excellent biocompatibility of PLCL (50:50) scaffolds with smooth muscle cells [43] Vergroesen et al. had encouraging results with PLCL as scaffold for hASC differentiation which after seeding attached readily, proliferated and differentiated into osteogenic phenotype [102]. PLCL has also been utilized as scaffold for hMSC cells with the intention of use in cardiac tissue regeneration [44].

6.3.4. Poly(methacrylamide-*co*-metharylic acid)

In a study by Singh et al. adult human and porcine RPE cells were cultured on non-biodegrable PMMA hydrogel in presence of FBS. Both methacrylamide and methacrylic acid monomers are found to be biocompatible and anti-immunogenic. Methacrylamide creates the hydrophilic part of the hydrogel. Ethylene glycol dimethacrylate was utilized as cross-linking agent. At first microporous and elastic films with approximate thickness of 25 µm and water content of 60% were manufactured. Films were then coated with poly-D-lysine and fibronectin. As both being natural ECM

factors aim was to enhance cellular attachment and proliferation. Poly-D-lysine coating was carried out in order to increase net positive charge on the film which would provide stronger electrostatic interactions between the film and cell membranes. Fibronectin coating in turn was carried out to improve cellular attachment and proliferation. The materials were seeded with either adult human RPE or porcine RPE and after reaching confluency the cell density and viability were determined. Both cell types attached and proliferated on hydrogel surface within 24 hours and in a few days formed a cell monolayer with characteristic polygonal morphology. The calculated viabilities of cells were around 90%. The study demonstrated that PMMA show potential as RPE cell culture substrate. [84]

6.3.5. Other synthetic materials

PHBV belongs to a group of bacterial polyesters, polyhydroxyalkanoates (PHAs). Due to good biocompatibility PHAs are under extensive research as tissue engineering constructs and drug delivery vehicles. Single PHB is relatively hard and brittle but more flexibility is gained by copolymerization with hydroxyvalerate (HV). PHBV degrades through hydrolytic surface erosion into D-3-hydroxybutyrate which is a normal constituent of blood. [90, 79] PHBV polyesters appear with 60-80% crystallinity and are therefore considered semicrystalline. PHBV polymers are also soluble in a number of organic solvents of which chloroform and dichloromethane have been most commonly used. [79]

In an early study Tezcaner et *al*. studied PHBV as substrate for D407 cell culture. Surfaces were oxygen plasma-treated applying different power and duration with the aim of rendering them more hydrophilic. Then effect of treatment on cell attachment, proliferation and morphology was assessed in a 7-day test. As result the PHBV film treated 10 min with 100 W was found to be the most suitable for re-attachment and proliferation of D407 cells. Cells reached confluency and formed a monolayer however in presence of FBS. [90]

Commercial **BD Purecoat™ amine and carboxyl** surfaces could be one alternative for RPE cell culture since they have been shown to support growth, expansion and differentiation of hASC and hMSC in serum-free conditions. Surfaces are chemically well-defined and xeno-free therefore ruling out the possible disease delivery and rejection reactions. Partridge et al. studied bone-marrow-derived hMSCs and adipose-derived hASC on amine surface with standard tissue culture treated vessels as controls. Cells reached confluency faster compared with standard surface and showed surface marker expression characteristic to hASC and hMSC cells. [76]

7. IMAGE ANALYSIS – STATE OF ART

The use of digital image processing provides advantages compared to traditional microscopy such as fast and automated analysis, efficient storage and reduction in technician-based errors. Recent advances in digital imaging have also speeded the development in automated analysis of cell properties from microscopic images, a field known as image cytometry. Due to large amount of data manual image analysis is found to be impractical [54].

Early studies from several groups have assessed the use of computer assisted image analysis for cell size and shape determination [53, 17, 108, 103, 63, 32]. Research has mainly been concerning phase contrast microscopic images of human corneal endothelium. Pioneer on this field has been Laing et al. trying to solve the problem of edge detection [53]. Cazuguel et al. have applied more sophisticated methods such as histogram equalization and top-hat filtering [17]. In addition Yu et al. have used techniques such as low pass filtering and matched filters [108]. However, cell boundary distinguishing in grey level images has been the main problem and none of these attempts have been successful. Also the diversity of initial images creates a challenge. Variance in contrast, noise level and lightning conditions between images makes automated process difficult. [103, 54]

Luc Vincent has made efforts on automated analysis of corneal endothelium cells. Vincent has developed an accurate method for segmenting grayscale images. First, extraction of corneal markers is carried out using dome extractor based on morphological grayscale reconstruction. Second, binary images of corneal cell network are obtained via marker-driven watershed segmentation. Histograms of cell sizes and number of neighbours are then created from the obtained images providing information on corneal condition. In addition a neighborhood graph is created and granulometric assay performed providing more detailed information on distribution of cells. Following these steps a model for corneal cell death was developed which, compared to experimental results, provided reliable outcome. Model enables estimation of amount of dead cells in examined tissue. [103]

Another study by Malpica et al. deals with segmentation of clustered nuclei applying watershed algorithms. The developed algorithm provides a tool that can be used for implementation of both gradient and domain-based algorithms which have been typical approaches in automatic segmentation. When applying this algorithm to peripheral blood and bone marrow samples, a high percentage (90%) of test clusters was correctly segmented. [63]

Gonzalez has taken a step further in his master's thesis which proposes automated system for image analysis and representation of cell morphology. Aim of the thesis was to build a feasible and user-friendly cell recognition system that would carry out the morphology analysis including segmentation, morphological data extraction, analysis and management. [32]

Several tools developed for automated image analysis exists including ImageJ, CellC, CellProfiler, and MCID Analysis. ImageJ is an open source Java-based image processing program. Basic tools for image enhancement, geometric operations, analysis and editing are included and most image file formats including TIFF, JPEG, BMP, GIF and "raw" can be operated. A major benefits are that ImageJ provides macro recording feature and enables development of own custom made plugins. Plug-ins created by users are free for downloading from the public domain and also exploited in this study. [2] ImageJ has been used by Lehmussola et al. in order to validate their simulation platform developed for generating synthetic images of fluorescence stained cell populations [54].

EXPERIMENTAL PART

8. MATERIALS AND METHODS

8.1. Overview

The materials chosen for this study included both natural-origin and synthetically fabricated materials. Each material, their origin, manufacturer and developmental status are presented in Table 8.1. In addition the hESC line used and culturing phase are mentioned. The practical work in this study was divided in two distinct phases (named phase I and phase II) in order to share the workload. The phase I included 14 synthetic materials of which Purecoat™ amine and carboxyl surfaces are commercially available yet each BioMade™ Gelators are still in developmental phase. The phase II included 3 synthetic materials of which PLGA, PDLLA and PLCL are commercially available. The total amount of natural materials was five including chitosan, type I collagen, type IV collagen, Matrigel™ and Substrate X of which all are commercially available excluding Substrate X which is still under development. Due to previous positive experiences type IV collagen was selected as control substrate in both phases and with both cell lines [100]. Hence phase II control substrates are titled as type IV collagen (08/017) and type IV collagen (08/023). Raw materials, equipment and premises for processing of PLGA, PDLLA and PLCL membranes and chitosan coatings were provided by TUT Department of Biomedical Engineering. Each of these materials was processed by Olli Kurkela.

Table 8.1 *The materials studied in thesis.*

Material origin	Name	Manufacturer	Status	Used in phase	Cell line	Analysis performed
Natural	Chitosan (91% deacetylation)	FMC BioPolymer	Commercially available	II	08/017	RT-PCR
	Type I collagen	Sigma-Aldrich	Commercially available	II	08/023	RT-PCR, staining
	Type IV collagen	Sigma-Aldrich	Commercially available	I, II	08/023, 08/017	RT-PCR, staining
	BD Matrigel™ matrix	BD Biosciences	Commercially available	II	08/023	RT-PCR, staining
	Substrate X	Finnish Red Cross	Under testing	II	08/017	RT-PCR, staining
Synthetic	OG1	BioMaDe	Under testing	I	08/017	-
	OG2	BioMaDe	Under testing	I	08/017	-
	HA-modified OG2	BioMaDe	Under testing	I	08/017	RT-PCR
	OG13	BioMaDe	Under testing	I	08/017	RT-PCR
	OG25	BioMaDe	Under testing	I	08/017	RT-PCR
	HA-modified OG25	BioMaDe	Under testing	I	08/017	RT-PCR
	OG30	BioMaDe	Under testing	I	08/017	RT-PCR
	RGD-modified OG30	BioMaDe	Under testing	I	08/017	-
	OG34	BioMaDe	Under testing	I	08/017	RT-PCR
	OG49	BioMaDe	Under testing	I	08/017	RT-PCR
	HA-modified OG49	BioMaDe	Under testing	I	08/017	RT-PCR
	OG51	BioMaDe	Under testing	I	08/017	-
	Purecoat™ amine	BD Biosciences	Commercially available	I	08/017	RT-PCR
	Purecoat™ carboxyl	BD Biosciences	Commercially available	I	08/017	-
	Poly(D,L-lactic-*co*-glycolic acid) (75:25)	Purac Biomaterials	Commercially available	II	08/017	-
	Poly(D,L-lactide) (96:4)	Purac Biomaterials	Commercially available	II	08/017	RT-PCR
	Poly(L-lactide-*co*-ε-caprolactone) (70:30)	Purac Biomaterials	Commercially available	II	08/017	-

The schedule for practical work is presented in Figure 8.1. The phase I started by preparation of materials for cell seeding. During phase I each well was photographed after each medium change (5 images/well, 3 times/week) excluding materials that showed poor performance during the culturing period. At the end point of phase I cells were lysed and lysate stored for further use in total RNA extraction and reverse transcriptase polymerase chain reaction (RT-PCR) analysis. Before start point of phase II PDLLA, PLGA and PLCL membranes together with chitosan coatings were processed at TUT and together with rest of the materials prepared for cell seeding. In phase II each well was photographed weekly (3 images/well, excluding type I and IV collagens, Matrigel™ and Substrate X). During the phase II gene expression analysis of cells from phase I materials was carried out. At the end point of phase II part of the cells were lysed and lysates stored for further use in gene expression analysis. Four wells on type I and IV collagens, Matrigel™ and Substrate X were fixed and stored for further use in immunofluorescence labeling. Gene expression analysis and immunofluorescence study of phase II was then carried out and practical work period was over at day 105.

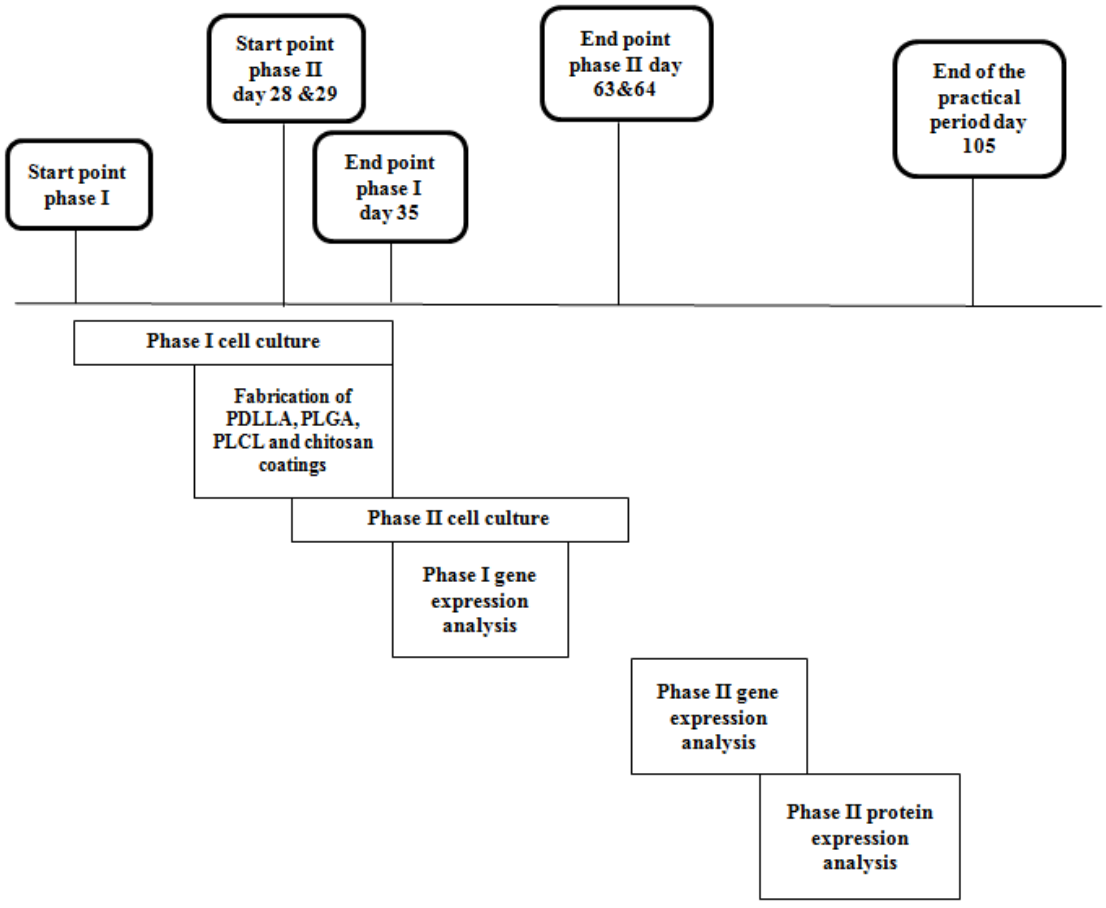

Figure 8.1*. The schedule of the practical work.*

8.2. Processing and preparation of materials for cell culture

8.2.1. Phase I materials

BioMade™ Gelators

Xeno-free BioMaDe™ Gelators included total of 12 materials. The materials were provided by Biomade Technology Foundation (Groningen, Netherlands). Materials were named as follows: OG1, OG2, OG13, OG25, OG30, OG34, OG49, and OG51. Modified versions of OG2, OG25 and OG49 with HA included in the structure were also provided together with modified version of OG30 with RGD included in the structure. Each BioMaDe™ Gelators are still under developmental phase. Structures of the materials are presented in Appendix 1. Materials were delivered on four 24-well cell culture plates each plate including two replicates of one type of material. Following delivery, the materials were stored (+4°C) for approximately two months. Condition of each plate was observed by eye and best two replicates of each material were selected for cell seeding. Selected plates were sterilized by UV-radiation (5 min) in laminar hood and washed once with Dulbecco's Phosphate Buffered Saline (DPBS) (Lonza Group Ltd, Biowhittaker, Basel, Switzerland). Eventually two of the delivered plates, titled plate A and plate B, were to be seeded with hESC RPE cells. During the first addition the cell culture medium turned from red to yellow indicating acidic conditions in some wells. Therefore DPBS wash was repeated in these wells in order to reach proper pH (7). Even though only best-conditioned replicates qualified for the cell culturing the condition of some materials were questionable since first medium change initiated tearing of surface.

Purecoat™ amine and carboxyl

BD Purecoat™ (BD Biosciences, Franklin Lakes, NJ, USA) surfaces included amine, a positively charged surface and carboxyl, a negatively charged surface. Surfaces are designed to improve overall culturing under serum-free or serum-reduced conditions, cell attachment and cell proliferation and enhance post-thaw recovery. Surface structures are xeno-free and well-defined, therefore potential for hESC RPE cell culturing. In addition surfaces do not interfere with imaging which is crucial for the study. [76] The conditions of plates at the beginning of culturing period were good. Wells were washed three times with DBPS prior to first medium addition. Two replicates on each plate were seeded with hESC RPE cells.

Type IV collagen

Type IV collagen (Sigma-Aldrich, St. Louis, MO, USA) from human placenta was the control material in both phase I and phase II. The coating protocol was similar in both

phases. Coatings with 5 µg of type IV collagen per cm^2 were prepared according to manufacturer's instructions on 24-well cell culture plates (Nunclon™, Sigma-Aldrich). Plates were placed in an incubator (+37°C) for approximately four hours. After incubation excess collagen was removed and wells were washed two times with DPBS.

8.2.2. Phase II materials

Numerous processing methods have been studied in manufacturing of polymer scaffolds for tissue engineering applications of which the most employed is solvent casting. [39] Another approach is use of compression molding technique. In this study these two methods are applied to for prepare chitosan coatings and PDLLA, PLGA and PLCL membranes. These two methods are briefly introduced in this chapter.

Solvent casting for preparing chitosan coatings

Solvent casting is practical and widely used method especially in biomaterial processing since it enables production of thin membrane structures or when insoluble porogens are used, a three-dimensional porous scaffold. Several scaffolds for subretinal transplantation have been manufactured utilizing solvent casting method mostly introducing PLGA as scaffold material [39, 60].

Solvent casting method includes polymer and organic solvent. Polymer is dissolved into solvent and shaped into desired geometrical form. Solvent evaporates creating desired structure. [39, 60] These solvents are toxic for living tissue and must be removed from the structure with the intention of use in medical applications. However, solvent casting method suits poorly for processing constructs with complex architecture and is typically utilized in manufacturing of thin polymer films. [39] Solvent casting method provides means to create smooth, homogenous surface on the bottom of the well as is required in this study. [39]

Protasan UP B 90/500 medical grade chitosan (FMC BioPolymer, New Jersey, USA) flakes with 91% acetylation grade were used to manufacture chitosan coatings. The lack of previous experience of applying solvent casting method to produce chitosan coatings obliged development of novel procedure. The principle of procedure is presented in Figure 8.2.

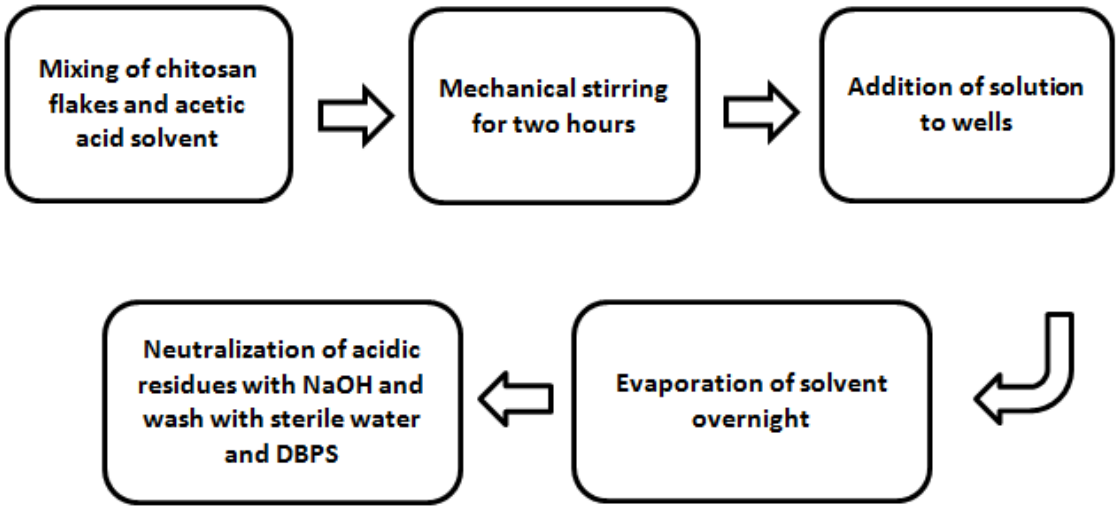

Figure 8.2. *The schematic figure of solvent casting method applied to produce chitosan coatings.*

First, the chitosan solution was prepared out of 0.75 g of chitosan flakes and 49.25 ml of de-ionized water. The mix was stirred mechanically for 2 hours. 0.75 ml of acetic acid was added and solution was left in ventilation hood to dissolve overnight. Next day 500 µl of chitosan solution was added to each well on a 24-well plate (Nunclon™, Sigma-Aldrich). Also four wells on another 24-well plate were coated. To assure thorough evaporation of acetic acid the plates were left to ventilation hood for two nights. Plates were sealed and delivered to Regea premises. After delivery, chitosan coatings were washed with sodium hydroxide (NaOH) (5 mol, 15 min) in order to neutralize acetic acid residues. Afterwards wells were washed with sterile water (15 times) to get rid of excess NaOH. However, after repeated sterile water wash the determined pH indicated alkaline conditions. Therefore DPBS wash was performed five times until proper pH (7) was confirmed.

Compression molding for preparing PDLLA, PLGA and PLCL membranes

Compression molding is a material processing technique typically used for compacting or sintering objects. The principal use is the production of large flat or moderately curved objects out of thermoset or thermoplastic polymers. Mano et al. have proposed compression molding as one alternative for scaffold production. [64] Pressure, heat, time and amount of material are main adjustable parameters. The principle of compression molding is following: raw material, typically in form of pellets, granules or sheets is placed in a mold with desired shape or structure. Molds with various shapes can be applied. The mold is placed between two heated platens and the pressure is applied. When applying the pressure heated material takes form of the mold. Thermoplastic materials are heated above their melting points, formed and cooled. [64] Compression molding equipment and conditions are presented in Figure 8.3.

In this study the aim was to create homogenous and smooth surface of particular biomaterial on the bottom of the well. hESC RPE cells were seeded and grown on these surfaces. Since the cell culture plates (Nunclon™, Sigma-Aldrich) planned to use in this study did not tolerate necessary solvents more suitable approach was to produce thin membranes by using compression molding method and place them on the bottom of wells. The equipment used in this study was Nike hydraulic arbor press with water circulated cooling and maximum compression value of 110 kN. The used molds were several identical metal plates with or without Teflon tape covering. The function of Teflon tape was to produce texture on material's surface to provide possible enhancement in attachment and proliferation of hESC RPE cells. Teflon tape also enables more trouble-free detachment of membrane from the mold. The material was placed between the metal plates, pre-heated and pressed. Various pre-heating times, pressure times and pressures were applied.

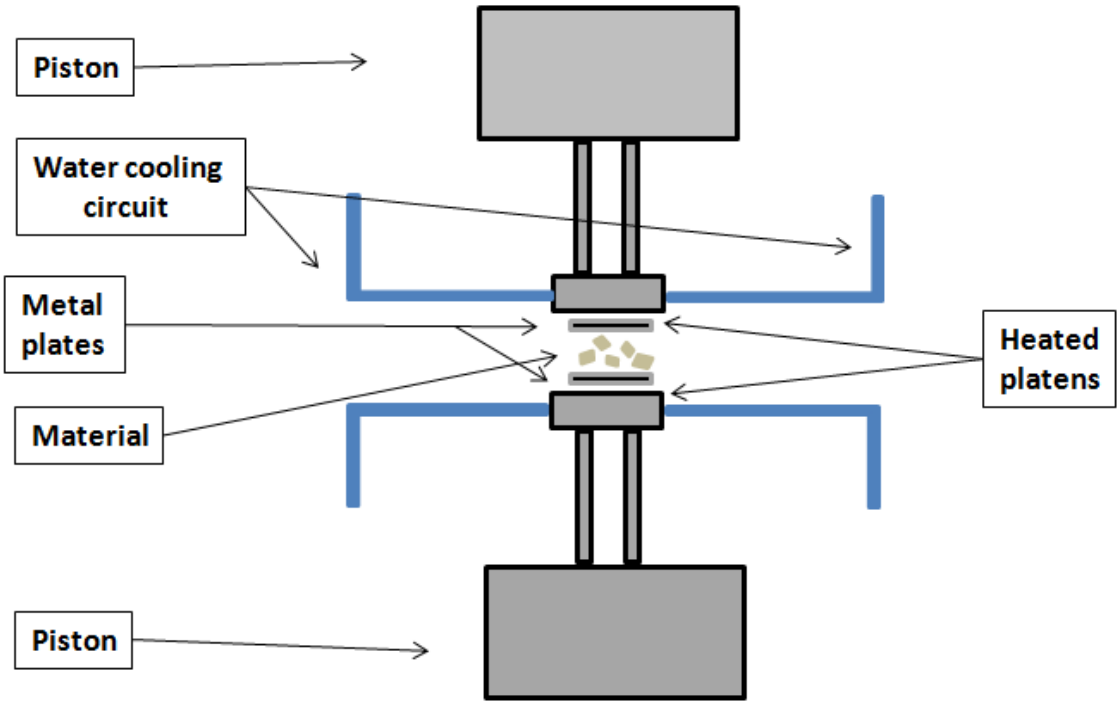

Figure 8.3 *Compression molding equipment and conditions.*

Purasorb® PLGA-granules (Purac Biomaterials, Gorinchem, Netherlands) with DL-lactide-glycolide ratio 75:25 were processed into thin membranes. The desired membrane structure was obtained by using compression molding method. Proper combination of parameters, these are, the amount of granules, pressure, time and temperature, had to be determined. Teflon tape was used on mold in order to provide textured surface and making the detachment of membranes easier from the molds. Possibly the texture could have enhancing effect on cellular behavior on the surface.

Membranes were de-attached from the moulds by heating slightly. In case the heating was not sufficient means to remove the membrane, 70% ethanol was used.

PDLLA membranes were processed from Purasorb® PDLLA granules (Purac Biomaterials, Gorinchem, Netherlands) with 96:4 D-lactide/L-lactide ratio. Similar compression molding method was utilized as with PLGA. Again suitable parameters had to be determined. Textured membrane was processed successfully but proper non-textured membrane was not obtained. Therefore a significantly thicker extrusion-made membrane was provided by TUT.

Granules of Purasorb™ PLC 7015 (Purac Biomaterials, Gorinchem, Netherlands) with L-lactide/E-caprolactone ratio of 70:30 were utilized to create thin membranes applying compression molding method as with PLGA and PDLLA. Again proper parameters had to be found. Both texture and non-texture membrane was obtained with appropriate thickness. Parameters used to obtain each membrane are presented in Table 8.2.

Table 8.2 *Parameters used in compression molding.*

Material	Amount (g)	T (°C)	P (MPa)	Time (s)	Teflon covering
PLGA	0.5	160	25	30	no
PLGA	1	170	25	30	yes
PDLLA	1	170	25	30	no
PLCL	1	120	25	30	no
PLCL	1	170	25	30	yes

Substrate X

Substrate X is a lectin with plant-origin. Since it is under developmental phase, limited amount of data concerning its structure and functions is available. Substrate X coatings were prepared according to manufacturer's instructions on a 24-well cell culture plate (Nunclon™, Sigma-Aldrich). Total six wells were coated to assure sufficient amount of cell material for gene and protein expression analysis. The stock solution was thawed overnight (+4°C). A total of 2280 µl of working solution (WS) was prepared with 1:6 ratio of stock and DPBS. 380 µl of WS were added to each well in order to obtain 28.6 µg of material per cm^2. Plates were stored overnight (+4°C) and washed next morning three times with DPBS.

Type I collagen

Type I collagen (Sigma-Aldrich, St. Louis, MO, USA) coatings with 5 µg per cm^2 were prepared according to manufacturer's instructions on 24-well cell culture plate. Plate

was placed in incubator (+37^{o}C) for approximately three hours. After incubation coatings were washed two times with DPBS.

Matrigel™

Growth factor-reduced Matrigel™ (BD Biosciences, Franklin Lakes, NJ, USA) coatings were prepared according to manufacturer's instructions on 24-well cell culture plate. A total of 250 µl of coating solution (1:30 ratio) was prepared for each well. Plate was incubated (+37°C) approximately two hours. After incubation wells were washed three times with DPBS.

8.3. Cell culture methods

8.3.1. Cell material

In this study two different hES cell lines were used: Regea 08/017 (46, XX) and Regea 08/023 (46, XY). Both cell lines have been derived from excess, early stage embryos. Early stage embryos are low quality surplus embryos donated by couples going through IVF treatments. Regea has approval from National Authority for Medicolegal Affairs Finland to do research with human embryos (Dnro 1426/32/300/05). Regea has also approval of the Ethics Committee of Pirkanmaa Hospital District to derive, culture and expand hESC lines from surplus embryos, which cannot be used in the infertility treatment of the donating couples. In addition Regea has approval to study hESC differentiation (R05116). Both cell lines are regularly characterized at Regea for assurance of pluripotent status, differentiation capacity and normal karyotype as described previously in [86]. The cell line used on each material are collected in Table 8.1. Differentiation of cells was carried out as described by Vaajasaari et al. [100]. The cells were grown as embryoid bodies (EB), that is, cell aggregates where the cells maintain differentiated RPE cell state. For both phases cells with different passages were pooled in order to ensure sufficient amount of cells. In addition cells had been differentiating as EBs for varying times (Table 8.3). EBs with long differentiation time were avoided to take into the study since that could result in poor cell aggregate degradation. EBs had been grown in a suspension in differentiation medium (RPE DM-). RPE DM- growth medium included Knockout™ D-MEM (Gibco, Invitrogen) supplemented with 15% Knockout™ Serum Replacement (Gibco, Invitrogen), 2 mM GlutaMAX™ -l Supplement (Gibco, Invitrogen), 1% MEM Non Essential Amino Acids (Camprex), 0.5% Penicillin/Streptomycin (Camprex) and 0.1 mM 2-mercaptoethanol (Gibco, Invitrogen).

Table 8.3 *Cells lines, their passages and time in differentiation before seeding.*

	Cell line	Passage	Time in differentiation (d)
Phase I	08/017	P20+5	246
		P27+2	112
		P33	98
Phase II	08/017	P27+4	141
		P33+2	127
		P38+3	89
	08/023	P29+5	109
		P30+3	100
		P31+3	70

8.3.2. Plating procedure and maintenance

Plating procedure was similar in both phase I and phase II however the number of EBs varied in each phase due to the different number of materials. In phase I and phase II plating procedure approximately 250 EBs (Regea 08/017 cell line) were collected into DPBS. However the type I and IV collagens, Matrigel™ and Substrate X were plated separately and for this procedure approximately 310 EBs (Regea 08/023 cell line) were collected into DPBS.

The EB structure was degraded with focus on pigmented areas by using 1x trypsin-ethylenediaminetetraacetic acid (EDTA) (Lonza Group Ltd) in DPBS. Before addition of trypsin EBs were washed once with DPBS. Detachment was enhanced with mechanical stirring with pipette every ten minutes. After one hour trypsin was inactivated by human serum (Paa Laboratories, Paschning, Austria) and solution was filtrated through 100 µm diameter Cell Strainer (BD Biosciences) in order to eliminate cell clumps. Cell suspension was centrifuged (400 g, 7 min) and supernatant was removed. Cells were re-suspended into 1 ml of RPE DM- medium. Cells were calculated with Neubauer Improved hemocytometer. Estimated cell count in phase I and phase II were 1.77 million cells and 4 million cells in total, respectively. With type I and type IV collagens, Matrigel™ and Substrate X the estimated cell count was 1.8 million cells in total. In the phase I each material was seeded with approximately 56 000 cells and in phase II with 100 000 cells. Total of 60 000 cells were seeded on each well on both type I and type IV collagens, Matrigel™ and Substrate X. The cells were seeded in 250 µl of DM- medium.

Cells were incubated in a humidified HeraCell 150 and 240 incubators (Thermo Electron Corporation, Thermo Fischer Scientific Inc., Walthan, MA, USA) at +37°C in 5% carbon dioxide atmosphere. Medium was changed three times a week. The amount of medium was increased from 0.5 ml to 1 ml during culture development. Fresh medium was prepared weekly. The condition of plates was inspected regularly before

and after each medium change both with stereomicroscope and phase contrast microscope. During imaging sessions plates were placed on a heated plate (+37°C).

8.4. Cell culture analysis methods

8.4.1. Cell attachment, proliferation and maturation monitoring

Cellular attachment, proliferation and maturation were observed using stereomicroscope (Nikon, SMZ800, Nikon Instruments Europe, B.V Amstelveen, Netherlands) and phase contrast microscope (Nikon Eclipse TE-2000s, Nikon Instruments). The initial amount of cells after first medium change indicated the level of attachment. The changes in number of cells during culturing period illustrated proliferation level of cells. Morphology change from attached round-shaped cells to cells with fibroblast-like morphology and finally to cobblestone-like, dense structure together with rise in pigmentation level marked cellular maturity. Typically before each medium change overall plate condition was inspected by eye before generating common concept of each well's condition with stereo microscope. After each medium change cellular condition was examined more carefully with phase contrast microscope.

In phase I each well was photographed regularly (5 images/well, 3 times a week) with the intention of providing enough image data for image analysis. As the cell culture samples had rather homogenous appearance number of images was reduced (3 images/well, once a week) in phase II. With type I and IV collagens (08/023), Matrigel™ and Substrate X only significant changes in cellular development were monitored since the materials were not included in the image analysis. Images were taken with 10x objective together with 10x ocular resulting in total magnification of 100x. Random images with 4x and 20x objective were taken to better illustrate cellular development. Image format was TIFF and images were taken with resolution 2560 x 1920. In addition with ImageJ, Adobe Photoshop CS2 and CS5 were used for graphics.

8.4.2. Gene expression analysis

The aim of gene expression analysis is to provide information about genotype of the cultured cells as one way to characterize cells. Studying the expression of specific marker genes at the end point culture illustrates the cellular maturation stage. Cell material from one replicate of each material was used for this purpose. However since the amount of cell material on some replicates was low cell material from two replicates were gathered. In order to provide genotypical data following procedures were carried out: cell lysis, total RNA extraction, complementary DNA (cDNA) translation and RT-PCR. Following materials were selected for gene expression analysis after phase I: HA-modified OG2, OG13, OG25, HA-modified OG25, OG30, OG34, OG49, HA-modified OG49, Purecoat™ amine and type IV collagen. After phase II chitosan, non-textured PDLLA, type IV collagen (08/017), type I and IV collagens (08/023), Matrigel™ and

Substrate X were selected. In case of chitosan and non-textured PDLLA cell material from both replicates was combined in order to obtain sufficient amount of cell material.

Cell lysis

Cell culture medium was removed and cells were washed two times with DPBS. Cells were detached by scraping with pipette or cell scraper and together with DPBS transferred to RNAse free eppendorf tubes. Cells were centrifuged (2000 rpm, 3 minutes) and supernatant was removed. A solution of 100 µl Lysis Buffer RA1 (Macherey-Nagel) and 2 µl of Reducing Agent tris(2-carboxyethyl)phosphine (TCEP) was added to each sample in order to inactivate the RNases. Cell pellets originated from phase II type IV collagen (08/017), type I and IV collagens (08/023), Matrigel™ and Substrate X were resuspended into 200 µl of Lysis Buffer RA1 + TCEP solution and divided into two eppendorf tubes due to great amount of cell material. Solution was vortexed (15 sec) and the tubes were stored (-70°C) for further use in total RNA extraction.

Total RNA extraction

Procedure was carried out using NucleoSpin™ RNA XS Kit (Macherey-Nagel, GmbH & Co. KG, Düren, Germany) and by following instructions provided by manufacturer. Carrier RNA working solution was prepared and 5 µl was added to each sample lysate. Each lysate were vortexed and spinned down briefly. NucleoSpin® Filters was used to filtrate the lysates in order to reduce viscosity and clear the lysate. Each filtrated lysate were centrifuged (11000 g, 30 sec). Filters were discarded and 200 µl of 70% ethanol was added to adjust RNA binding conditions. Each lysate was stirred by pipetting up and down five times. Lysates were pipetted on the NucleoSpin® RNA XS column membrane and centrifuged (11000g, 30 sec) in order to bind RNA. Column was placed into a new collection tube and 100 µl of Membrane Desalting Buffer was added to remove salts and dry the membrane. For each lysate DNAse reaction mixture was prepared out of 3 µl of reconstituted rDNAse and 27 µl of Reaction Buffer for rDNAse. The function of DNase reaction mixture was to remove contaminating DNA from the lysate. 25 µl of DNase reaction mixture was added to membrane of the column. Lid was closed and column incubated in room temperature (RT) for 15 min. Three-step wash procedure was carried out to wash and dry the silica membrane. 100 µl of Wash Buffer RA2 was added and lysate was incubated (2 min) and centrifuged (11000 g, 30 sec) to inactivate rDNAse. 400 µl of Wash Buffer RA3 was then added to the column and the lysate was centrifuged again (11000 g, 30 sec). Finally, 200 µl of Buffer RA3 was added to the column and again the lysate was centrifuged (11000g, 3.5 min). Then column was placed into a nuclease free collection tube and incubated (2.5 min). Total RNA was eluted by 10 µl of RNAse-free water and centrifuged (11000 g, 30 sec). Obtained samples were stored (-70°C) for further use in cDNA translation.

Complementary DNA translation

cDNA was translated from the obtained total RNA samples using enzyme reverse transcriptase. In order to carry out the cDNA translation concentrations of total RNA in prepared samples were determined using NanoDrop ND-1000 spectrophotometer (NanoDrop Technologies, Wilmington, DE, USA). cDNA translation was performed using High-Capacity cDNA Reverse Transcription Kit (Applied Biosystems, Foster City, CA, USA). Reagents used in the procedure are presented in Table 8.4. RNAse inhibitor was provided by Fermentas, Glen Burnie, MD, USA while all other reagents were provided by Applied Biosystems. Procedure required specific total RNA sample concentration (20 ng/µl) therefore necessary dilutions were carried out.

Table 8.4 *Reagents for cDNA translation reaction for one total RNA sample.*

Reagent	Amount
10 x Buffer RT	2 µl
25 x dNTP Mix 100mM	0.8 µl
10 x RT Random Primers	2 µl
MultiScribe™ Reverse Transciptase	1 µl
RNAse Inhibitor (10 U/µl) in 1 x RT Buffer	1 µl
Sterile water	11.2 µl
Extracted total RNA sample 20 ng/µl	2 µl
Total reaction volume	**20 µl**

Total amount of reaction mixture without the total samples was prepared into an eppendorf tube before division into separate PCR tubes. Total RNA samples were then added to each appropriate PCR tube. The cDNA translation incubation cycle was carried out as follows: 10 min at 25°C, 120 min at 37°C and 5 min at 85°C. Resulted cDNA was stored (-20°C).

Reverse transcriptase-PCR

Gene expression analysis was performed by studying expression of specific marker genes. Marker genes were selected so that whole typical RPE cell life span would be sufficiently covered. The same selected marker genes were examined in both phase I and phase II. The RPE marker genes used and their functions are listed in Table 8.5. Gene expression analysis was performed in two sessions, first including glyceraldehyde 3-phosphate dehydrogenase (GADPH), a widely studied gene participating in glycolysis

[65] and also RAX and MITF. The second session, in turn, included RPE65, Bestrophin and SRY (sex determining region Y)-box 2 (SOX2), a gene indicating differentiation towards neural lineage [78].

Table 8.5 *RPE marker genes used in RT-PCR. T_{ann} (annealing temperature).*

Gene name	T_{ann} (°C)	Marker function
GADPH	55	housekeeping
RAX	55	precursor marker
SOX2	55	neuromarker
MITF	52	mature RPE marker
Bestrophin	55	mature RPE marker
RPE65	52	mature RPE marker

The RT-PCR protocol was carried out similarly in both phase I and phase II. The reagents used in mastermix solutions are presented in Table 8.6. First, mastermix solutions were prepared containing specific primers for each gene. 24 µl of each mastermix solution were added to appropriate PCR tubes. Then 1 µl of sample was added to each particular PCR tube. Following PCR program was applied. In the first step samples were incubated at 95°C (3 min). Then a loop of following steps were repeated 38 times: incubation at 95°C (30 sec), incubation at T_{ann} (30 s) and incubation at 72°C (1 min). Obtained PCR samples were stored at +7°C.

Table 8.6 *Reagents and amounts used in each mastermix solution in RT-PCR procedure. Primer F and Primer R depend on gene under examination.*

Reagent	Amount
Sterile water	16.6 µl
10 x Buffer without Mg^{2+} with KCl	2.5 µl
MgCl (25mM)	2.5 µl
dNTP Mix (2 mM)	1.25 µl
Primer F (5 mM)	1.0 µl
Primer R (5 mM)	1.0 µl
Taq polymerase	0.125 µl
cDNA sample	1 µl
Total reaction volume	**25 µl**

The visualization of gene expression was performed using agarose gel electrophoresis. First 2% agarose gel was prepared by mixing 2 g of agarose and 100 ml of buffer solution containing tris base, boric acid and EDTA (TBE). Solution was heated in a microwave oven until reaching boiling point. Heating was repeated until the solution turned clear. 5.5 µl of ethidium bromide was then added to the solution, solution was stirred and left to cool in a ventilation hood until reaching temperature approximately 50°C. Gel electrophoresis equipment was assembled and gel was poured into the gel rack. 20-spike combs were added and gel was left to cool. After reaching RT combs were removed and gels were transferred together with the racks into gel tank**.** Tank was filled with TBE until whole gel was below the surface. GeneRuler marker dilution including 1.5 µl of DNA ladder, 1 µl of 6x loading dye and 3.5 µl of sterile water was prepared according to manufacturer's instructions (10x, 50 bps, Fermentas) and vortexed briefly. 5 µl of 6x loading dye was added to each PCR tube including the cDNA samples. 20 µl of these samples together with 6x loading dye were added to particular wells on the gel. Electrophoresis was carried out with following parameters: 90 V, 400 mA, 100 W and 50 min. After electrophoresis gels were illuminated with UV lightbox (BioRad) and photographed 3-4 times each. The program used for administration of images was Quantity One (v 4.5.2).

8.4.3. Indirect immunofluorescence analysis

Indirect immunofluorescence stainings were used to assess the RPE maturation specific protein expression and localization of cells grown on type I and IV collagens (08/023), Matrigel™ and Substrate X. Total four wells of each material were fixed and stained. Staining procedure included two steps: cell fixation and cell staining. Cell fixation was carried out using following protocol: cell culture medium was removed from the each well destined for staining and the cells were washed carefully three times with DBPS. Each well was fixed with 500 µl of 4% paraformaldehyde (PFA) and incubated in ventilation hood (RT, 10 min). Cells were washed three times with DPBS to remove excess PFA. DPBS was left on the well and plates were sealed and stored (+4°C).

Each well was treated with different primary and secondary antibodies presented in Table 8.7. Selection of antibodies was done so that RPE maturity could be sufficiently indicated. First 300 µl of 0.1% Triton® X-100 (4-(1,1,3,3-tetramethylbutyl)phenyl-polyethylene glycol) (Sigma-Aldrich) was added to permeabilize cells. After incubation (10 min) cells were washed two times with DPBS. 3% bovine serum albumin in DPBS (BSA-DPBS) was added to each well and plate was incubated (RT, 1 hour) in order to block non-spesific protein binding. Primary antibody was added in with 0.5% BSA-DPBS and incubated (RT, 1 hour). Cells were washed again three times with DPBS before addition of secondary antibody with 0.5% BSA-DPBS. Secondary antibody binds to the primary antibody. Again cells were incubated (RT, 1 hour) and wash-procedure was performed three times. DPBS was removed carefully and 20 µl of Vectashield mounting medium containing 4',6'-diamidino-2-phenylindole (DAPI) (Vector Laboratories, Inc., Burlingame, CA, USA) was added on

each fixed cell population. Cover slips were placed on each stained well and plates were sealed with foil and stored (+4°C). Imaging was done with Zeiss axiovert microscope with 20x magnification.

Table 8.7 *The primary and secondary antibodies used in immunofluorescence labeling.*

Antibodies		**Dilution**	**Origin**	**Manufacturer**
Primary	Bestrophin	1:500	rabbit	Abcam
	CRALBP	1:1000	rabbit	Abcam
	MITF	1:350	mouse	Abcam
	ZO-1	1:250	mouse	Molecular Probes
Secondary	Alexa 568 IgG anti-rabbit	1:5000	goat	Molecular Probes, Invitrogen
	Alexa 568 IgG anti-mouse	1:500	goat	Molecular Probes, Invitrogen

8.4.4. Image analysis with ImageJ-software

Images taken during culturing period were analyzed with ImageJ-software. ImageJ is an open source Java-based image processing program. Downloading from the public domain is free of charge and therefore ImageJ was chosen for this study. Basic tools for image enhancement, geometric operations, analysis and editing are included and these operations can be performed to 8-bit, 16-bit and 32-bit images. ImageJ can operate on most image file formats including TIFF and JPEG which were formats used in this study. In order to create automated process macro recording feature was used. [2]

Ten images were selected for the analysis (Figure 8.4). Images represented different time points of culturing period so that typical developmental phases in the cell culture would be covered. The material should also be sufficiently suitable for cell culturing so that different phases could be monitored. Therefore the control material, type IV collagen, was chosen. Images were mainly taken from the same well and from a particular area of the well to ensure realistic development. Image quality and imaging conditions corresponds to a typical imaging session.

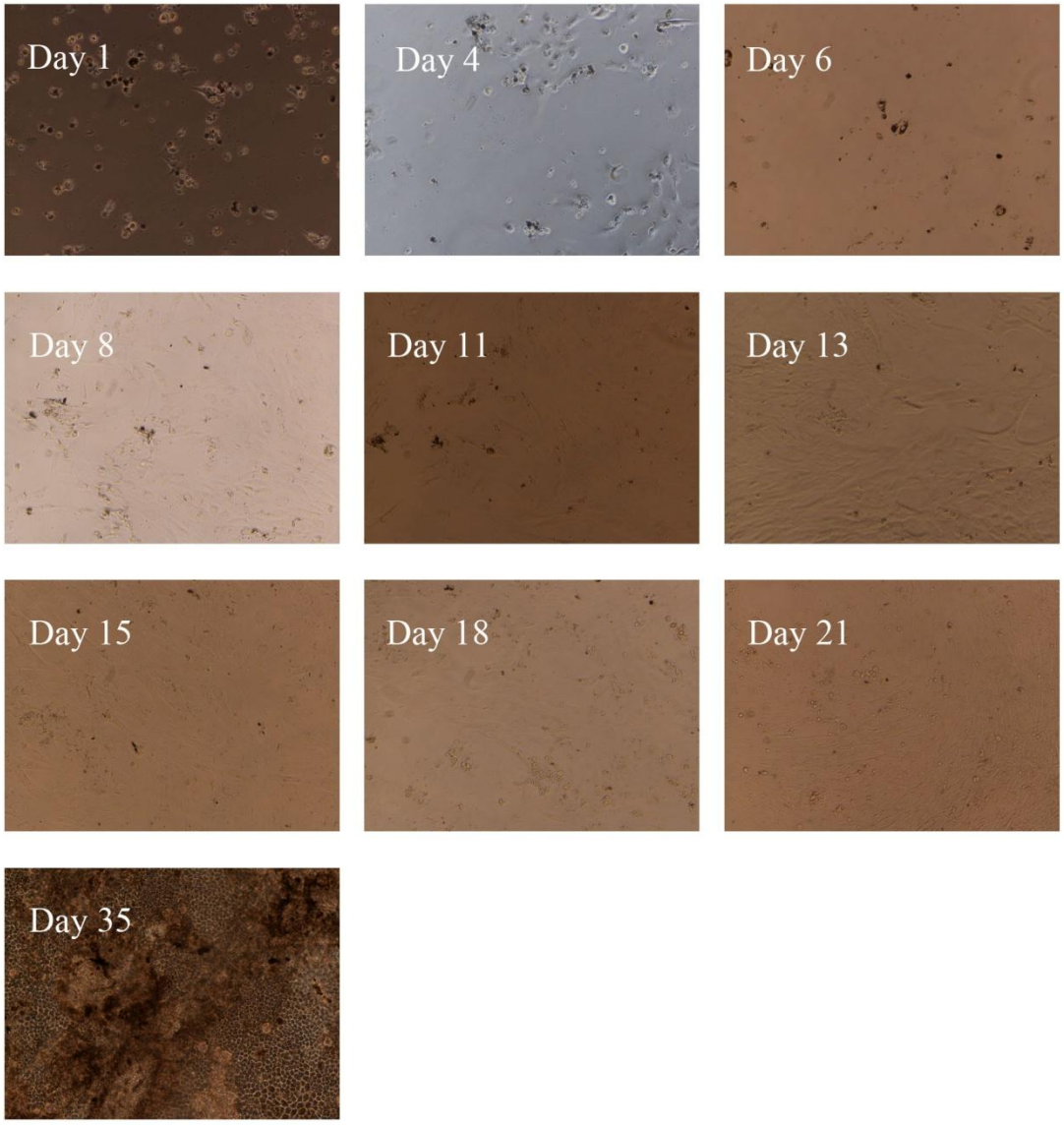

Figure 8.4 *The images selected for image analysis using ImageJ-software.*

The experiment based strongly on Luc Vincent's study with corneal endothelial cells [103]. Aim was to by using macro recording feature create a single macro by optimizing the use of tools presented in Table 8.8. Created macro should provide reliable cell count, distinguish different cell morphologies and provide information about pigmentation level. In addition the previously described aim was to be accomplished by creating as user-friendly process as possible.

Table 8.8 *Tools utilized in image analysis [41].*

Tool	Description
8-bit	Converts the image to 8-bit grayscale by linearly scaling pixel values between min (0) and max (255).
Sharpen	Increases contrast and highlights detail in the image or selection but may also highlight noise. Each pixel is replaced with a weighted average of the 3x3 neighborhood. Following weighting factors are used -1 -1 -1 -1 12 -1 -1 -1 -1
Automatic threshold	Segments the image into features of interest and background by automatically setting lower and upper values for thresholding. The default function carries this out by taking a test threshold and computing the average of the pixels at or below the threshold and pixels above. Then it computes the average of those two, increments the threshold and repeats the process. Incrementing stops when the threshold is larger than the composite average threshold = (average background + average objects)/2 16 different automatic thresholding methods can be selected.
Convert to mask	Converts the image into black and white regarding to the threshold values set or calculated by automated thresholding tool with inverted lookup table (black is 255 and white is 0) as default.
Erode	Removes pixels from the edges of the objects. This can be carried out using minimum filter which does the grayscale erosion by replacing each pixel in the image with the smallest pixel value in that pixel's neighborhood.
Watershed	Automatically separates or cuts apart particles that touch. First, Euclidian distance map (EDM) is calculated to determine the ultimate eroded points (UEP). Then each UEPs (peaks or local maxima of the EDM) are dilated until the edge of the particle is reached or edge of another growing UEP is found. Watershed is found to work best with smooth convex objects that do not overlap too much.
Analyze particles	Measures particles in existing area selection in binary or thresholded images. The tool scans the selection until edge of an object is found. It then outlines the object, measures it and fills it to make it invisible. Scan is resumed until the end of selection is reached. Adjustable parameters are *size* and *circularity*. Particles outside the range specified in these parameters are ignored. *Size* values may range between 0 and infinity. Determined values are expressed in square units or in pixels. *Circularity* value is counted as follows and ranges from 0 (infinitely elongated polygon) to 1 (perfect circle). $\text{circularity} = 4\pi \frac{\text{Area}}{\text{Perimeter}^2}$
Measure	Based on the chosen values calculates and displays area statistics, line lengths and angles or point coordinates. With area selections following parameters can be measured: area, center of mass, centroid, perimeter, bounding, rectangle, shape, descriptors, fitted ellipse, Feret's diameter, skewness, kurtosis and area fraction.

9. RESULTS

9.1. Cellular attachment, proliferation and maturation monitoring

Study was divided into two five-week culturing periods (phase I and phase II). During the culturing periods varying number of photos were taken of each well in order to provide sufficient image data for image analysis. In phase I the initial number of images was five images per well after each medium change (three times a week). On some substrates clear cellular development stopped after a few days in culture. In these cases, the number of pictures taken was reduced remarkably or stopped entirely. However at the end point of culturing period each substrate was photographed. Due to homogeneity of the images the number was reduced to three images per well once a week in the phase II excluding the type I and IV collagens (08/023), Matrigel™ and Substrate X. These substrates were not included in the image analysis and therefore only random pictures were taken to provide image data of most important developmental changes. In phase I first images (day 4) were taken prior to medium change but following images were taken after each medium change so that detached and dead cells would not disturb observations. Also notes were taken regularly regarding cellular condition and changes on each substrate. The data concerning attachment, proliferation and maturation on each substrate is illustrated as a series of images from different time points. Time points represent morphological status after first days in culture, at the approximately middle of the culturing period and at the end point. Since imaging frequency differed slight variation in time points between materials exists. At the end of the chapter cellular behavior on each material is summarized in Table 9.1. The cell attachment, proliferation and maturation are scaled to ease comparison.

9.1.1. Phase I monitoring

Type IV collagen

Cell attachment and development on type IV collagen are illustrated in Figure 9.1. Due to reliable coating procedure and desired cellular behavior type IV collagen was selected as control material for the study [100]. In phase I the coating procedure was carried out successfully, cells attached readily and fibroblast-like morphology appeared already on the first days. Both wells reached confluency and at the end point clear cobblestone-like morphology and heavy pigmentation was observed in the center area

of the well. However on the peripheral area of the well de-pigmented fibroblast-like morphology was dominant.

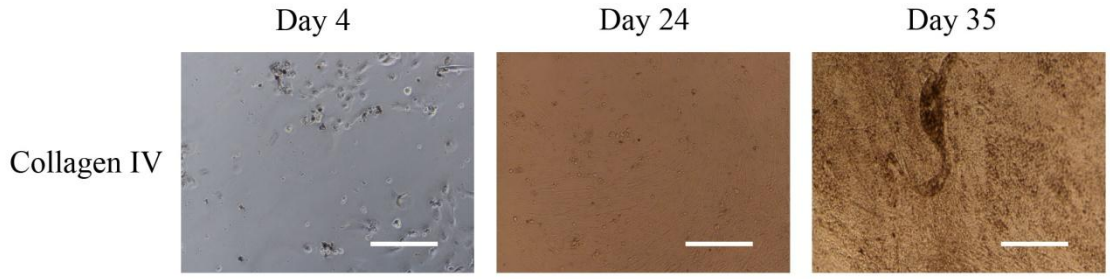

Figure 9.1 *hESC RPE cells cultured on type IV collagen surface at different time points. Scale bar length 200 µm.*

Purecoat™ amine and carboxyl

On both Purecoat™ amine and carboxyl surfaces the cells attached relatively well and indicated signs of spreading by obtaining slight fibroblast-like morphology (Figure 9.2). However the development stopped rapidly after a few days in culture. Some spread cells appeared with vesicles in the ends of elongated cells. At the end point number of cells remained small and cells were scarcely distributed. On amine surface the development was slightly more advanced and therefore it was selected for further analysis.

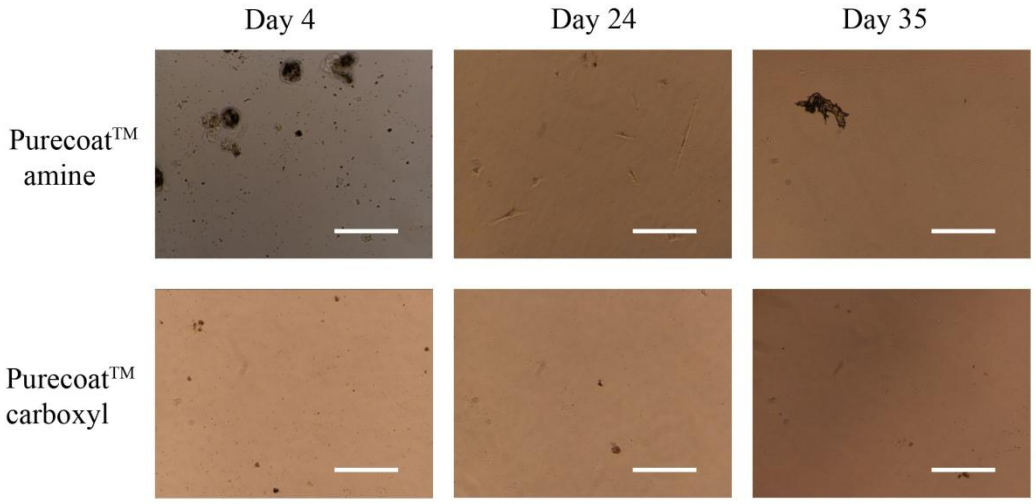

Figure 9.2 *hESC RPE cells cultured on Purecoat™ amine and carboxyl surfaces at different time points. Scale bar length 200 µm.*

BioMaDe™ Gelators plate A

The cellular attachment, proliferation and maturation of BioMaDe™ Gelators are illustrated in Figure 9.3 (plate A) and Figure 9.4 (plate B). Total four plates with two replicates of each material were provided for this study. First observations demonstrated

the poor initial condition of some materials, especially HA-modified OG2. Some wells were just partly covered with the material and some surfaces seemed to already been torn partly. Some wells had material on the well edges. The conditions of each replicate were estimated and two best-conditioned replicates of each Gelator entered the plating procedure. Because of the halted proliferation and maturation on plate A the imaging was stopped after three weeks. However at the end point each well was photographed.

Despite the good condition of OG1 and OG2 surfaces the first observations demonstrated poor attachment of cells (Figure 9.3). Typical for every BioMaDe™ Gelators cells tend to form large heavily pigmented clusters. Cell loss was extensive already at early days in culture and although slight spreading was observed cellular proliferation did not occur. After one week of culturing the material started to tear off in both OG2 wells. At the end point only few pigmented clusters and random individual cells were present yet some had obtained slight fibroblast-like morphology.

HA-modified OG2 slightly excelled the non-modified OG2 in initial cellular attachment even thought early observations indicated tearing in the material possibly occurred already in the first medium change during the plating procedure (Figure 9.3). The second well was in better condition and showed better attachment and slight spreading of cells yet no clear proliferation was observed. Cell number constantly decreased during the culturing period in both wells and end point observations illustrated presence of only few clusters and individual cells located mainly in the center of the wells. However cells on HA-modified OG2 entered further analysis.

The surface of OG13 had clear structural irregularities that slightly disturbed the observations and imaging. Cellular attachment was poor and even though slight spreading was observed cells did not proliferate (Figure 9.3). Development stopped entirely after a few days in culture and cell number reduced constantly yet a few cells obtained slight fibroblast-like morphology. At the end point just few clustered and random individual cells were present however cells on OG13 were selected for further analysis.

OG51 surface was smooth and enabled relatively good cell attachment yet no spreading was observed after first days. Again the cluster-form was dominant yet a few individual fibroblast-like cells appeared during the culturing period (Figure 9.3). No proliferation was observed and cell number decreased constantly during the culturing period. End point observations illustrated presence of only few clusters and random individual cells.

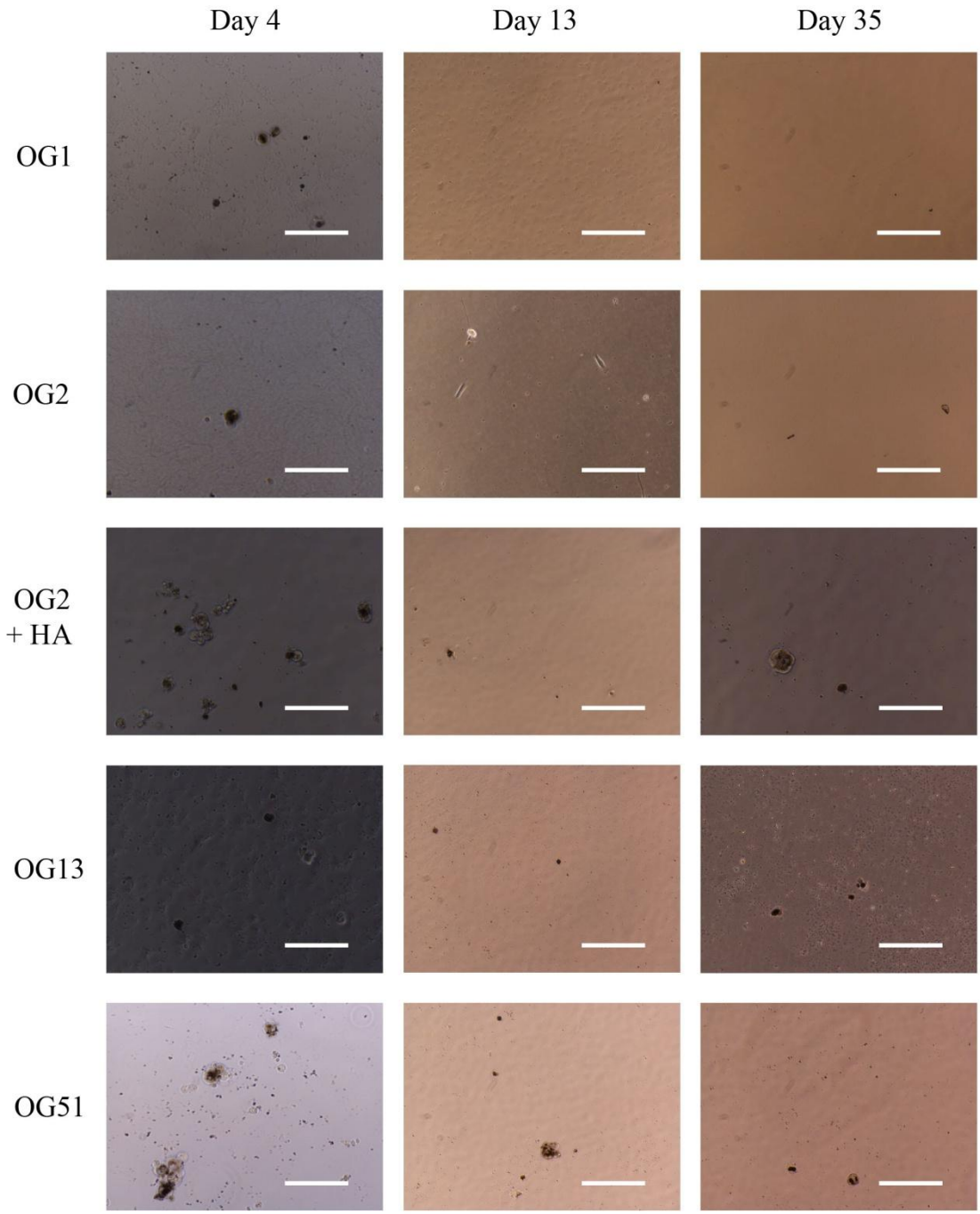

Figure 9.3 *hESC RPE cells on BioMaDe™ Gelators (plate A) at different time points. Scale bar length 200 µm.*

BioMaDe™ Gelators plate B

Irregular surface of OG25 caused slight difficulties in distinguishing cells from the surface. Cell attachment was relatively good and cells were distributed equally around the well. However no spreading was observed after first days (Figure 9.4). In the second well the material started to tear off and particles were observed in the center of the well throughout the culturing period. Cells however remained attached yet no proliferation

was observed. Even though a few clustered and individual cells with heavy pigmentation were present development was stopped entirely at the end point. However OG25 was estimated to possess enough cell material to enter further analysis.

HA-modified OG25 surface had smooth areas in the center well but granular-like irregularities in the peripheral area which slightly disturbed cell observations. Attachment was relatively good yet no spreading was observed after first days of culture (Figure 9.4). Material started to tear off after two weeks yet cells remained mostly attached. Even though the condition of material was very poor at the end point number of cells remained rather constant. Cells were mainly clustered and fibroblast-like morphology was not observed however HA-modified OG25 was chosen for further analysis.

Also in the case of OG30 surface was granular-like and in the second well partly torn off making cell distinguishing difficult (Figure 9.4). Attachment was relatively good yet cell loss was extensive after first days in culture. No spreading or proliferation was observed. At the end point a few clusters and random individual cells were present and in the second well the substrate was nearly entirely torn off. The first well however contained sufficient amount of cell material and proceeded to further analysis.

Also modified version of OG30 was included in the test with RGDs included in the structure. RGD-modified OG30 had also irregular surface and despite the modification showed poor attachment of cells (Figure 9.4). After first days no spreading or proliferation was observed. Material started to tear off after a few days yet cells seemed to remain attached. However constant decrease in cell number was observed and at the end point only few clusters and random individual cells were present.

OG34 had a smooth surface with similar appearance with type IV collagen. Relatively good attachment and slight spreading was observed after first days in culture (Figure 9.4). Cells remained attached and slight fibroblast-like morphology started to appear. However some irregularities emerged on the surface and distinguishing fibroblast-like cells from the substrate became difficult. Shortly after development halted yet at the end point relatively many clusters and fibroblast-like cells had remained attached therefore cells on OG34 entered further analysis.

The surfaces of OG49 and HA-modified OG49 were smooth and in good condition at the preliminary observations. Cells attached relatively well and slight spreading occurred after first days (Figure 9.4) on both surfaces. Cells remained attached although material started to tear off. In the second well of OG49 fibroblast-like morphology emerged. Also in the case of both OG49s substrate appearance made it complicated to distinguish the fibroblast-like cells from the irregular surface. No proliferation was observed but the amount of cells remained nearly constant throughout the culturing period. At the end point relatively large amount of clusters and spread cells were observed therefore both surfaces were selected for further analysis.

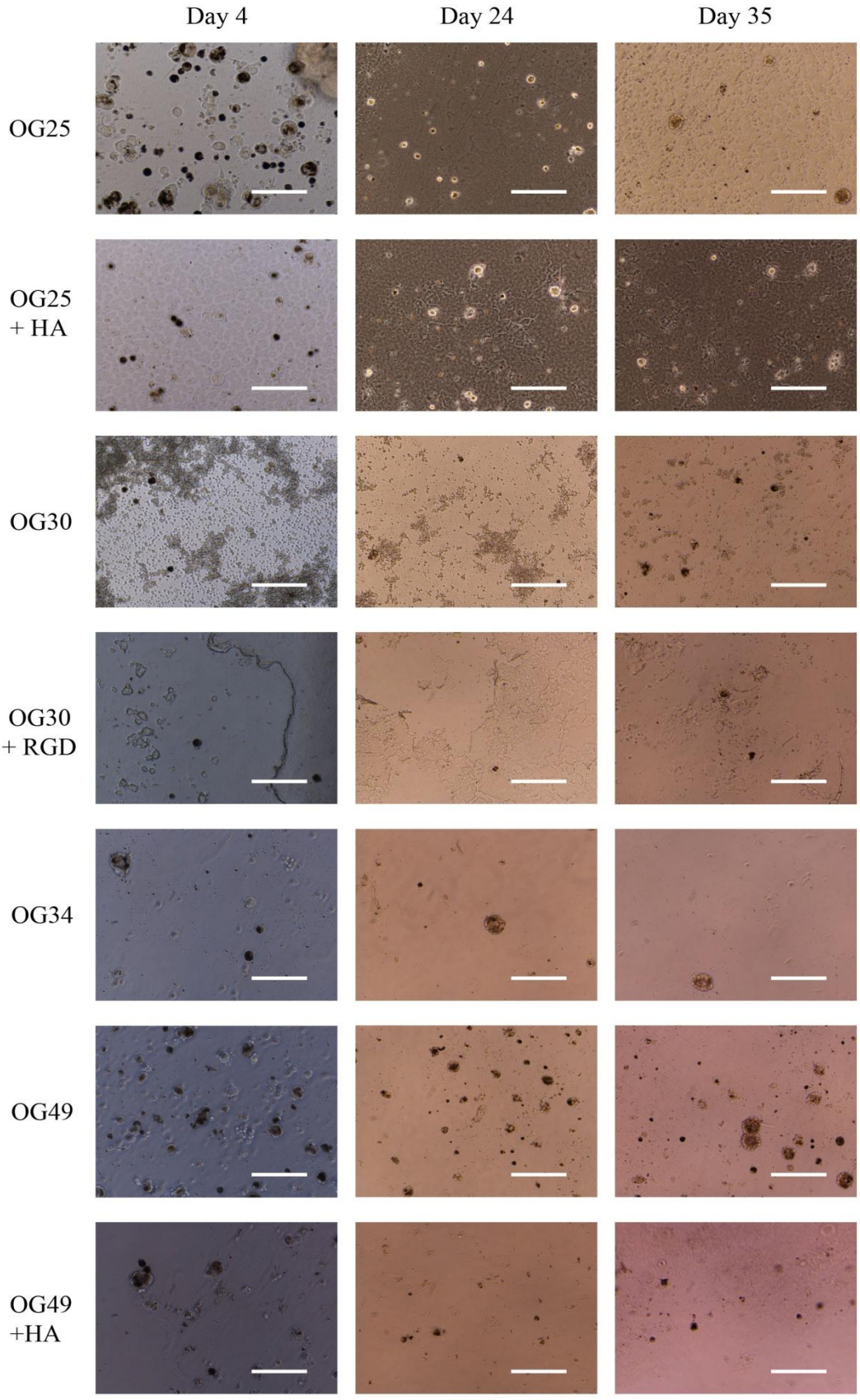

Figure 9.4 *hESC RPE cells on BioMaDe™ Gelators (plate B) at different time points. Scale bar length 200 µm.*

9.1.2. Phase II monitoring

Type IV collagen (08/017)

Type IV collagen, seeded with 08/017 hESC RPE cells, was used as a control substrate in both phase I and phase II for other than type I collagen, Matrigel™ and Substrate X. In these cases the control material was type IV collagen seeded with 08/023 hESC RPE cells. Coating procedure was carried out similarly as in phase I resulting in a smooth-surfaced coating. However on each well tearing occurred on the well edge after two weeks of culturing and at the end point the cell layer was nearly entirely folded into the center of the well. Nevertheless attachment was very good and cells started to spread and proliferate already after first days of culture. Clear trans-differentiation and cobble-stone-like stages were observed on unfolded areas (Figure 9.5).

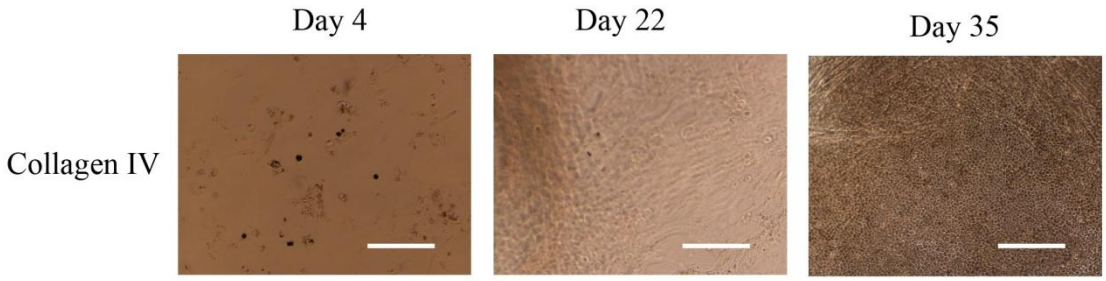

Figure 9.5 *hESC RPE cells (08/017) cultured on type IV collagen at different time points. Scale bar length 200 µm.*

Chitosan

Solvent casting-produced chitosan surface remained smooth throughout the culturing period. Cells attached relatively well and equally throughout the well (Figure 9.6). Characteristic to chitosan surface was the presence of numerous individual round-shaped cells compared to other substrates on which the cells mainly appeared in cluster-form (excluding type I and IV collagens, Matrigel™ and Substrate X). After first days slight spreading was observed however cells did not proliferate. Number of cells remained rather constant throughout the culturing period. Pigmentation level varied from heavily pigmented to nearly entirely depigmented. At the end point both small clusters and individual cells were present in sufficient number therefore chitosan was selected for further analysis.

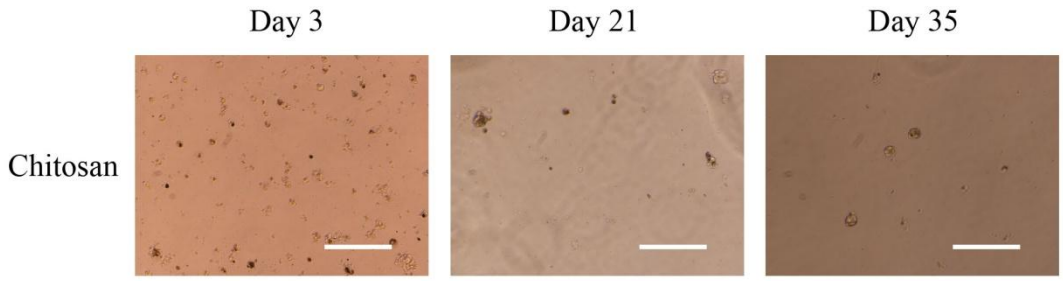

Figure 9.6 *hESC RPE cells on chitosan coatings at different time points. Scale bar length 200 µm.*

PDLLA, PLGA and PLCL

After processing PDLLA, PLGA and PLCL membranes were cut into pieces to fit into a well of 24-well culture plate. After ethanol desinfection pieces were attached to the bottom of the well with Scaffdex Cellcrown™ cell culture inserts. The attachment of PDLLA, PLGA and PLCL membranes was questioned since Scaffdex Cellcrown™ cell culture inserts used were second-hand possibly resulting in weakened docking capability. Questionable attachment was supported by first observations on each substrate which indicated the presence of a number of cells below the membranes (Figure 9.7).

The PDLLA substrate remained clear throughout the culturing period. Cells attached relatively good on both non-textured and textured surface however mainly on the peripheral area of the well (Figure 9.7). Even though no proliferation was observed slight changes in cell morphology occurred after first days in culture. At the end point mainly big clusters with heavy or partly lost pigmentation were present with the ones attached on non-textured surface being slightly larger in size. Also random individual cells with clear fibroblast-like morphology were observed. However cell material on non-textured PDLLA was sufficient and therefore it proceeded for further analysis.

The PLGA material was brownish and the texture was clearly visible (Figure 9.7). Substrate transparency reduced remarkably during the culture period and close to the end point small round-shaped holes appeared. Attachment was poor however slightly better on non-textured surface and no spreading or proliferation occurred. Again clusters were observed below the membrane. At the end point only few large, heavily pigmented clusters were present on both surfaces.

Cell attachment on PLCL non-textured surface excelled slightly the attachment on textured one however being poor in both cases and occurring mainly on the peripheral area between well edge and cell crown (Figure 9.7). Again a few clusters appeared to be located below the membrane. However after first days in culture slight spreading of cells were observed yet cells did not proliferate. At the end point only large clusters with heavy or partly lost pigmentation were present on both surfaces situated mostly on the peripheral area of the well. Transparency of the substrate also reduced during the culturing period.

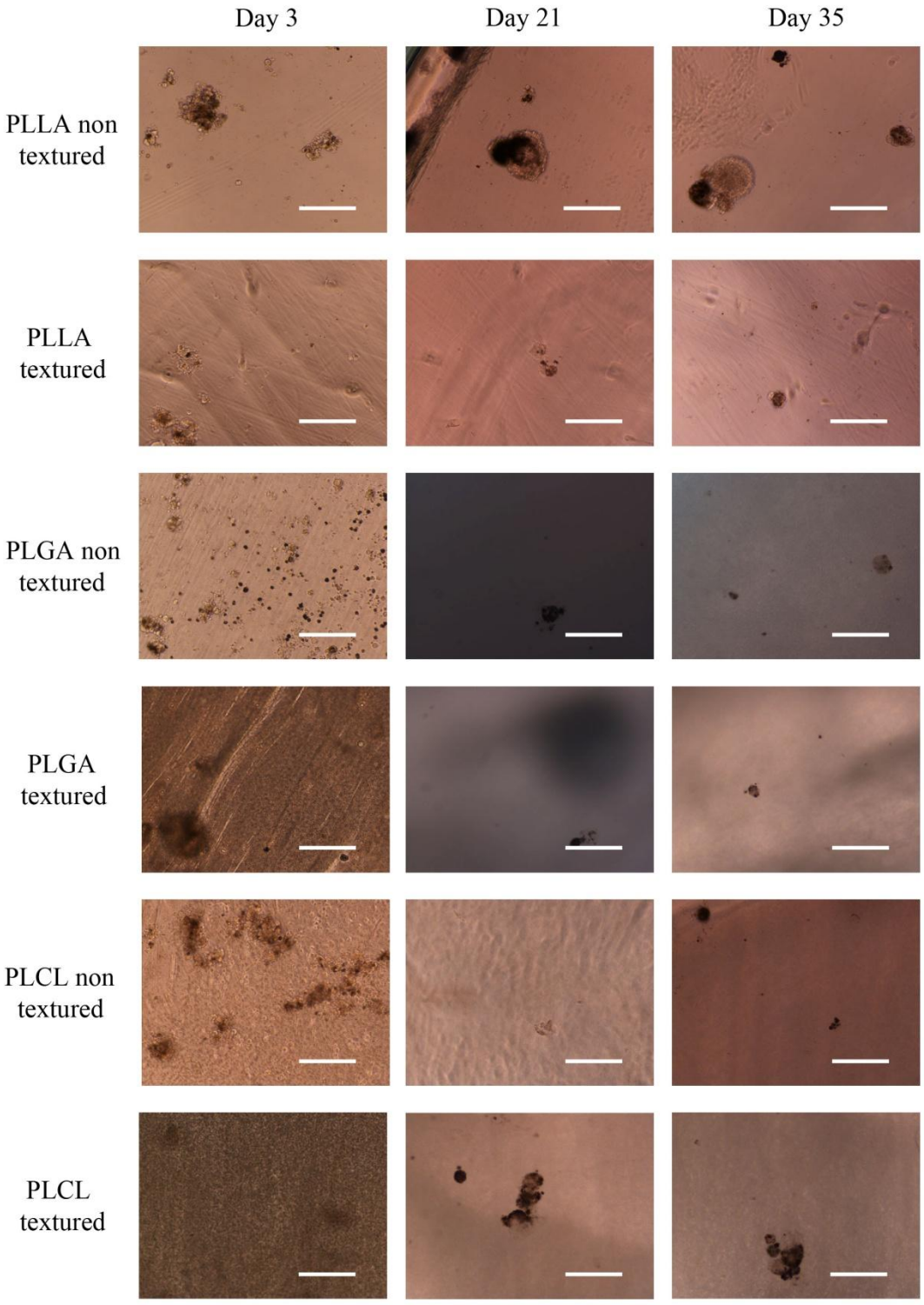

Figure 9.7 *hESC RPE cells cultured on PDLLA, PLGA and PLCL membranes at different time points. Scale bar length 200 µm.*

Substrate X

The coating protocol of Substrate X was successful resulting in smooth surface. Cells attached readily and first observations demonstrated relatively large cell number and

already initiated spreading of cells (Figure 9.8). Significantly large, heavily pigmented cell clusters were observed out of which, as the culturing period proceeded, large areas with fibroblast-like morphology spread. In addition individual round-shaped and fibroblast-like cells were observed mainly in the center area. However the spreading of fibroblast-like areas stopped in the middle of the culturing period and areas started to shrink yet simultaneously initiating and increasing pigmentation and ultimately leading to cobblestone-like structure. The cell condition was questioned as its appearance had similarities with folded type IV collagen (phase II, 08/017). At the end point slight differences between sizes and pigmentation level of fibroblast-like areas were observed between the wells.

Type I and type IV collagen (08/023)

Coating procedures for type I and type IV collagen (08/023) was carried out successfully providing smooth surfaces. However type IV collagen started to tear from the well edge at the final days of culture. Attachment was good although slightly lower on type I collagen (Figure 9.8). Both substrates reached confluency in two weeks. In general cultures on type I collagen and type IV collagen developed in a similar fashion yet cobblestone-like areas appeared a few days earlier on type IV collagen. In addition pigmentation on type IV collagen at the end point was slightly more advanced. Cobblestone-like areas formed mostly on the peripheral area of the well while the center of the well was densely occupied by fibroblast-like cells. Slight differences between wells were observed regarding cobblestone-like cell area number.

Matrigel™

Also Matrigel™ surface coating procedure was carried out successfully creating smooth surface. Attachment was equal throughout the well outmatching type I and IV collagens and spreading was rather advanced already after first days (Figure 9.8). Also confluency was reached before type I and IV collagens resulting in rapid formation of high number of cobblestone-like centers equally distributed throughout well. Pigmentation increased in faster pace resulting in clearly higher level compared to type IV collagen. Undoubtedly development on Matrigel™ was the most advanced at the end point.

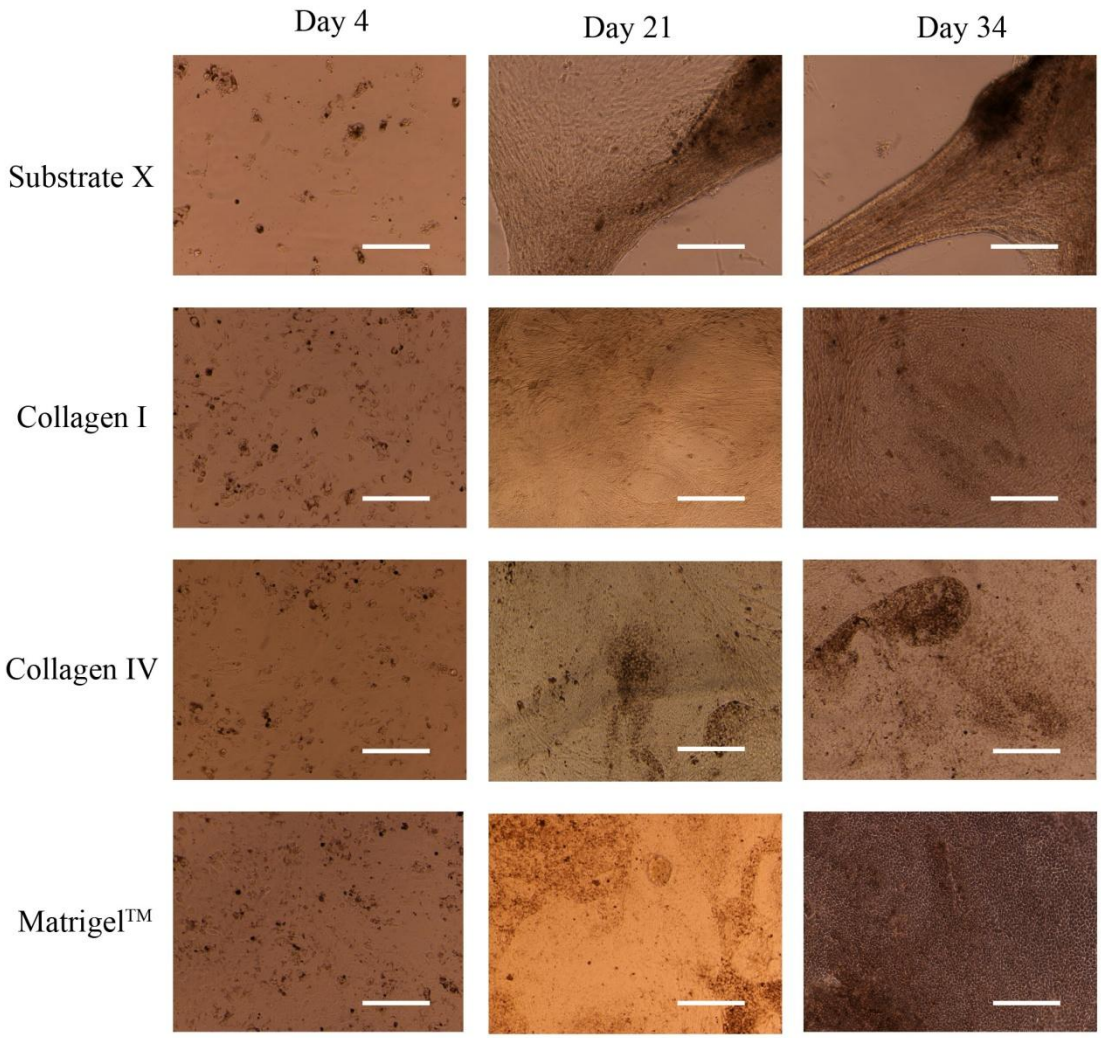

Figure 9.8 *hESC RPE cells cultured on Substrate X, type I and IV collagens (08/023) and Matrigel™ at different time points. Scale bar length 200 µm.*

Table 9.1 *Comparison of cellular attachment, proliferation and maturation on tested materials. The scale of grading is following: - for zero level attachment, proliferation or maturation, + for slight, ++ for equal to control (type IV collagen) and +++ for outmatching control.*

Material origin	Name	Phase	Cell line	Attachment	Proliferation	Maturation
Natural	Chitosan (91% deacetylation)	II	08/017	+	-	-
	Type I collagen	II	08/023	++	++	++
	Type IV collagen	I	08/017	++	++	++
	Type IV collagen	II	08/017	++	++	++
	Type IV collagen	II	08/023	++	++	++
	BD Matrigel™ matrix	II	08/023	+++	+++	+++
	Substrate X	II	08/017	++	++	++
Synthetic	OG1	I	08/017	+	-	-
	OG2	I	08/017	+	-	-
	HA-modified OG2	I	08/017	++	-	-
	OG13	I	08/017	+	-	-
	OG25	I	08/017	++	-	-
	HA-modified OG25	I	08/017	++	-	-
	OG30	I	08/017	+	-	-
	RGD-modified OG30	I	08/017	+	-	-
	OG34	I	08/017	+	-	-
	OG49	I	08/017	+	-	-
	HA-modified OG49	I	08/017	++	-	-
	OG51	I	08/017	++	-	-
	Purecoat™ amine	I	08/017	+	+	-
	Purecoat™ carboxyl	I	08/017	+	-	-
	PLGA non-textured	II	08/017	+	-	-
	PLGA textured	II	08/017	+	-	-
	PDLLA non-textured	II	08/017	++	-	-
	PDLLA textured	II	08/017	+	-	-
	PLCL non-textured	II	08/017	+	-	-
	PLCL textured	II	08/017	+	-	-

9.2. Gene expression analysis

9.2.1. Phase I testing

After phase I gene expression analysis was performed to cells on substrates with sufficient amount of cell material. Not many substrates met this requirement and therefore all materials that had sufficient amount of cell material were selected without concentrating on other aspects such as maturation stage. After phase I following materials qualified for further analysis: HA-modified OG2, OG13, OG25, HA-modified OG25, OG30, OG34, OG49, HA-modified OG49, Purecoat™ amine and the control, type IV collagen.

Cell material from one replicate of each substrate was collected for total RNA extraction and RT-PCR. At first cells were lysed and stored (-70°) until total RNA extraction which was then carried out. Concentrations of obtained total RNA samples were determined using spectrophotometer (Table 9.2). As expected, concentrations of most samples were relatively low but sufficient to carry out RT-PCR procedure which required 20 ng of RNA. Surprisingly amount of total RNA from cells grown on type IV collagen was exceptionally low. Purity of samples was questionable since 260/280 ratio differed remarkably from value for pure RNA (2.00).

Table 9.2 *Total RNA concentrations measured with Nanodrop ND-1000 spectrophotometer.*

Substrate	Concentration (ng/µl)	Purity 260/280
HA-modified OG2	60.94	1.04
OG13	75.08	3.87
OG25	24.46	3.49
HA-modified OG25	23.78	3.65
OG30	55.65	3.37
OG34	55.65	3.37
OG49	28.81	4.66
HA-modified OG49	45.47	3.29
Purecoat™ amine	41.04	3.46
Type IV collagen	64.20	2.41

cDNAs were translated out of mRNAs of obtained total RNA samples and RT-PCR was used to determine the expression of following marker genes: GADPH, RAX, SOX2, MITF, Bestrophin and RPE65. Results are presented in Figure 9.9.

Cells cultured on HA-modified OG2 exhibited relatively mature expression however RPE65 was not expressed indicating that maturation has not advanced to natural RPE level. Unwanted SOX2 expression was not observed indicating that cells had not differentiated towards neural retina. In addition RAX was not expressed indicating that cells at precursor state necessary for transdifferentiation were not present. Cells on OG13 weakly expressed Bestrophin, the mature RPE marker. The absence of housekeeping gene GADPH questions the reliability of the result. Cells on OG25 expressed precursor marker RAX and mature RPE marker Bestrophin. Presence of RAX could be a sign of initiated trans-differentiation. Again the absence of GADPH is questioning the reliability of the result. Cells on HA-modified OG25 expressed GADPH, MITF and Bestrophin which indicates mature expression of cells. Cells cultured on OG30 had similar expression indicating also mature stage of cellular development. Cells on OG34 showed mature expression since each mature markers including RPE65 was present. Positive RAX expression indicates that cells in precursor state were also present and could sign initiated transdifferentiation. Cells on OG49 with or without HA-modification also expressed each mature RPE marker excluding RPE65. In addition, RAX was expressed indicating precursor state-cell presence. None of the substrates induced neurodifferentiation since SOX2 was absent in each sample.

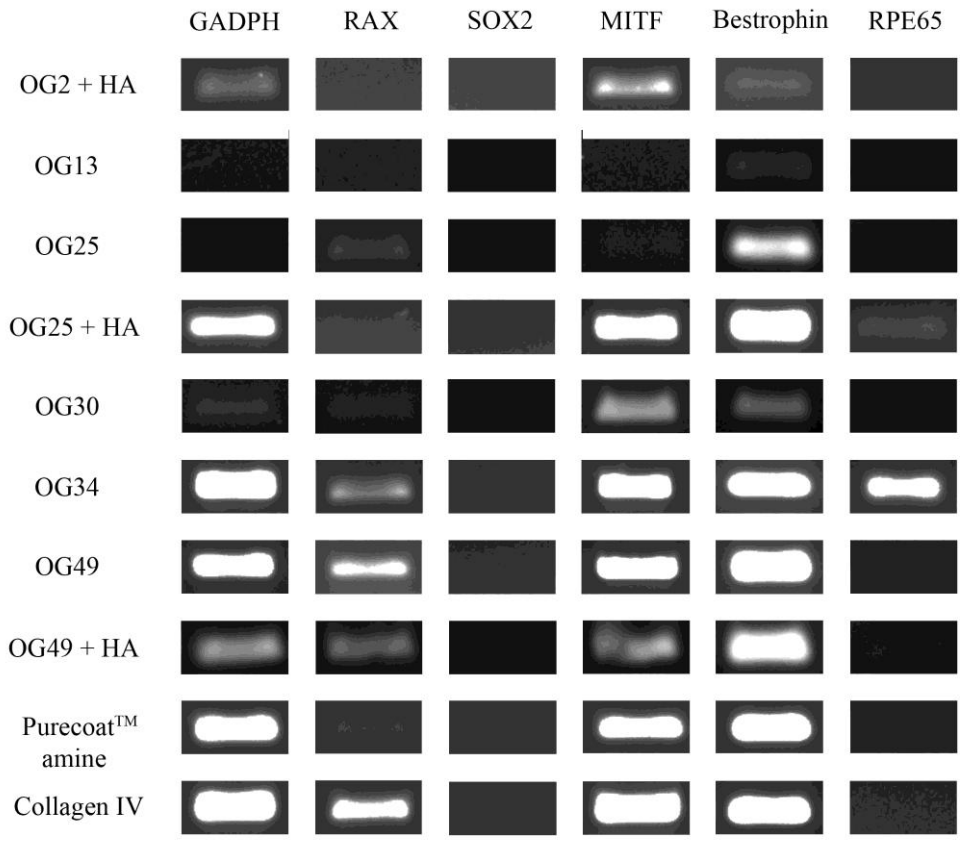

Figure 9.9 *Marker gene expression of cells cultured on phase I substrates.*

9.2.2. Phase II testing

After the phase II culturing period substrates were selected for further analysis according to the same principle as after phase I, that is, the sufficient amount of cell material. Excluding type I and IV collagens (08/023), Matrigel™ and Substrate X, not many replicates met the requirement and therefore each substrate that had sufficient amount of cell material qualified for gene expression analysis. The substrates that proceeded to analysis were following: both type I and IV collagens (08/023), Matrigel™, Substrate X, non-textured PDLLA, chitosan and type IV collagen control (08/017). EB sample collected from the pooled 08/023 cell line EBs (see Table 8.3) in the beginning of the phase II was also included to provide information about initial stage of seeded cells.

One replicate of each substrate was treated to provide total RNA with exception of PDLLA and chitosan in which two replicates were included in order to obtain enough cell material. Cells were lysed following similar protocol as in phase I and stored (-70°C) until use in total RNA extraction. Total RNA extraction was carried out and concentrations were measured using spectrophotometer (Table 9.3). Concentration measurement was repeated for Substrate X since the concentration was exceptionally low which was in contradiction with visual data obtained during culturing period. In addition not enough total RNA was extracted from cells grown on chitosan and PDLLA in order to run a proper RT-PCR analysis.

Table 9.3 *Total RNA concentrations measured with Nanodrop ND-1000 spectrophotometer.*

Substrate	Concentration (ng/µl)	Purity 260/280
Start EBs	47.83	2.55
Type IV collagen (08/023)	134.40	2.25
Type I collagen	74.93	2.41
Matrigel™	87.91	2.28
Substrate X	10.26	3.05
PDLLA non-textured	0.31	- 0.10
Chitosan	- 5.46	1.17
Type IV collagen (08/017)	188.82	2.17

Similarly as after phase I mRNAs from obtained total RNA samples were translated into cDNA and RT-PCR was used to determine the expression of following marker genes: GADPH, RAX, SOX2, MITF, Bestrophin and RPE65. Cells at the EB state expressed only GADPH with very weak band. Therefore reliable comparison of cellular state at the end point to the initial state is impossible. On Substrate X sample no

bands were observed. In addition both type IV collagen samples expressed GADPH with strong band yet other markers were not present. Type I collagen sample also expressed GADPH weakly yet no other bands were present. Matrigel™ sample, with most advanced development on the culture plate, expressed also only GADPH. These results are in contradiction with the development observed on the cell culture plate and also with measured concentrations. Samples from non-textured PDLLA and chitosan also resulted negative however in these cases amount of extracted total RNA was relatively low. However since visual observations demonstrate good attachment, proliferation and maturation on type I and type IV collagen (08/023), Matrigel™ and Substrate X the phase II RT-PCR analysis is considered to be failed.

9.3. Indirect immunofluorescence analysis

Four materials entered the staining phase: Substrate X, type I and IV collagens (08/023) and Matrigel™. Four different antibodies were used to indicate maturity: Bestrophin, CRALBP, MITF and ZO-1. Also DAPI staining was performed in order to visualize the nuclei. Typically in a mature RPE cell CRALBP and ZO-1 are located on the cellular membrane while MITF is typically located in nucleus. Bestrophin in turn is located on the cell membrane and the cytoplasm. [104, 100] Each staining was photographed using fluorescence microscope with 20x magnification. In addition bright-field images were taken.

Staining procedure was carried out successfully. On Substrate X Bestrophin protein was observed both on cell membrane and cytoplasm (Fig 9.10). CRALBP in turn was present in lower quantity. MITF protein, located in cell nucleus, was expressed by only few cells. ZO-1 antibody formed partly disconnected web-like staining pattern indicating uneven disposition of ZO-1 protein. DAPI staining indicated that many cells did not express any of selected marker proteins.

On type I collagen Bestrophin protein was expressed in low quantity however on both cell membrane and in cytoplasm (Figure 9.11). Both CRALBP and MITF protein was present in larger quantities. MITF protein was exceptionally located on cell membrane instead of nucleus. ZO-1 protein was also expressed in rather large quantity and formed a partly disconnected network.

On type IV collagen (08/023) (Figure 9.12) Bestrophin protein was present rather large amounts both in cytoplasm and on cell membrane. CRALBP in turn was expressed to lower extent. In addition MITF protein expression was rather low however ZO-1 protein was present as a continuous web-like pattern.

Bestrophin protein was expressed to large extent on Matrigel™ (Figure 9.13). In addition the quantity of CRALBP was high. MITF protein was also expressed extensively and indicated presence of clustered, partly overlapping cells. The ZO-1 antibody formed a clear continuous staining pattern demonstrating protein presence in large amounts. Matrigel™ showed strongest staining with each antibody.

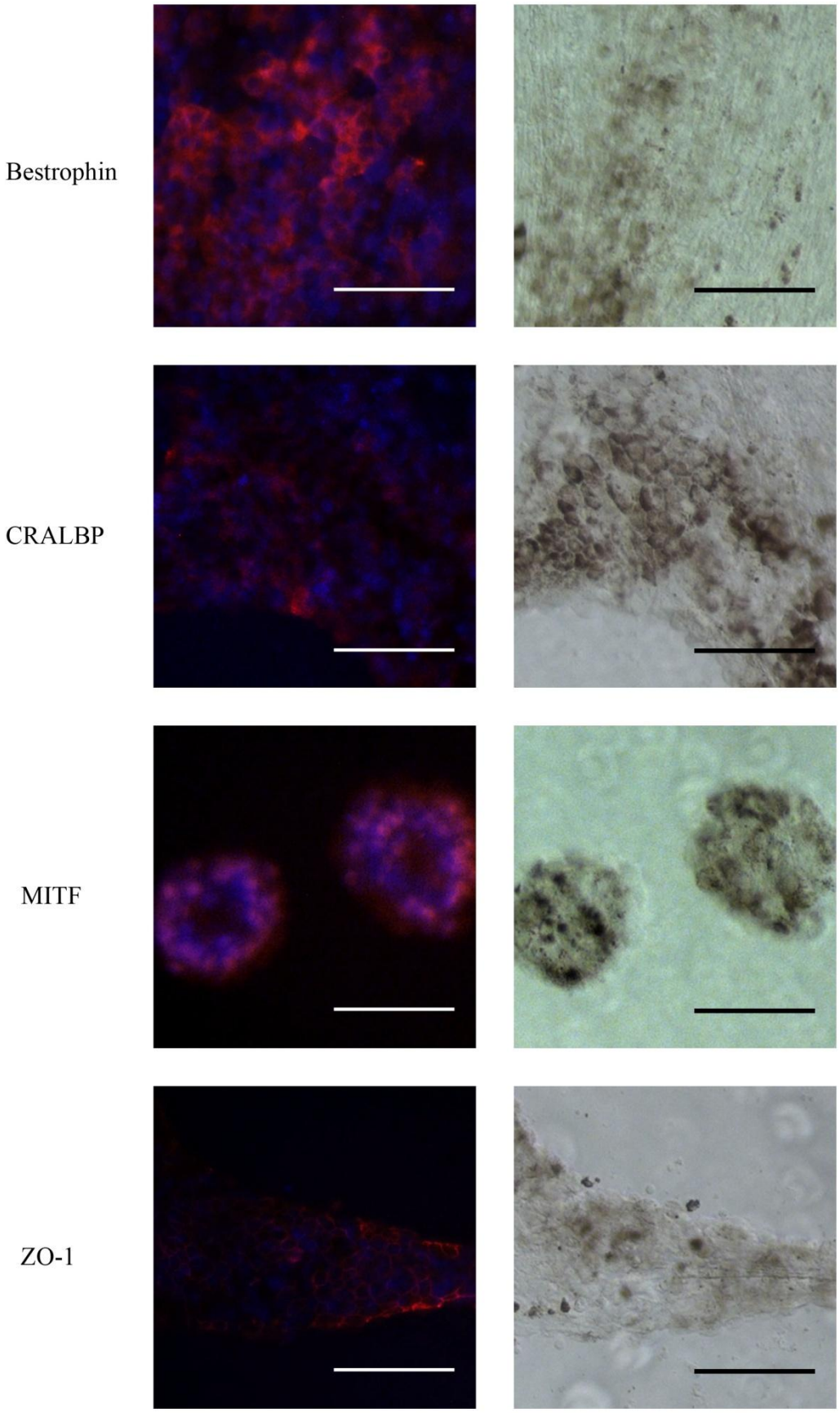

Figure 9.10 *Protein expression of hESC RPE cells cultured on Substrate X. Scale bar length 100 µm.*

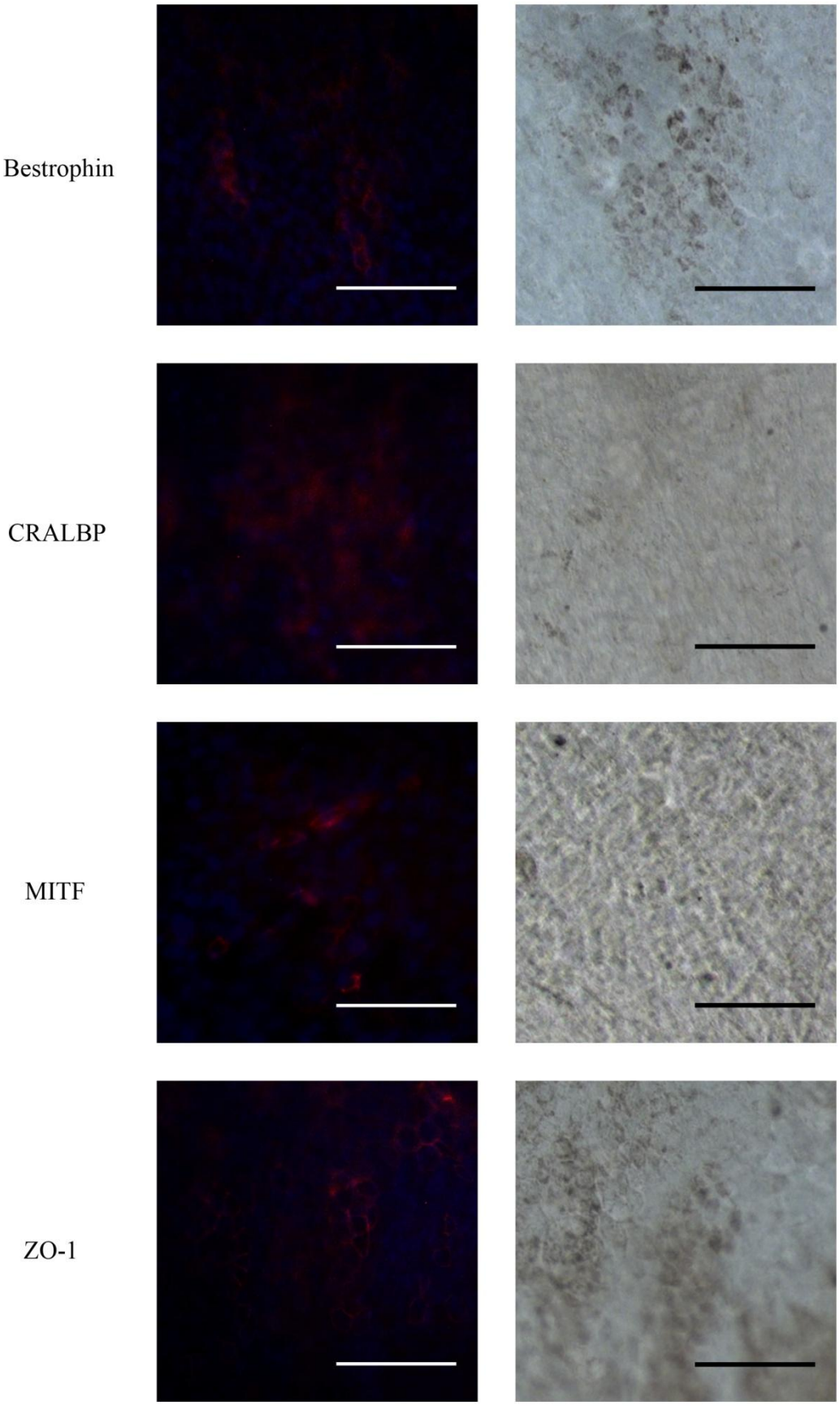

Figure 9.11 *Protein expression of hESC RPE cells cultured on type I collagen. Scale bar length 100 µm.*

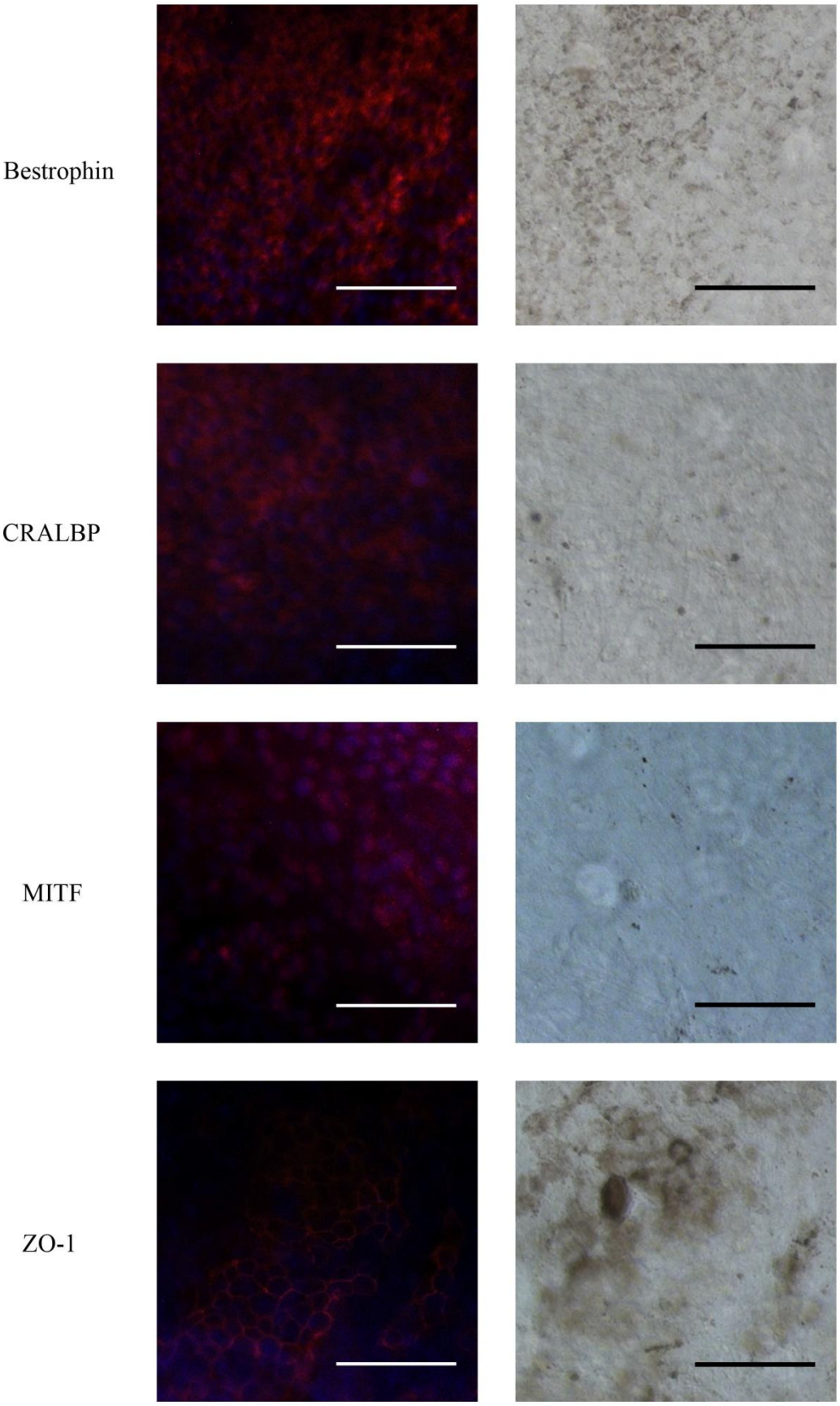

Figure 9.12 *Protein expression of hESC RPE cells cultured on type IV collagen (08/023). Scale bar length 100 µm.*

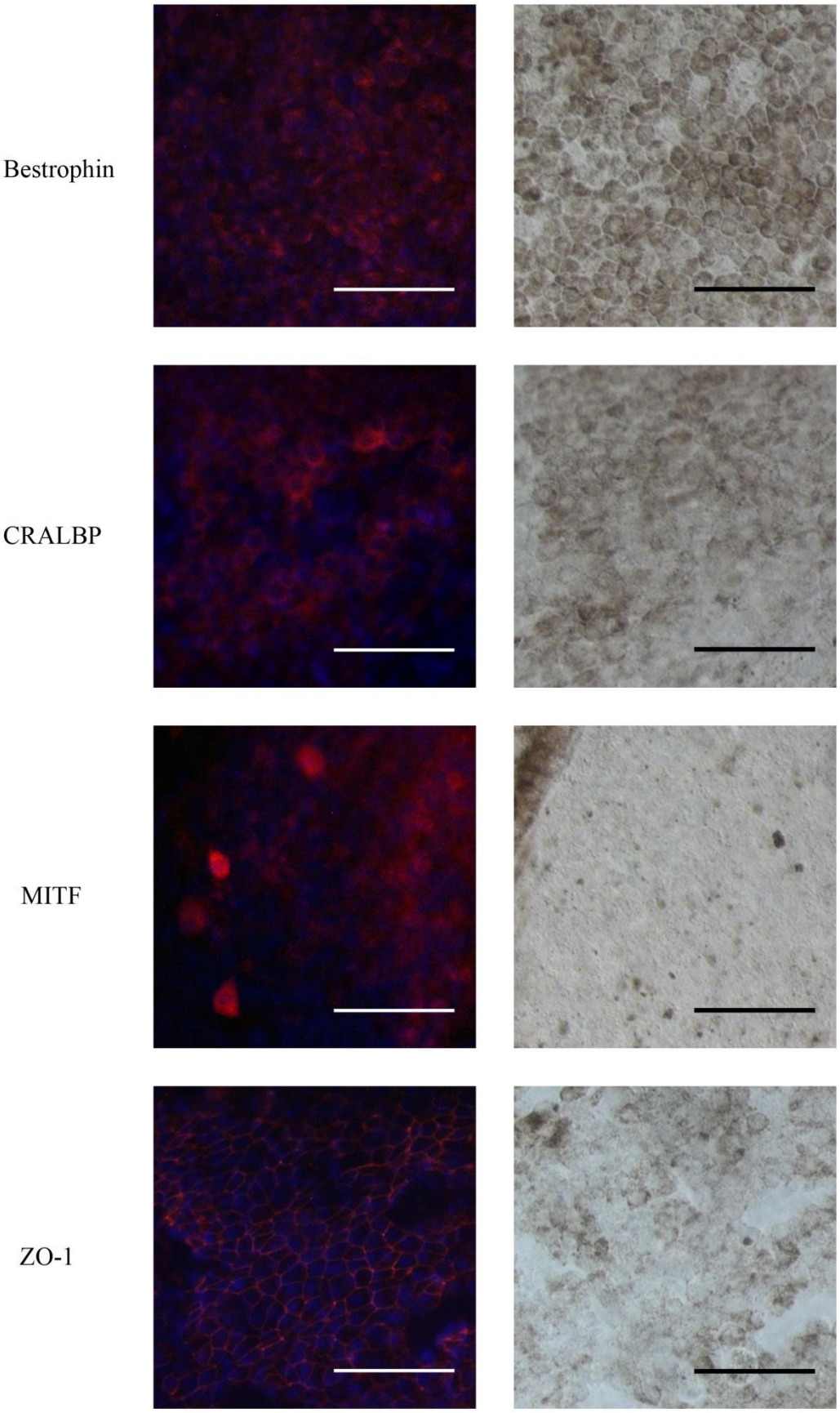

Figure 9.13 *Protein expression of hESC RPE cells cultured on Matrigel™. Scale bar length 100 µm.*

9.4. The image analysis with ImageJ-software

With the intention of producing an automatic image analysis tool for proliferation and maturation monitoring 10 images (Figure 8.4) were analysed using ImageJ-software. Images were taken during the culturing period and selected from different time points in order to present typical growth phases and situations in cell culture. Cells on type IV collagen behaved as expected [100, 104] therefore it was chosen for image analysis.

At first individual macros were created for each photo separately with the intention of combining them later into one single macro. It was found useful to create three different macro types, one for cell count before appearing of cobblestone-like morphology, one for cobblestone-like cell count and one for pigmentation level measuring. Basic tools used in each macro differed. Structures of developed macros are presented in Table 9.4.

Table 9.4 *Basic tools used in different macros*

Tool	Macro for cell count measuring	Macro for cobblestone-like cell count measuring	Macro for pigmentation level measuring
8-bit	Step 1	Step 1	Step 1
Sharpen	Step 2	Step 2	Step 2
Automatic threshold	Step 3	Step 3	Step 3
Convert to mask	Step 4	Step 4	Step 4
Erode		Step 5	
Watershed		Step 6	
Analyze particles	Step 5	Step 8	
Measure			Step 5

However when applying created macros unreliable results were obtained. Proper value for threshold could not be adjusted automatically for each image due to the great variance in background color. After running the macro for cell count measuring results were compared to manual observations. The developed macro could not distinguish two slightly overlapping cells properly and in most cases counted both as one cell. No proper values for size and circularity were obtained, therefore macro could not reliably count in only wanted particles. Finally, macro could not detect edges of fibroblast-like morphology. The most promising results were obtained with other two macros. Cobblestone-like morphology was rather well distinguished by using watershed tool. It was also found that pigmentation measuring could be carried out with a straight-forward macro however a proper threshold-value applicable to all images was not found.

10. DISCUSSION

Malfunctions in RPE can cause retinal degenerative diseases, such as AMD, that affect millions of people worldwide [77, 12]. As being structurally simple however crucial for maintaining overall retinal health [12, 88, 89] RPE is considered to be potential target for tissue engineering [77]. However to date experiments using cell sheets and suspensions have been discouraging [39, 39]. Therefore approach utilizing RPE cells grown on a substrate has raised interest [60, 39]. However, the biocompatibility of allologous or xenologous cell culture substrata meets the requirements poorly. Therefore a xeno-free material is desired option in order to use the cultured cells in therapeutic transplantations [60, 100]. Another obstacle is the limited amount of source tissue which could be addressed by utilizing hESC RPE cells. [77] In addition by using automated image analysis a non-invasive, simple and accurate method to determine the developmental status of RPE cells during the culturing period could be obtained.

This thesis examined the capability of a few specific cell culture substrata to enable attachment, proliferation and maturation of hESC RPE cells towards RPE epithelium. In case a studied material would have performed as desired it could be further utilized as RPE delivery vehicle into subretinal space of patients with retinal diseases. Secondly, this thesis aimed to define how successfully and easily statistical data about the maturation stage of the RPE cells could be obtained by using automated image analysis tool. As being open-source and user-friendly, ImageJ was chosen for the task. [2]

Both synthetic and natural-based materials were selected for this study. Materials included 12 synthetic xeno-free BioMaDe™ Gelators, commercial synthetic Purecoat™ amine and carboxyl surfaces, synthetic PDLLA, PLGA and PLCL membranes, chitosan, Substrate X, type I collagen, Matrigel™ and type IV collagen from human placenta as control. During the culturing period development on materials was monitored by taking images with specific intervals. After culturing period the expression of housekeeping gene GADPH, precursor marker RAX, neural marker SOX2, and mature RPE markers MITF, Bestrophin and RPE65 were determined. In addition, expression and localization of Bestrophin, CRALBP, MITF and Z0-1 proteins was determined with type I and IV collagens, Matrigel™ and Substrate X.

10.1. Type IV collagen controls

Type IV collagen from human placenta was selected as control material for both phase I and phase II mainly due previous positive experiences at Regea [100]. As being natural component of RPE ECM it has performed well as culture substrate in many RPE

experiments [68, 27, 46, 100]. In addition to natural tendency to support cell attachment degradation time (2-7 weeks for not cross-linked collagen) can be easily tailored by cross-linking to suit RPE transplantation [68].

Cell **attachment** of 08/017 and 08/023 cell lines was excellent and spreading was observed already after first days in culture. Cells obtained clear fibroblast-like morphology, proliferated to confluency and formed cobblestone-like centers surrounded by fibroblast-like areas. In phase II with 08/017 cell line material started to tear off from well edge and fold towards center of the well. Nevertheless cells on unfolded area developed in a similar fashion as in phase I. Similar tearing was observed with type IV collagen with 08/023 cell line however into a smaller extent. No remarkable differences between replicates were observed.

Type IV collagen was selected for **gene expression analysis** using RT-PCR in both phases. In phase I total RNA concentration was found rather low (64.20 ng/µl) which was contradictory to visual observations at end point. In addition the purity of sample was questionable (260/280 = 2.41). In phase I cells from type IV collagen expressed all markers excluding SOX2 and RPE65. In phase II total RNA concentration (08/017) was surprisingly high excelling others (188.82 ng/µl), which was surprising since a large area of the coating had been folded. However, the purity of sample was again questioned (260/280 = 2.17). Total RNA concentration obtained from cells on type IV collagen (08/023) was found sufficient (134.40 ng/µl) however with questioned purity (260/280 = 2.25). Gene expression analysis in phase II resulted negative although the procedure was repeated. **Immunofluorescence labeling** showed that cells (08/023) exhibited mature RPE expression of MITF, Bestrophin, CRALBP and ZO-1 proteins [49, 100].

It can be **concluded** that visual observations of type IV collagen control together with gene expression analysis supports the proliferation hypothesis of RPE cells represented by Vugler et al [104]. The cell maturity is supported by marker gene and protein expression profiles which demonstrated typical mature RPE expression as shown in previous studies [104, 74, 15, 49, 100]. As exception, cells on type IV collagen did not express RPE65 indicating that maturity was not complete which could be due to insufficient culture time (5 weeks).

Type IV collagen enables comparison between different cell lines (08/017 and 08/023) since both type IV collagen controls were prepared according to similar protocol. No clear difference on attachment, proliferation and maturation between different cell lines could be observed. Most remarkable difference was the position and size of cobblestone-like areas in the well. Cells from 08/017 cell line formed a large cobblestone-like area in the center of the well as cells from 08/023 cell line appeared as smaller cobblestone-like centers present equally around the well. However, reason for this behavior is probably due to different distribution of cells during seeding procedure or alterations in coating density around the well than cellular differences between cell lines.

Since the measured total RNA concentrations were found sufficient failed gene expression analysis was probably caused by failure in cDNA translation. A suggested explanation for initiation of tearing in phase II is defected batch. In addition, exceptionally warm summer (average app. +40°C) could have affected humidity inside the laboratory.

Despite the serum-free conditions cells attached readily supporting previous results of type IV collagen as material enhancing cellular attachment, proliferation and maturation [68, 27, 46]. However the complex, ill-defined structure of type IV collagen limits its use [87, 68].

10.2. BioMaDe™ Gelators

The BioMaDe™ Gelators were kindly offered to us by BioMaDe Technology Foundation. These nanofibrous scaffolds aim to provide a matrix morphologically similar to natural ECM [10, 111, 33]. In addition, previous promising results concerning hESC-derived cardiomyocyte cultures on HA-modified OG2 and OG8 (unpublished data) raised interest to utilize them in hESC RPE culturing also. Additional replicates of OG2, OG25 and OG49 were modified with HA aiming to enhance the cellular attachment. Also two additional replicates of OG30 had RGD included in the structure.

Attachment varied only little between different Gelators as cells mostly attached in small numbers as large heavily pigmented clusters. Clear proliferation was not observed on any of Gelators however slight spreading of cells was observed on few (OG1, OG2, HA-modified OG2, OG13, OG34, OG49, HA-modified OG49). The number of cells decreased constantly during the culturing period. Cells retained the clustered form throughout the culturing period with no clear changes in pigmentation. HA-modified OG25 and OG30 surface had granular-like irregularities somewhat disturbing cell distinguishing. No clear differences were observed with modified Gelators compared to unmodified ones.

HA-modified OG2, OG13, OG25, HA-modified OG25, OG30, OG34, OG49 and HA-modified OG49 were selected for **gene expression analysis** using RT-PCR. Total RNA concentrations were sufficient for cDNA translation excluding the OG25, HA-modified OG25 and OG49 samples. However, the purity of most samples was questionable. As expected from the visual observations at the end point RPE cells on Gelators mostly exhibited typical mature RPE gene expression with GADPH, MITF and Bestrophin present and RAX and SOX2 absent [104, 74, 15, 49, 100]. On OG13 and OG25 GADPH band was not observed questioning the reliability of the result. On OG25, OG34, OG49 and HA-modified OG49 also RAX was observed indicating presence of precursor state cells.

As a conclusion, BioMaDe™ Gelators supported poorly the attachment of hESC RPE cells. Reason for poor attachment could be the use of RPE DM- medium which due to absence of serum lacks various factors that enhance cell attachment [100, 1]. The attached cells did not proliferate and seemed to retain the clustered form similar to

differentiated EBs from which they have been separated prior to seeding. Gene expression analysis, excluding exceptions with OG13 and OG25, supported the assumption by indicating typical mature RPE cell expression defined in previous studies. [104, 74, 15, 49, 100]. During hESC differentiation towards different lineages they spontaneously cluster into EBs. Low-binding vessels are used to induce EB formation [51]. If cells on Gelators retained EB state it could be assumed that surfaces instead of supporting cell growth would maintain EB state of cells.

The initial shape of Gelators was questionable since tearing on some materials occurred after first days of culture and with HA-modified OG2 already on the first medium change. This could be due to their relatively long storage time (2-3 months at +7°C). Tearing of material that took place during the culturing period could be due to their short degradation time of two weeks (unpublished data). According to the previous studies the maturation of RPE cell culture into a proper state for transplantation occurs typically in 4-6 weeks [104, 74, 15, 49, 100]. Therefore degradation time must be prolonged in order to further utilize the material in RPE transplantation.

Second reason for poor attachment could be the improper pH on the surface of the coating. Some of the wells turned yellow when medium was added first time indicating acidic conditions. This could have affected negatively on cell survival since RPE cells prefer physiological pH. Improper pH was probably due to the residues of hydrochloric acid which is used as solvent during the manufacturing process (unpublished data). Proper pH indicated after DBPS wash could have been temporal however later during the culturing period no problem with pH was detected.

In addition, the main advantage with utilization of hydrogels as scaffold materials is the obtained three-dimensional structure and cellular organization into multiple layers [50]. In RPE transplantation monolayer is the desired organization of cells [60] therefore hydrogels would not be most suitable alternatives to achieve this goal.

Despite the promising results in the literature [110, 22] HA and RGD modified Gelators did not stand out in the test. However no previous studies exist utilizing these bioactive ligands especially in RPE cell culture substrates. Since there is no assurance of the proper initial condition of the Gelators no clear conclusions should be drawn on attachment-enhancing effect of RGD and HA modifications.

10.3. Purecoat™ amine and carboxyl

Commercial xeno-free Purecoat™ amine and carboxyl surfaces were also included in the study mainly due to promising results by Partridge et al. which demonstrated that these surfaces support cellular growth, expansion and differentiation of hASC and hMSC towards adipogenic and osteogenic lineages in serum-free conditions [76]. Furthermore, encouraging results with primary cells of both animal and human origin and with a few established cell lines exists. Amine surface is positively charged while

carboxyl surface in turn possess negative net charge. These properties could provide an alternative for biological attachment factor incorporation. [76]

The **attachment** on both surfaces was relatively good and different from that of BioMaDe™ Gelators since individual cells were present and distributed equally around the well. After first days of culture clear spreading was observed however no proliferation occurred. Morphology of RPE cells was somewhat different from spread cells on type IV collagen with small vesicles appearing in the ends of slightly elongated cells. However after a few days spreading halted and cell number started to decrease. At the end point amine surface excelled slightly the carboxyl surface in the amount of cell material.

Purecoat™ amine surface was selected **for gene expression analysis**. Obtained total RNA concentration (41.04 ng/µl) was found rather low and the sample purity questionable (260/280 = 3.46). Purecoat™ amine expressed GADPH and all mature markers excluding RPE65 indicating typical mature RPE expression [104, 74, 15, 49, 100].

As a **conclusion,** Purecoat™ surfaces supported attachment rather well however they did not enable proliferation of hESC RPE cells. In general, end point observations demonstrated that no clear alterations in cell morphology had been occurred indicating that cells probably retained the EB state. However, a few individual cells obtained an unexpected morphology not typical for RPE cell development [104]. Visual observations were supported by exhibited gene expression. However the purity of the sample brings uncertainty to obtained results. Amine surface excelled carboxyl surface slightly which is probably due to interactions between negatively charged cell glycocalyx and positively charged surface [82]. Despite the promising results with hMSC and hASC differentiation [76] Purecoat™ amine and carboxyl surfaces show no potential as hESC RPE cell substrates at least in serum-free conditions (RPE DM-) [1, 100].

10.4. Poly(D,L-lactide) (96:4)

PDLLA membranes were manufactured specifically for this study. As being approved by FDA for use in humans PDLLA has been widely studied in different tissue engineering applications. Fetal RPE and ARPE-19 cells have been reported to grow successfully on PDLLA substrates [68, 30, 93]. However no study including hESCs has been carried out.

During manufacturing process PDLLA membranes were detached from the plates used in compression moulding using 70% ethanol. Also the desinfection was carried out using 70% ethanol (1 h, dried overnight in laminar hood). Membranes were attached to the bottom of the well with CellCrown™ cell culture inserts.

Attachment on PDLLA was poor occurring mainly close to well edge and CellCrown™ inserts. Cells appeared as pigmented clusters in a similar fashion as on BioMaDe™ Gelators and remained that way throughout the culturing period however

the number of cells constantly decreased. Only few individual de-pigmented cells were observed. When approaching the end point transparency of the membranes started to decrease which could sign initiated degradation.

Non-textured PDLLA was estimated to possess enough cell material to carry out cDNA translation thus it was selected for **gene expression analysis**. Total RNA concentration was not found sufficient (0.31 ng/µl) however cDNA translation was carried out. The purity of sample was again an issue (260/280 = -0.10). RT-PCR analysis resulted negative despite the repetitions.

As a **conclusion**, PDLLA membranes performed poorly as cell culture substrates for hESC RPE cells. Cells remained mostly as pigmented clusters throughout the culturing period adopting no clear morphological changes. This could demonstrate similar development as concluded previously with BioMaDe™ Gelators, that is, cells retained the EB state throughout the culturing period. If EB state was maintained PDLLA could have similar low-binding effect as vessels used in EB induction [51]. Non-textured surface outmatched textured one only slightly. This is rather welcomed piece of information since the detachment of non-textured membranes from the plates during processing is rather difficult.

Poor outcome with PDLLA is rather surprising since large body of literature exists with encouraging results concerning RPE cell cultures on PDLLA [68, 30, 93]. A crucial point is that the cells used in these studies, ARPE-19 and fetal RPE cells, may not be as selective as hESC RPE cells regarding to their growth environment. In addition in each experiment culture medium included FBS. In this study cells were cultured in serum-free medium (RPE DM-) which could be reason for poor attachment on all xeno-free synthetic substrates [1, 100].

One reason explaining poor performance could be improper desinfection method. Alcohols have been used in permeabilization of RPE cells for example in immunofluorescence labeling therefore they are expected to have ill effect on cell survival [24]. During the process material could have absorbed ethanol which due to insufficient drying procedure could have resulted in poor attachment and survival of the cells [24, 5, 100].

In addition, PDLLA degrade into mildly acidic degradation products [68]. This could have caused temporal changes in pH which could have affected cell survival. Degradation was observed during the culturing period as reduction in transparency however no change in pH was indicated by changes of medium color.

One reason affecting poor outcome could be the Teflon tape that was used to provide texture on the surface of PDLLA. During the processing and detachment of membranes, residues of Teflon could have attached to membrane and remained there through wash procedure ultimately leading to poor cell survival. However no clear differences between textured and non-textured surfaces were observed.

Obtained PDLLA membranes were significantly thick however this factor was not in focus since the membranes were not porous. Therefore it was not expected for transportation of nutrients to occur through the membrane. Despite the fact that

thickness is important factor concerning membrane degradation in this study it was considered to have small role since culturing period was short compared to degradation time [68]. More significantly thickness could have affected the amount of ethanol absorbed in the structure. Also in the future when implanting the cell-membrane structure into subretinal space thickness must be significantly smaller.

An important factor is that attachment of PDLLA membranes to the bottom of the well was questionable since the conditions of at least some CellCrown™ cell culture inserts were not proper due to the second hand use. Even though attachment was confirmed before cell seeding loosening could have occurred during medium changes. This was supported by observations of cell growth underneath the membrane.

Despite the fact that the amount of seeded cells was high the attachment was poor. The negative result of gene expression could be due to following factors. The amount of total RNA could have been insufficient for proper cDNA translation. In addition the protein content of total RNA sample could have disturbed the cDNA translation and result in negative outcome.

10.5. Poly(D, L-lactide-*co*-glycolic acid) (75:25)

Also PLGA membranes were manufactured specifically for this study. FDA approval for use in humans has resulted in extensive research in many biomedical applications [68]. As with PDLLA, ARPE-19 and D407 have been grown successfully on PLGA substrates [30, 95, 59, 93] however no study including hESC RPE cells has been carried out.

Detachment and desinfection was carried out using 70% ethanol (1 h, dried overnight in laminar hood). Membranes were attached to the bottom of the well with CellCrown™ cell culture inserts.

Attachment of cells on PLGA membranes was similar to PDLLA, that is, low and located mainly close to well edge and CellCrown™ inserts. Cells formed mainly pigmented clusters and remained that way throughout the culturing period however the number of cells decreased in faster pace than on PDLLA. Also with PLGA a few individual de-pigmented cells were observed. At the end point cell material was not found sufficient for gene expression analysis. Also with PLGA transparency of the membranes started to decrease when approaching the end point.

As a **conclusion**, PLGA performed poorly as cell culture substrate for hESC RPE cells. As with PDLLA, cellular development can be only concluded from visual observations. Despite the high amount of seeded hESC RPE cells attachment was poor. Similarly as on BioMaDe™ Gelators and PDLLA cells remained mostly as pigmented clusters throughout the culturing period indicating no clear morphological changes. This supports the assumption that cells retained the EB state throughout the culturing period. In case assumption is right PDLLA could possess similar low-binding tendency as vessels used in EB induction [51]. Again no clear differences in cellular behavior were observed related to texture on the membranes.

Since many successful experiments utilizing PLGA as RPE cell culture substrata exist [30, 95, 59, 93] poor support of cellular attachment and growth in this test was surprising. However each of these studies utilized FBS in their culture medium which is known to enhance cellular attachment [1]. ECM influence on hESC RPE cells is rather poorly known (dissertation of MSc H. Hongisto partly covers this topic) and more research must be carried out to understand the complex interactions better.

As with PDLLA reason for poor outcome could be high selectivity of hESC RPE cells on their growth substrata. In addition it is possible that serum-free conditions did not support sufficiently enough the cellular attachment. [1, 100] In addition similar desinfection method was used for PLGA as with PDLLA, that is, 70% ethanol wash for 1 h and overnight drying in laminar hood. Ethanol residues could have remained in the structure causing alterations in cell membrane [24, 5, 100]. Also the membrane attachment to the bottom of the well could have been improper causing the membrane to move during culturing period which was supported by the fact that cells were observed underneath the membrane.

One factor affecting negatively on survival of the cells could be initiated degradation of PLGA which was observed as decrease in transparency. As PLGA degrade into mildly acidic degradation products pH on the surface could have decreased however this was not observed as change in medium color [68]. A factor possibly affecting poor outcome could be the Teflon tape that was used to provide texture on the surface. As with PDLLA residues of Teflon could have attached to membrane and remained there through wash procedure ultimately affecting to cell survival. However no clear differences between textured and non-textured surfaces were observed. In the following studies monitoring of surface could provide information on these issues.

Better survival could hardly be obtained with different monomer ratio since PLGA (75:25) has degradation time approximately 4-5 months [68]. Use of PLGA (50:50) could result in too fast degradation (1-2 months). This can be only reasoned in theory since no membranes with other ratios were involved.

10.6. Poly(L-lactic acid-*co*-ε-caprolactone) (70:30)

Also PLCL membranes were produced especially for this study. To date PLCL has been mainly studied for drug delivery and bone regeneration applications [102, 44, 19] however it was chosen for this study due to its well-fitting properties [68, 58, 90]. Similar desinfection protocol was carried out as with PDLLA and PLGA using 70% ethanol (1 h, dried overnight in laminar hood). Again, CellCrown™ cell culture inserts were used to attach membranes to the bottom of the well.

Similarly as on PDLLA and PLGA **attachment** on PLCL membranes was low and occurred mainly close to well edge and CellCrown™ inserts. Cells were mainly clustered in a similar fashion as with PLGA and PDLLA and remained that way throughout the culturing period. The number of cells was found to decrease slightly faster than on PDLLA. At the end point cell material was not found sufficient for gene

expression analysis. The clustered cells remained pigmented throughout the culturing period. Also with PLCL reduction in membrane transparency was observed during the culturing period possibly indicating initiated degradation.

It can be **concluded** that PLCL performed poorly as cell culture substrate for hESC RPE cells. The high amount of seeded cells did not result as high attachment. Again cellular development can be only concluded from visual observations. Similar conclusion can be drawn as previously with BioMaDe™ Gelators, PDLLA and PLGA, that is, cells retained the EB state throughout the culturing period. This could indicate that PLCL maintain EB state in a similar fashion as low-binding vessels [51]. Again, texture on the membrane surface had no notable effect on cell attachment or survival. Despite the encouraging results in bone regeneration applications [102, 44, 19] PLCL showed poor suitability as hESC RPE cell substrate. However, as this study was first of a kind and a few reliability decreasing factors were involved too final conclusions should not be drawn.

Also with PLCL high hESC RPE selectivity in addition with serum-free medium (RPE DM-) [1, 100] could be reasons for poor outcome. Again, similar desinfection method was used as with PDLLA and PLGA, that is, 70% ethanol wash for 1 h and overnight drying in laminar hood which could have left alcohol residues inside the membrane structure. This factor is highlighted with PLCL since the material has high permeability [68, 44]. Alcohol release from the structure during culturing period could have affected negatively on cell survival [24, 15, 100].

Also with PLCL cells were spotted below the membrane indicating poor attachment of second-hand CellCrown™ inserts. As with PDLLA and PLGA a factor affecting poor performance could be initiated degradation of PLCL membranes which could have lowered surface pH [68] however this was not indicated as color change in culture medium. One factor affecting attachment and cell survival on textured membranes could be Teflon tape residues as was reasoned with PDLLA and PLGA.

Lactic acid and ε-caprolactone monomer ratio could hardly have effect in this study since the degradation time of pure poly(ε-caprolactone) and pure poly(lactid acid) is significantly longer than culturing period in this study (app. 2 years and app. 6 months) [68]. However this can be only reasoned in theory since no membranes with other ratios were involved.

10.7. Chitosan

Despite the fact that no studies exist combining chitosan and RPE cells, the material was included in the study due to its wide use in biomedical applications [80]. Chitosan properties, including good biocompatibility and easy processing to thin smooth structures [68] fit well for utilization as RPE scaffold [80]. Furthermore, positive surface charge could function as attachment enhancing factor due to negative charge of cell glycocalyx [82]. As being polysaccharide with natural origin [68] good cellular attachment was hoped.

Attachment on chitosan was relatively good and equal around the well. Instead of forming clusters cells appeared more as individuals however no clear spreading was observed. Again the cell number decreased constantly during the culturing period however with lower rate compared to poly-α-esters. At the end point both pigmented cells and cells with partly lost pigmentation were observed.

The amount of cell material was estimated to be sufficient to carry out cDNA translation therefore it was selected for **gene expression analysis**. Total RNA measuring was not reliable (-5.46 ng/µl) in addition to questionable purity (260/280 = 1.17). Unsurprisingly, RT-PCR resulted negative.

The **results** showed that performance of chitosan coatings as cell culture substrates for hESC RPE cells was poor. Despite the rather good attachment no proliferation occurred. Some cells however lost their pigmentation during the culturing period. Unfortunately, no gene expression data was obtained. When compared to Purecoat™ amine similarity in cell behavior could be observed including presence of individual cells and equal distribution around the well. In addition amount of cell material at the end point was slightly higher than with xeno-free materials. This could be due to positive surface charge of both chitosan and Purecoat™ amine [76] which could have at least to some extent enhanced cell attachment. In the future studies this factor should be taken into closer examination.

The main reason for poor success of chitosan could be the improper surface pH. This factor is highlighted since chitosan is highly pH sensitive [68, 80]. During the wash procedure the removal of excess NaOH could have been insufficient resulting in poor survival of cells. Despite that pH measuring was carried out after DBPS wash surface pH could have been only temporarily proper. However no changes in medium color were observed during the culturing period. In the future monitoring the surface pH during the culturing period could answer to this issue.

Other reasons affecting poor performance could be serum-free medium (RPE DM-) [1, 100] combined with hESC RPE cells high selectivity of substrate material. Since a few factors decreases reliability of obtained result no final conclusions should be made on chitosan suitability to RPE cell culturing. In addition as novel approach to produce chitosan coatings was applied optimization of different steps of production process need to be done with special emphasis on desinfection procedure.

10.8. Substrate X

Substrate X is a lectin with plant-origin provided for this study by Finnish Red Cross. Since it is still under development available data concerning its structure and functions is limited. Basic function of Substrate X is to provide binding sites for RPE cell glycocalyx components therefore supporting cellular attachment. To date no studies including RPE cells grown on Substrate X have been reported.

Attachment on Substrate X was good however significantly different than on other natural-derived materials. At first cells formed a few remarkably large clusters

which then started to spread creating large areas with fibroblast-like morphology ultimately turning into cobblestone-like areas with slight pigmentation. Confluency was not reached and development was observed to halt before end point.

However, Substrate X was selected for **gene expression analysis** and immunofluorescence labeling. Contradictory to visual observations total RNA concentration was found to be very low (10.26 ng/µl) with low purity (260/280 = 3.05) however cDNA translation and RT-PCR analysis was carried out with negative result. **Immunofluorescence study** showed typical mature RPE cell expression [104, 100] of Bestrophin, CRALBP, MITF and ZO-1.

As a **conclusion** Substrate X supported hESC RPE cell attachment, proliferation and maturation however with rather different morphological development of cell culture compared to type I and IV collagens. On the spread areas the individual cell development was found to be typical for RPE cells [104]. This was supported by protein expression study which indicated presence of mature RPE markers [104, 100]. In general, Substrate X shows potential as hESC RPE cell culturing substrate. Unfortunately gene expression could not be determined which was probably due to two factors: insufficient amount of total RNA and failure in cDNA translation.

Reason for exceptional culture appearance could be folding of material as was the case with type IV collagen (08/017) control since appearances in both cases had clear similarities. Folding could be due to failures in carrying out Substrate X coating protocol otherwise stability of the coating can be questionable.

The plant-origin can form a limiting factor for further use of Substrate X in RPE transplantation [87]. However no publications to provide basis for comparison exist. Since a few factors reduces the reliability of this result final conclusions on suitability of Substrate X for hESC RPE culturing should not be drawn.

10.9. Type I collagen

Type I collagen, a natural component of RPE ECM, has natural tendency to enhance cellular attachment and proliferation [68, 58, 27]. In addition degradation time can be tailored to some extent by cross-linking in order to better suit RPE transplantation [68]. Encouraging results have been reported concerning hESC differentiation towards RPE lineage in addition to cell culture experiments with ARPE-19 cells [49, 58, 97].

The **attachment** on type I collagen was excellent and spreading was observed already after first days. Cells reached confluency after approximately two weeks and started to obtain cobblestone-like morphology. At the end point cell material was extensive.

Type I collagen was selected for both **gene expression analysis** and immunufluorescence study. Contradictory to visual end point observations total RNA concentration (74.93 ng/µl) was low however sufficient to carry out cDNA translation. Purity (260/280 = 2.41) was again an issue. RT-PCR analysis resulted negative despite the repetitions. However type I collagen showed typical mature RPE cell **expression**

and localization of Bestrophin, CRALBP and ZO-1 excluding MITF which was exceptionally located on cell membrane instead of nucleus [104, 100].

As a **conclusion**, type I collagen performed well in this study which was expected due to previous successful studies [58, 49, 97]. The substrate clearly supports hESC RPE cell attachment, and more significantly, in serum-free conditions [1, 100]. Cells obtained fibroblast-like and cobblestone-like morphologies typical for developing RPE cell culture [104]. Maturity of RPE cell culture was supported by immunofluorescence labeling of mature RPE markers however MITF was located untypically [104, 100]. Unfortunately no gene expression data was obtained which is probably due to failure in cDNA translation since total RNA concentration was found sufficient.

The primary functions of type I and type IV collagens differ as type I collagen is present in structures that have to tolerate high forces while type IV collagen is part of loose fibrillar networks directing cell migration, attachment and differentiation. [58, 27, 46] This study enabled comparison of these two RPE ECM proteins in terms of morphology and protein expression. As expected a few slight differences between type I and type IV collagens were observed. These include slightly better attachment, appearing of cobblestone-like morphology a few days earlier and slightly more advanced pigmentation on type IV collagen.

Despite the encouraging results further use of type I collagen as RPE delivery vehicle faces challenges. Further knowledge about complex structure must be obtained in order to minimize unexpected behavior [87, 68]. In addition further knowledge could enable enhancement of mechanical properties more efficiently [68].

10.10. Matrigel™

Commercial Matrigel™ has been in extensive use as cell platform in many cell culturing studies [72, 104, 31, 105] and good results have been reported with both normal and transformed anchorage dependent cells [72]. Matrigel™ has also been used as platform for RPE differentiation [104, 31]. Matrigel™ is rich in different proteins and GFs naturally occurring in RPE ECM [72]. However its tumor-origin [72] creates a clear obstacle for further use in RPE applications [87].

Attachment on Matrigel™ slightly excelled both collagens. Cells spread, proliferated to confluency and formed cobblestone-like centers with heavy pigmentation. At the end point amount of cell material was extensive. Matrigel™ was clearly the most advanced material with highest attachment, fastest proliferation and largest cobblestone-like areas with most advanced pigmentation.

Due to high amount of cell material Matrigel™ was selected for **gene expression analysis**. The relatively low concentration of extracted total RNA sample (87.91 ng/µl) was surprising since cells on Matrigel™ had clearly reached confluency. Again, problems existed concerning purity of the sample (260/280 = 2.28). Despite the proper amount of total RNA RT-PCR analysis resulted negative. The **immunofluorescence**

labeling indicated that cells exhibited typical mature RPE expression and localization of MITF, Bestrophin, CRALBP and ZO-1 [104, 100].

As a **conclusion** Matrigel™ supports well RPE cell culturing which was expected from previous results [72, 104, 31]. As with type I and IV collagens typical phases of cellular growth were observed [104]. However, pigmentation and amount of cobblestone-like structures were slightly higher compared to type I and type IV collagens which probably results from rich protein and GF content [72]. Maturity of RPE cell culture was further confirmed by protein expression [104, 100]. Although sufficient total RNA concentration was obtained RT-PCR analysis resulted negative which is probably due to failure in cDNA translation.

Though studies applying Matrigel™ as cell differentiation substrate exists [104, 31] this study was first of a kind in examining its possible use as RPE cell maturation substrate. Major obstacle impeding further use as RPE delivery vehicle is the xenologous origin [72] that does not meet GMP standards [87]. Complex structure including numerous components with complex biological effects must be more specifically examined [72].

10.11. Image analysis with ImageJ-software

A specific series of images (type IV collagen) from different time points of culture were analyzed using ImageJ-software. ImageJ-software was chosen mainly due to previous positive experiences and its user-friendliness. In addition it is freely downloadable from public domain together with multiple plugins. [2] Aim of this part of the thesis was to define how successfully and easily ImageJ could be used to provide statistical data about the maturation stage of the RPE cells. Examined factors were cellular proliferation rate, morphology and the amount of pigmentation.

The approach used in this thesis based strongly on study by Luc Vincent in which he presented an effective way to analyze corneal endothelium cells [103]. Furthermore the approach was also influenced by work of Lehmussola et al. [54]. As appearances of mature corneal and RPE epitheliums have significant similarities the presented techniques could be applied also in RPE epithelium images [100, 103]. However, when Vincent's focus was on images with cobblestone-like morphology [103] this study tried to cover all typical phases of growth including early attachment, proliferation as fibroblast-like cells and finally the maturation into cobblestone-like morphology [104].

To achieve this goal three different basic macros [2] were created to determine cell count at early and proliferation stages, at cobblestone-like mature stage and to estimate amount of pigmentation. Basic tools used in each macro differed. Proper value for threshold could not be adjusted automatically for each image due to the high variance in background color. The estimation of pigmentation level was carried out with simpler macro.

Following problems arose during the process. First, the differences between images in exposure, lightning conditions, colors and focus varied greatly which are widely occurring technician-based problems in image processing [54]. Therefore creating a single macro to process all of the images was impossible since finding proper thresholding value to cover all images could not be achieved. In general, RPE cell culture in random stage can appear with all of the typical cell types including recently attached round-shaped cells, elongated fibroblast-like cells with hardly distinguishable borders and emerging cobblestone-like morphology [104, 100, 49, 60]. Therefore setting proper values for size and circularity parameters is extremely challenging. According to Lehmussola et al, no extensive models for cell shape determining have been proposed to date that cover all variations of cell shape [54].

Second, the cells with fibroblast-like morphology do not have easily distinguishable edges [104, 100, 49, 60]. Third, at the early phases of cell culture period the cells formed aggregates in which they appeared to overlap creating difficulties in distinguishing the actual cell count both manually and automatically. Also situations in which two or more cells have attached to each other created problems since many times watershed tool could not understand them as separate objects. Fourth, the round-shaped objects that were rather straightforward to distinguish automatically in most cases represented detached cells. Therefore when estimating cell attachment they should not be counted in. This created problems in determining proper circularity values for appropriate use of analyze particles-tool. Similar problem arose with necrotic cells and cell debris as being easy to distinguish manually but difficult automatically.

The images analyzed in this study represent products of typical imaging session. In order to achieve more homogenous images imaging conditions should be more carefully considered including especially lightning conditions and color. This could also be helped by developing better image restoration algorithms as has been stated by Lehmussalo et al. [54].

11. CONCLUSIONS

The aim of the study was to examine potential of a few specific xeno-free and natural-based materials to be used as cell culture substrates for hESC RPE cells and ultimately as cell transplantation vehicle in therapies to cure retinal diseases. During the culturing period cells were monitored by taking images with regular time intervals, the end point gene expression analysis was carried out using RT-PCR techniques and immunofluorescence labeling of mature RPE markers was carried out for type I and type IV collagens, Matrigel™ and Substrate X. In addition potential of ImageJ-software to function as automated analysis tool for cell count, morphology and pigmentation measuring was determined.

As a conclusion, xeno-free synthetic materials performed poorly in the test and did not support hESC RPE cell culturing. Incorporation of bioactive ligands with BioMaDe™ Gelators and surface-patterning with poly-α-esters did not result in enhanced attachment. The attached cells seemed to retain the clustered form similar to EBs which was supported by gene expression analysis. Result was unexpected since large body of literature reports promising results concerning RPE culturing on PDLLA and PLGA [68, 95, 30, 59, 93]. On the contrary, natural materials showed opposite behavior which correlated with existing literature [58, 49, 68, 27, 46, 97]. On type I and type IV collagens, Matrigel™ and Substrate X cells attached, proliferated and maturated readily which was verified by both microscopic observations and immunofluorescence labeling. As exception, cellular behavior on chitosan was more similar to synthetic substrates however differences in cell number and distribution were observed.

Several factors could explain the poor performance of xeno-free materials and chitosan. Residues of solvents (BioMaDe™ Gelators), NaOH (chitosan) and ethanol (poly-α-esters) used in manufacturing could have remained in the structure despite wash and neutralization procedures. Culture medium containing ill-defined serum may cause unpredictability to cell behavior and is therefore undesired [1]. However, the absence of serum in this study could have caused too scarce culture conditions for hESC RPE cells. Also should be emphasized that existing RPE experiments on poly-α-esters have been carried out mainly using ARPE-19 and D407 cell lines [58, 90, 97, 59, 93] which are not as selective as hESC RPE cells for their culture substrata.

Study also demonstrated that image analysis using ImageJ was not successful. Reliable results were obtained solely when analyzing cobblestone-like morphology and pigmentation, that is, on a narrow segment of cellular development. Main issue is the heterogeneity of images which makes impossible to use single macro for every image.

In addition, a typical RPE cell culture consists of a wide variety of particles with different shapes which creates challenge for cell distinguishing.

However, the reliability of the conclusions is questioned by several factors including poor initial condition of BioMaDe™ Gelators and questionable membrane attachment of poly-α-esters which could have affected cell attachment and proliferation negatively. Due to insufficient amount of cell material in phase I only gene expression data was obtained to confirm cellular maturity in addition to visual observations. In addition, gene expression analysis in the phase II resulted negative therefore only immunofluorescence labeling provided data about cellular maturation stage. Despite these factors it can be concluded that the aims of this thesis were reached.

11.1. Future aspects

Despite the poor outcome BioMaDe™ Gelators should be further studied since poor initial condition of materials decreases reliability of the result. The typical time of RPE cell culture to reach maturity is approximately 3-5 weeks [100] therefore degradation time of Gelators needs to be prolonged to suit better RPE culturing. In addition poly-α-esters should be also further studied however with more careful removal of ethanol residues. A possible solution could be vacuum drying however a more throughout sterilization method is necessary when clinical trials are considered. Utilization of solvent casting method to produce smooth poly-α-ester coatings has already been reported [39]. Since RPE cells are known to prefer smooth surfaces when cultured *in vitro* [90] this method could provide superior surface than what is obtained by compression molding and therefore enhance cell attachment. Despite the good results with hMSC and hASC [76] Purecoat™ surfaces show no potential for RPE culturing.

As being natural components of RPE ECM type I and IV collagens support readily cellular attachment, proliferation and maturation of hESC RPE cells. In addition Substrate X showed similar behavior. Chitosan, on the other hand, showed poor performance and future research should be on other natural materials. The main problem regarding the use of natural-based proteins is the ill-defined and complex structure that is prone to alterations in physiological environment. A solution for this problem could be isolation of functional groups participating in cell attachment and uniting them with synthetic well-defined body. This way the strengths of both approaches could be combined. In addition, reasons for high selectivity of hESC RPE are poorly understood. Additional information on hESC RPE and ECM interactions together with better exploiting of hESC N-glycome profile will be steps forward on this goal.

The main issue concerning the effective use of ImageJ in image analysis was heterogeneity of images. The severity of this problem can be minimized by paying attention to imaging conditions. In addition ImageJ allows development of custom plugins however this feature was not exploited in this study due to lack of programming skills. In further use of ImageJ this possibility should be considered.

REFERENCES

[1] Abraham, E. J. & Thompson K. Advanced Cell Culture Surfaces: BD Purecoat surfaces provide improved cell attachment and growth of many cell types compared to standard tissue culture vessels. Application note 470. BD Biosciences.

[2] Abramoff, M. D., Magelhaes, P. J., Ram, S. J. 2004. Image Processing with ImageJ. Biophotonics International, 11, 7, pp. 36-42.

[3] Aisenbrey, S., Zhang, M., Bacher, D., Yee, J., Brunken, W., J. & Hunter, D. D. 2006. Retinal pigment epithelial cells synthesize laminins, including laminin 5, and adhere to them through α3- and α6-containing integrins. Investigative Opthalmology & Visual Science 47, 12, pp. 5537-5544.

[4] Amabile, G. & Meissner, A. 2009. Induced pluripotent stem cells: current progress and potential for regenerative medicine. Trends in Molecular Medicine 2, pp. 59-68.

[5] Arden, G. B., Wolf, J. E., Singcartl, F., Berninger, T. E., Rudolp, G. & Kampik, A. 2000. Effect of alcohol and light on the subretinal pigment epithelium of normal subjects and patients with retinal dystrophies. British Journal of Ophthalmology 84, pp. 881-883.

[6] Auer, S., Lappalainen, R. S., Skottman, H., Suuronen, R., Narkilahti, S. & Vikholm-Lundin, I. 2009. An Antibody Surface for Selective Neuronal Cell Attachment. Journal of Neuroscience Methods 186, 1, pp. 72-76.

[7] Bajpai, S. K., Singh, S. 2006. Analysis of swelling behavior of poly(methacrylamide-*co*-methacrylic acid) hydrogels and effect of synthesis conditions on water uptake. Reactive and Functional Polymers 66, pp. 431-440.

[8] Bharti, K., Nguyen, M-T., Skunz, S., Bertuzzi, S. & Arnheiter, H. 2006. The other pigment cell: Spesification and development of the pigmented epithelium of vertebrate eye. Pigment Cell & Melanoma Research 19, pp. 380-394.

[9] Binder, S., Stanzel, B. V., Krebs, I., Glittenberg, C. 2007. Transplantation of the RPE in AMD. Progress in Retinal and Eye Research 26, pp. 516-554.

[10] BioMaDe Technology Foundation. [WWW]. Sited: 31.3.2011. Available: http://www.biomade.nl/.

[11] Blasi, P., Schoubben, A., Giovagnoli, S., Perioli, L., Ricci, M., Rossi, C. 2007. Ketoprofen Poly(lactide-co-glycolide) Physical Interaction. American Association of Pharmaceutical Scientists 8.

[12] Bok, D. 1993. The retinal pigment epithelium: a versatile partner in vision. Journal of Cell Science – Supplement 17, pp. 189-195.

[13] Braam, S. R., Zeinstra, L., Litjens, S., Ward-van Oostwaard, D., van den Brink, S., van Laake, L., Lebrin, F., Kats, P., Hochstenbach, R., Passier, R., Sonnenberg, A. & Mummery, C. L. 2008. Recombinant vitronectin is a functionally defined substrate that supports human embryonic stem cell self-renewal via alphavbeta5 integrin. Stem Cells 26, 9, pp. 2257-65.

[14] Buchholz, D. E., Hikita, S. T., Rowland, T. J., Friedrich, A. M., Hinman, C. R., Johnson, L. V. & Clegg, D. O. 2009. Derivation of functional retinal pigmented epithelium from induced pluripotent stem cells. Stem Cells 27, pp. 2427-34.

[15] Carr, A. J, Vugler, A., Lawrence, J., Chen, L. L., Ahmado, A., Chen, F. K., Semo, M., Gias, C., da Cruz, L., Moore, H. D., Walsh, J. & Coffey P. J. 2009. Molecular characterization and functional analysis of phagocytosis by human embryonic stem cell-derived RPE cells using a novel human retinal assay. Molecular Vision 15, pp. 283-295.

[16] Carr, A. J., Vugler, A. A., Hikita, S. T., Lawrence, J. M., Gias, C., Chen, L. L., Buchholz, D. E., Ahmado, A., Semo, M., Smart, M. J., Hasan, S., da Cruz, L., Johnson, L. V., Clegg, D. O., Coffey, P. J. 2009. Protective effects of human iPS-derived retinal pigment epithelium cell transplantation in the retinal dystrophic rat. PLoS ONE 4:e8152.

[17] Cazuguel, G. & Mimouni, F. 1989. Extraction automatique des contours cellulaires de l'endothelium cornèen humain. Innovation and Technology in Biology and Medicine 10, pp. 659-667.

[18] Chambers, I. & Tomlinson, S. R. 2009. The transcriptional foundation of pluripotency. Development 136, pp. 2311-22.

[19] Coombes, A. G. A., Rizzi, S. C., Williamson, M., Barralet, J. E., Downes, S. & Wallace, W. A. 2004. Precipitation casting of polycaprolactone for applications in tissue engineering and drug delivery. Biomaterials 25, pp. 315-325.

[20] Da Cruz, L., Chen, F. K., Ahmado, A., Greenwood, J. & Coffey, P. 2007. RPE transplantation and its role in retinal disease. Progress in Retinal and Eye Research 26, pp. 598-635.

[21] Del Priore, L. V. & Tezel, T. H. 1998. Reattachment rate of human retinal pigment epithelium to layers of human Bruch's membrane. Archives of Ophthalmology 116, pp. 335-341.

[22] Doran, M. R., Frith, J. E., Prowse, A. B. J., Fiztpatrick, J., Wolvetang, E. J., Munro, T. P., Gray, P. P. & Cooper-White, J. J. 2010. Defined high protein content surfaces for stem cell cultures. Biomaterials 31, pp. 5137-5142.

[23] Dunn, K. C., Aotaki-Keen, A. E., Putkey, F. R. & Hjelmeland, L. M. 1996. ARPE-19, A Human Pigment Epithelial Cell Line with Differentiated Properties. Experimental Eye Research 62, pp. 155-169.

[24] Eldred, W. D., Zucker, C., Karten, H. J. & Yazulla, S. 1983. Comparison of fixation and penetration enhancement techniques for use in ultrastructural immunocytochemistry. The Journal of Histochemistry and Cytochemistry 31, pp. 285-292.

[25] Farrokh-Siar, L., Rezai, K. A., Patel, S. C., Ernest, J. T. 1999. Cryoprecipitate: An autologous substrate for human fetal retinal pigment epithelium. Current eye research 19, pp. 89-94.

[26] Ferris, F. L., Fine, S. L. & Hyman, L. 1984. Age-related macular degeneration and blindness due to neovascular maculopathy. Archives of Ophthalmology 102, pp. 1640-1642.

[27] Friess, W. 1998. Collagen – biomaterial for drug delivery. European Journal of Pharmaceutics and Biopharmaceutics 45, pp. 113-136.

[28] Fuhrmann, S. 2010. Eye morphogenesis and patterning of the optic vesicle. Current Topics in Developmental Biology 93, pp. 61-84.

[29] Fujisaki, H., Adachi, E., Hattori, S. 2008. Keratinocyte Differentiation and Proliferation are Regulated by Adhesion to the Three-Dimensional Meshwork Structure of Type IV Collagen. Connective tissue research 49, pp. 426-436.

[30] Giordano, G. G., Thomson, R. C., Ishaug, S. L., Mikos, A. G., Cumber, S., Garcia, C. A., Lahiri-Munir, D. 1997. Retinal pigment epithelium cells cultured on synthetic biodegradable polymers. Journal of Biomedical Materials Research 34, pp. 87-93.

[31] Gong, J., Sagiv, O., Cai, H., Tsang, S. H., Del Priore, L. V. 2008. Effects of extracellular matrix and neighboring cells on induction of human embryonic stem cells into retinal or retinal pigment epithelial progenitors. Experimental Eye Research 86, pp. 957-65.

[32] Gonzàlez-Garcia, J. Proposal for a Vision-based Cell Morphology Analysis System. Master's Thesis. Linköping Institute of Technology 2008. 116 pages.

[33] Guillame-Gentil, O., Semenov, O., Roca, A. S., Groth, T., Zahn, R., Vörös, J. & Zenobi-Wong, M. 2010. Engineering the Extracellular Environment: Strategies for Building 2D and 3D Cellular Structures. Advanced Materials, pp. 1-20.

[34] Gupta, A. P., Kumar, V. 2007. New emerging trends in synthetic biodegradable polymers – Polylactide: A critique. European Polymer Journal 43, pp. 4053-4074.

[35] Hamel, C. 2006. Retinitis pigmentosa. Orphanet Journal of Rare Diseases 11.

[36] Haug, E., Sand, O., Sjaadstad, Ö. & Toverud, K. Ihmisen fysiologia. 1-2. edition. Porvoo 1999, WSOY. 536 p.

[37] Hirami, Y., Osakada, F., Takahashi, S., Yamanaka, S., Kurimoto, Y. & Takahashi, M. 2009. Generation of retinal progenitor cells from human induced pluripotent stem cells. ARVO Annual Meeting; 2009 May 3–7; Fort Lauderdale, Florida.

[38] Ho, T. C. & Del Priore, L. V. 1997. Reattachment of cultured human retinal pigment epithelium to extracellular matrix and human Bruch's membrane. Investigative Ophthalmology & Visual Science 38, 6, pp. 1110-8.

[39] Hynes, S. R & Lavik, E. B. 2010. A tissue-engineered approach towards retinal repair: scaffolds for cell transplantation to the subretinal space. Graeve's Archive for Clinical and Experimental Ophthalmology 248, pp. 763-778.

[40] Idelson, M., Alper, R., Obolensky, A., Ben-Shushan, E., Hemo, I., Yachimovich-Cohen, N., Khaner, H., Smith, Y., Wiser, O., Gropp, M., Cohen, M. A., Even-Ram, S., Berman-Zaken, Y., Matzrafi, L., Rechavi, G., Banin, E. &

Reubinoff, B. 2009. Directed differentiation of human embryonic stem cells into functional retinal pigment epithelium cells. Cell Stem Cell 5, 4, pp. 396-408.

[41] ImageJ Image Processing and Analysis in Java. [WWW]. [Cited 6.4.2011]. Available at: http://rsbweb.nih.gov/ij/index.html.

[42] In Pyo Park, P., Jonnalagadda, S. 2006. Predictors of glass transition in the biodegradable poly-lactide and poly-lactide-co-glycolide polymers. Journal of Applied Polymer Science 100, pp. 1983-1987.

[43] Jeong, S. I., Kim B-S., Kang, S. W., Kwon, J. H., Lee, Y. M., Kim, S. H. & Kim, Y. H. 2001. In vivo biocompatility and degradation behavior of elastic poly(L-lactide-co-ε-caprolactone) scaffold. Biomaterials 25, pp. 5939-5946.

[44] Jin, J., Jeong, S. I., Shin, Y. M., Lim, K. S., Shin, H. S., Lee, Y., M., Koh, H. C. & Kim, K-S. 2009. Transplantation of mesenchymal stem cells within a poly(lactide-co-ε-caprolactone) scaffold improves cardiac function in a rat myocardial infarction model. European Journal of Heart Failure 11, pp. 147-153.

[45] Katta, S., Kaur, I. & Chakrabarti, S. 2009. The molecular genetic basis of age-related macular degeneration: an overview. Journal of Genetics 88, 4, pp. 425-49.

[46] Khoshnoodi, J., Pedchenko, V. & Hudson, B. G. 2008. Mammalian collagen IV. Microscopy Research and Technique 71, 5, pp. 357-70.

[47] Klassen, H., Sakaguchi, D. S., Young, M. J. 2004. Stem cells and retinal repair. Progress in Retinal and Eye Research 23, pp. 149-181.

[48] Klimanskaya, I. 2006. Retinal pigment epithelium. Methods in Enzymology 418, pp. 169-94.

[49] Klimanskaya, I., Hipp, J., Rezai, K. A., West, M., Atala, A. & Lanza, R. 2004. Derivation and comparative assessment of retinal pigment epithelium from human embryonic stem cells using transcriptomics. Cloning and Stem Cells 6, 3, pp. 217-45.

[50] Kloxin, A. M., Kloxin, C. J., Bowman, C. N. & Anseth, K. S. 2010. Mechanical properties of cellularly responsive hydrogels and their experimental determination. Advanced Materials 17, 22, pp. 3484-3494.

[51] Kurosawa, H. 2007. Methods for Inducing Embryoid Body Formation: In Vitro Differentiation System of Embryonic Stem Cells. Journal of Bioscience and Bioengineering 103, pp. 5939-5946.

[52] Lachke, S. A & Maas, R. L. 2010. Building the developmental oculome: systems biology in vertebrate eye development and disease. Wiley Interdisciplinary Reviews. Systems biology and Medicine 2, pp. 305-232.

[53] Laing, R-A., Brenner, J-F., Lester, J-M., Mcfarland, J. L. 1981. Automated morphometric analysis of endothelial cells. Investigative Ophthalmology and Visual Science 20, pp. 407-410.

[54] Lehmussola, A., Ruusuvuori, P., Selinummi, J., Huttunen, H. & Yli-Harja, O. 2007. Computational Framework for Simulating Fluorescence Microscope

Images With Cell Populations. IEEE Transactions on Medical Imaging 26, pp. 1010-1016.

[55] Lin, C-C. & Anseth, K. S. 2009. PEG Hydrogels for the Controlled Release of Biomolecules in Regenerative Medicine. Pharmaceutical Research 26, pp. 631-643.

[56] Liu, C., Xia, Z. & Czernuska, J. T. 2007. Design and Development of Three-dimensional Scaffolds for Tissue Engineering. Chemical Engineering Research and Design 85, pp. 1051-1064.

[57] Liu, W., Yin, Y., Long, X., Luo, Y., Jiang, Y., Zhang, W., Du, H., Li, S., Zheng, Y., Li, Q., Chen, X., Liao, B., Xiao, G., Wang, W. & Sun, X. 2009. Derivation and characterization of human embryonic stem cell lines from poor quality embryos. Journal of Genetics and Genomics 36, 4, pp. 229-39

[58] Lu, J. T., Lee, C. J., Bent, S. F., Fishman, H. A. & Sabelman, E. E. 2007. Thin collagen films for retinal epithelial cell culture. Biomaterials 28, pp. 1486-1494.

[59] Lu, L., Garcia, C. A. & Mikos, A. G. 1999. *In vitro* degradarion of thin poly(D,L-lactic-co-glycolic acid) films. Journal of Biomedical Materials Research 46, pp. 236-244.

[60] Lu, L. Yaszemski, M. J. & Mikos, A. G. 2001. Retinal pigment engineering using synthetic biodegradable polymers. Biomaterials 22, pp. 3345-3355.

[61] Lund, R. D., Wang, S., Klimanskaya, I., Holmes, T., Ramos-Kelsey, R., Lu, B., Girman, S., Bischoff, N., Sauvé, Y. & Lanza, R. 2006. Human embryonic stem cell-derived cells rescue visual function in dystrophic RCS rats. Cloning Stem Cells 8, pp. 189-99.

[62] Madhavan Nampoothiri, K., Nair, N. R., John, R. P. 2010. An overview of the recent developments in polylactide (PLA) research. Bioresource Technology 101, pp. 8493-8501.

[63] Malpica, N., de Solorzano, C. O., Vaquero, J. J., Santos, A., Vallcorba, I., Garcia-Sagredo, J. M., del Pozo, F. 1997. Applying Watershed Algorithms to the Segmentation of Clustered Nuclei. Cytometry 28, pp. 289-297.

[64] Mano, J. F, Silva, G. A., Azevedo, H. S., Malafaya, P. B., Sousa, R. A, Silva, S. S., Boesel, L. F., Oliveira, J. M., Santos, T. C., Marques, A. P., Neves, N. M. & Reis, R. L. 2007. Natural origin biodegradable systems in tissue engineering and regenerative medicine: present status and some moving trends. Journal of the Royal Society Interface 4, pp. 999-1030.

[65] Mazzola, J. L. & Sirover, M. A. 2003. Subcellular localization of human glyceraldehydes-3-phospate dehydrogenase is independent of its glycolytic function. Biochimica et Biophysica Acta 1622, pp. 50-56.

[66] Meyer, J. S., Shearer, R. L., Capowski, E. E., Wright, L. S., Wallace, K. A., McMillan, E. L., Zhang, S-C. & Gamm, D. G. 2009. Modeling early retinal development with human embryonic and induced pluripotent stem cells. Proceedings of National Academy of Science of the United States of America 106, pp. 16698-703.

[67] Montezuma, S. R., Loewenstein, J., Scholz, C. & Rizzo, J. F. 2006. Biocompatibility of materials implanted into the subretinal space of Yucatan pigs. Investigative Ophthalmology & Visual Science 47, pp. 3514-22.

[68] Nair, L. S. & Laurencin, C. T. 2007. Biodegradable polymers as biomaterials. Progress in Polymer Science 32, 8-9, pp. 762-798.

[69] Nistor, G., Seiler, M. J., Yan, F., Ferguson, D. & Keirstead, H. S. 2010. Three-dimensional early retinal progenitor 3D tissue constructs derived from human embryonic stem cells. Journal of Neuroscience Methods 190, pp. 63-70.

[70] Niwa, H. 2001. Molecular mechanism to maintain cell renewal in ES cells. Cell Structure and Function 26, pp. 137-148.

[71] Oganesian, A., Gabrielian, K., Ernest, J. T & Patel, S. C. 1999. A new model of retinal pigment epithelium transplantation with microspheres. Archives of Opthalmology 117, pp. 1192-1200.

[72] Ohashi, K., Yokoyama, T., Nakajima, Y. & Kosovsky, M. Methods for BD Matrigel™ Matrix into Mice and Tissue Fixation. Technical Bulletin 455. BD Biosciences.

[73] Ohno-Matsui, K., Ichinose, S., Yoshida, T., Kojima, A., Mochizuki, M., Morita, I. 2005. The Effects of Amniotic Membrane on Retinal Pigment Epithelial Cell Differentiation. Molecular Vision 6, 11, pp. 1-10.

[74] Osakada, F., Ikeda, H., Mandai, M., Wataya, T., Watanabe, K., Yoshimura, N., Akaike, A., Sasai, Y. & Takahashi, M. 2008. Toward the generation of rod and cone photoreceptors from mouse, monkey and human embryonic stem cells. Nature Biotechnology 26, pp. 215-224.

[75] Osakada, F., Jin, Z. B., Hirami, Y., Ikeda, H., Danjyo, T., Watanabe, K., Sasai, Y. & Takahashi, M. 2009. In vitro differentiation of retinal cells from human pluripotent stem cells by small-molecule induction. Journal of Cell Science 122, pp. 3169-79.

[76] Partridge, J., Thompson, K. E. & Abraham, E. J. 2010. BD Purecoat Surfaces Support Growth, Expansion and Differentiation of Stem Cells. Application Note 485. BD Biosciences.

[77] Petrukhin, K. 2007. New therapeutic targets in atrophic age-related macular degeneration. Expert Opinion on Therapeutic Targets 11, pp. 625-639.

[78] Pevny, L. H. & Nicolis, S. K. 2010. SOX2 roles in neural stem cells. The International Journal of Biochemistry & Cell Biology 42, pp. 421-424.

[79] Pouton, C. W. & Akhtar, S. 1996. Biosynthetic polyhydroxyalkanoates and their potential in drug delivery. Advanced Drug Delivery Reviews 18, pp.133-162.

[80] Prabaharan, M. 2008. Review Paper: Chitosan Derivatives as Promising Materials for Controlled Drug Delivery. Journal of Biomaterials Applications 23, pp. 5-36.

[81] Rezai, K., Farrokh-Siar, L., Botz, M., Godowski, K., Swanbom, D., Patel, S. & Ernest, J. 1999. Biodegradable polymer film as a source for formation of human

fetal retinal pigment epithelium spheroids. Investigative Ophthalmology & Visual Science 40, pp. 1223-1228.

[82] Satomaa, T., Heiskanen, A., Mikkola, M., Olsson, C., Blomqvist, M., Tiittanen, M., Jaatinen, T., Aitio, O., Olonen, A., Helin, J., Hiltunen, J., Natunen, J., Tuuri, T., Otonkoski, T., Saarinen, J. & Laine, J. 2009. The N-glycome of human embryonic stem cells. BMC Cell Biology 10, 18 pages.

[83] Simo, R., Villaroel, M., Corraliza, L., Hernandez, C. & Garcia-Ramirez, M. 2010. The Retinal Pigment Epithelium: Something More than a Constituent of the Blood-Retinal Barrier – Implications for the Pathogenesis of Diabetic Retinopathy. Journal of Biomedicine and Biotechnology, 15 pages.

[84] Singh, S., Woerly, S. & Mclaughlin, B. J. 2001. Natural and artificial substrates for retinal pigment epithelial monolayer transplantation. Biomaterials 22, pp. 3337-3343.

[85] Sistiabudi, R., Paderi, J., Panitch, A. & Ivanisevic, A. 2009. Modification of native collagen with cell-adhesive peptide to promote RPE cell attachment on Bruch's membrane. Biotechnology and Bioengineering 102, pp. 1723-1729.

[86] Skottman, H. 2010. Derivation and characterization of three new human embryonic stem cell lines in Finland. In Vitro Cellular & Developmental Biology 46, pp. 206-9.

[87] Skottman, H., Dilber, M. S. & Hovatta, O. 2006. The derivation of clinical-grade human embryonic stem cell lines. FEBS Letters 580, 12, pp. 2875-8.

[88] Steinberg, R. H. 1985. Interactions between the retinal pigment epithelium and the neural retina. Doc Ophthalmol 60, pp. 327-344.

[89] Strauss, O. 2005. The retinal pigment epithelium in visual function. Physiological reviews 85, pp. 845-881.

[90] Tezcaner, A., Bugra, K. & Hasirci, V. 2003. Retinal pigment epithelium cell culture on surface modified poly(hydroxybutyrate-*co*-hydroxyvalerate) thin films. Biomaterials 24, pp. 4573-4583.

[91] Tezcaner, A. & Hicks, D. 2007. *In vitro* characterization of micropatterned PLGA-PHBV8 blend films as temporary scaffolds for photoreceptor cells. Journal of Biomedical Materials Research, Part A 86, pp. 170-181.

[92] Tezel, T. H. & Del Priore, L. V. 1996. Reattachment to a substrate prevents apoptosis of human retinal pigment epithelium. Graefe's Archive for Clinical and Experimental Ophthalmology 235, 1, pp. 41-7.

[93] Thomson, H. A., Treharne, A. J., Walker, P. Grosselm, M. C. & Lotery, A. J. 2011. Optimisation of polymer scaffolds for retinal pigment epithelium (RPE) cell transplantation. The British Journal of Ophthalmology 95, pp. 563-568.

[94] Thomson, J. A., Itskovitz-Eldor, J., Shapiro, S. S., Waknitz, M. A., Swiergiel, J. J., Marshall, V. S. & Jones, J. M. 1998. Embryonic stem cell lines derived from human blastocysts. Science 282, 5391, pp. 1145-7.

[95] Thomson, R. C., Giordano, G. G., Collier, J. H., Ishaug, S. L., Mikos, A. G., Lahiri-Munir, D. & Garcia, C. A. 1996. Manufacture and characterization of

poly(hydroxy ester) thin films as temporary substrates for retinal pigment epithelium cells. Biomaterials 17, pp. 321-327.

[96] Thumann, G., Schraermeyer, U., Bartz-Schmidt, K. U. & Heimann, K. 1997. Descemet's membrane as membranous support in RPE/IPE transplantation. Current eye research 16, pp. 1236-1238.

[97] Thumann, G., Viethen, A., Gaebler, A., Walter, P., Kaempf, S., Johnen, S., Salz, A. K. 2009. The *in vitro* and *in vivo* behaviour of retinal pigment epithelial cells cultured on ultrathin collagen membranes. Biomaterials 30, pp.287-294.

[98] Timpl, R. & Brown, J. C. 1994. The laminins. Matrix Biology 14, pp. 275-281.

[99] Tunggal, P., Smyth, N., Paulsson, M. & Ott, M-C. 2000. Laminins: Structure and genetic regulation. Microscopy Research & Technique 51, pp. 214-227.

[100] Vaajasaari, H., Ilmarinen, T., Juuti-Uusitalo, K., Rajala, K., Onnela, N., Narkilahti, S., Suuronen, R., Hyttinen, J., Uusitalo, H. & Skottman, H. Toward the defined and xeno-free differentiation of functional human pluripotent stem cell-derived retinal pigment epithelial cells. Molecular Vision 17, pp. 558-575.

[101] Vacanti, J. P. & Langer, R. 1999. Tissue engineering: the design and fabrication of living replacement devices for surgical reconstruction and transplantation. The Lancet 354, Supplement 1, pp. S32-S34.

[102] Vergroesen, P-P. A., Kroeze, R-J., Helder, M. N. & Smit, T. H. 2011. The Use of Poly(L-lactide-*co*-caprolactone) as a Scaffold for Adipose Stem Cells in Bone Tissue Engineering: Application in a Spinal Fusion Model. Macromolecular Bioscience 11, 9 pages.

[103] Vincent, L. 1992. Morphological Image Processing and Network Analysis of Corneal Endothelial Cell Images. Proceedings SPIE 1796 "Image Algebra and Morphological Image Processing III", pp. 212-226.

[104] Vugler, A., Carr, A. J., Lawrence, J., Chen, L. L., Burrell, K., Wright, A., Lundh, P., Semo, M., Ahmado, A., Gias, C., da Cruz, L., Moore, H., Andrews, P., Walsh, J. & Coffey P. 2008. Elucidating the phenomenon of hESC-derived RPE: anatomy of cell genesis, expansion and retinal transplantation. Experimental Neurology 214, pp. 347-61.

[105] Ward, D. A. & Barnhill, M. A. 1997. Extracellular matrix promotes differentiation of retinal pigment epithelium. *In Vitro* Cellular & Developmental Biology 33, pp. 588-591.

[106] WebVision. Simple Anatomy of the Retina. [WWW]. John Moran Eye Center University of Utah. Updated May, 2009. [Cited 31.3.2011]. Available at:http://webvision.med.utah.edu/sretina.html.

[107] Wimmers, S., Karl, M. O. & Strauss, O. 2007. Ion channels in the RPE. Progress in Retinal and Eye Research 26, pp. 263-301.

[108] Yu, J-H., Hsieh, M-M., Su, J-L. & Hung, B-N. 1991. Algorithm for Automatic Analysis of Corneal Endothelial Images. In 13th Annual International Conf. of the IEEE Engineering in Medicine and Biology Society, pp. 273-275.

[109] Zarbin, M. A. 2004. Current consepts in the pathogenesis of age-related macular degeneration. Archives of Ophthalmology 122, pp. 598-614.

[110] Zhou, M., Smith, A. M., Das, A. K., Hodson, N. W., Collins, R. F., Uljin, E. V. & Gough, J. E. 2009. Self-assembled, peptide-based hydrogels as scaffolds for anchorage dependent cells. Biomaterials 30, pp. 2523-2530.

[111] Zhu, J. 2010. Bioactive modification of poly(ethylene glycol) hydrogels for tissue engineering. Biomaterials 31, pp. 4639-4656.

APPENDIX 1: STRUCTURES OF BIOMADE™ GELATORS

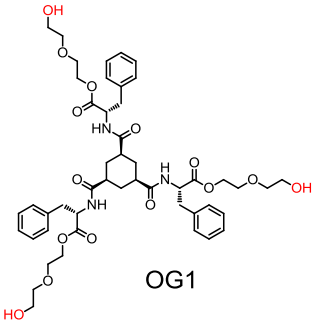

OG1

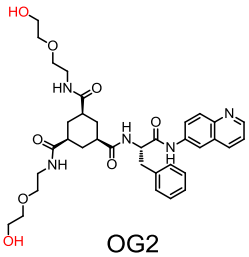

OG2

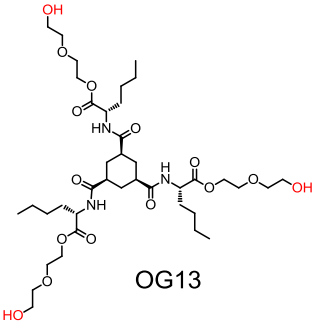

OG13

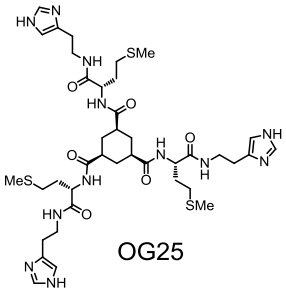

OG25

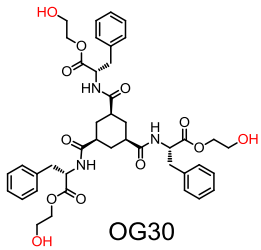

OG30

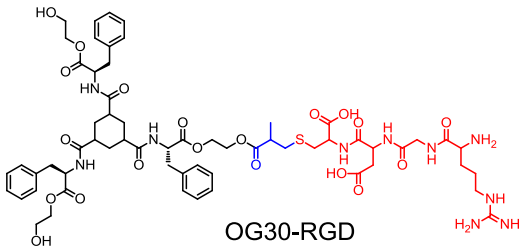

OG30-RGD

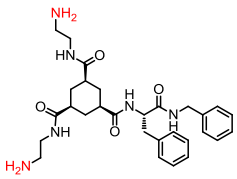

OG34

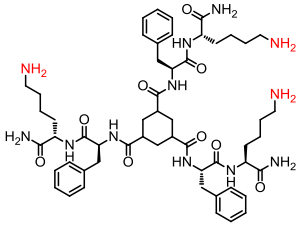

OG49

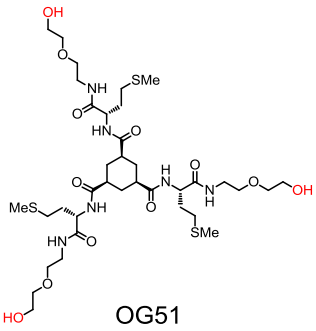

OG51